The geomagnetic polarity timescale for the Triassic: linkage to stage boundary definitions

Mark W. Hounslow and Giovanni Muttoni

Geological Society, London, Special Publications 2010; v. 334; p. 61-102
doi:10.1144/SP334.4

The geomagnetic polarity timescale for the Triassic: linkage to stage boundary definitions

MARK W. HOUNSLOW[1]* & GIOVANNI MUTTONI[2]

[1]*Centre for Environmental Magnetism and Palaeomagnetism, Lancaster Environment Centre, Lancaster University, Bailrigg, Lancaster, UK LA1 4YQ*

[2]*Dipartimento di Scienze della Terra, Università di Milano, Via Magiagalli 34, I-20133 Milan, Italy (e-mail: giovanni.muttoni1@unimi.it)*

**Corresponding author (e-mail: m.hounslow@lancs.ac.uk)*

Abstract: Studies of Triassic magnetostratigraphy began in the 1960s, with focus on poorly fossilferous nonmarine red-beds. Construction of the Triassic geomagnetic polarity timescale was not consolidated until the 1990s, when access to magnetometers of sufficient sensitivity became widely available to measure specimens from marine successions. The biostratigraphically-calibrated magnetostratigraphy for the Lower Triassic is currently largely based on ammonoid zonations from Boreal successions. Exceptions are the Permian–Triassic and Olenekian–Anisian boundaries, which have more extensive magnetostratigraphic studies calibrated by conodont zonations. Extensive magnetostratigraphic studies of nonmarine Lower Triassic successions allow a validation and cross-calibration of the marine-based ages into some nonmarine successions. The Middle Triassic magnetostratigraphic timescale is strongly age-constrained by conodont and ammonoid zonations from multiple Tethyan carbonate successions, the conclusions of which are supported by detailed work on several nonmarine Anisian successions. The mid Carnian is the only extensive interval in the Triassic in which biostratigraphic-based age calibration of the magnetostratigraphy is not well resolved. Problems remain with the Norian and early Rhaetian in properly constraining the magnetostratigraphic correlation between the well-validated nonmarine successions, such as the Newark Supergroup, and the marine-section-based polarity timescale. The highest time-resolution available from magnetozone correlations should be about 20–30 ka, with an average magnetozone duration of *c*. 240 ka, for the Lower and Middle Triassic, and about twice this for the Upper Triassic.

The early pioneering work of Brunhes (1906) and Matuyama (1929) recognized that volcanic rocks recorded magnetization directions similar to the orientation of the present day Earth's magnetic field (i.e. of normal polarity), but also that some volcanic rocks recorded older magnetization directions that were in the opposite direction (i.e. of reverse polarity). Motonori Matuyama was the first to suggest that these directions recorded the reversal in the main (i.e. dipole) component of the Earth's magnetic field (see discussion of early developments in Jacobs 1963). The first studies on the natural remanent magnetization and magnetic properties of sedimentary rocks were conducted in the late 1930s and 1940s, often with the focus on Pleistocene continental sediments (e.g. McNish & Johnson 1938; Ising 1942; Nagata 1945; Graham 1949; Torreson *et al.* 1949). In the 1950s, more comprehensive work on Neogene volcanic rocks showed a consistent stratigraphic pattern in the recorded polarity of magnetizations, that is, a magnetostratigraphy (see Irving 1964; Hailwood 1989; and McElhinney & McFadden 2000 for a review of these early developments).

Palaeomagnetic data from Triassic red-bed sediments were first published by Clegg *et al.* (1954) and Creer *et al.* (1954). The later authors also undertook the first published magnetostratigraphic study, focussing on the Late Proterozoic from the UK. Palaeomagnetic work on other Triassic successions, from the USA, quickly followed (Graham 1955; Runcorn 1955; Du Bois 1957), demonstrating that other sediments also recorded magnetizations of both reverse and normal polarity. Radiometric evidence, providing convincing support that the Earth's magnetic field polarity changes were synchronous on a global scale, was firmly established in the early 1960s (Irving 1964; see review in McElhinney & McFadden 2000), which Vine & Matthews (1963) used in their sea-floor spreading model, linking Earth's magnetic field polarity changes with sea-floor magnetic anomaly lineations.

Roots of a Triassic Geomagnetic Polarity Timescale (GPTS)

Most of the palaeomagnetic work in the 1950s and 1960s was directed to providing data to support the concepts of continental drift (Irving 1964). Work by Creer (1958, 1959) on part of the UK Triassic

From: LUCAS, S. G. (ed.) *The Triassic Timescale*. Geological Society, London, Special Publications, **334**, 61–102.
DOI: 10.1144/SP334.4 0305-8719/10/$15.00

was the earliest Triassic palaeomagnetic study that placed a set of palaeomagnetic samples into stratigraphic order to produce a simple magnetostratigraphy.

The early pioneer in the development of magnetostratigraphy for stratigraphic correlation was A. N. Khramov, who published the seminal summary of on-going Russian work in 1958 (Khramov 1958). This was primarily focused on extensive studies of Neogene and Quaternary successions in western Turkmenistan (Cheleken Peninsula), but was also significant (Irving 1964; Glen 1982) in that it discussed fundamental magnetostratigraphic concepts, such as the use of multiple sections, minimum sampling requirements to define magnetozones, and palaeomagnetic data quality. It also anticipated the construction of a geomagnetic polarity timescale (GPTS) for dating and correlation. In addition, Khramov (1958) outlined a rudimentary working knowledge (without details) of the magnetostratigraphy from Upper Permian and Lower Triassic sections in the Vyatka River region of the Moscow Basin. Details of this multiple-section magnetostratigraphic study appeared subsequently (Khramov 1963), and it was quickly followed by studies on the Chugwater Formation in the western USA (Picard 1964) and the German Upper Buntsandstein (Burek 1967, 1970).

The focus of Triassic magnetostratigraphic studies in the 1950s to early 1980s was on terrestrial red-bed successions, since these provided natural remanent magnetizations that could be easily measured on the early astatic magnetometers and the later fluxgate spinner magnetometers then available (Collinson *et al.* 1957; Gough 1964). During this period, the development of routine magnetic cleaning techniques, referred to as demagnetization (As & Zijderveld 1958; Creer 1959; Wilson 1961) and more rigorous analysis (i.e. using least-square best fitting methods: Kirschvink 1980) of palaeomagnetic data, were developed into methodologies that are routinely used today. The widespread use of full demagnetization techniques, now accepted as standard for extracting primary magnetizations, was only fully embraced in the 1970s. As such there is some scepticism about the validity of palaeomagnetic data generated prior to the 1970s, which is in part expressed in the quality criteria suggested by Opdyke and Channell (1996) for classifying magnetostratigraphic data.

It was not until the development of superconducting quantum interference device (SQUID) magnetometers in the 1970s (Goree & Fuller 1976), and their widespread use since the 1980s and 1990s, that the weakly magnetic specimens found in many marine Triassic successions could be suitably measured, demagnetized, and primary magnetization components extracted. This development finally heralded the expansion of detailed studies on the construction of a Triassic GPTS, after earlier attempts to apply the new instrumentation to limestone successions of other ages (e.g. Martin 1975; Heller 1977). The seminal magnetostratigraphic works of Lowrie & Alvarez (1977) and Channell *et al.* (1979) on Cretaceous limestones of the Apennines and the Southern Alps, respectively, were influential and were followed by work on the Triassic by Heller *et al.* (1988), McFadden *et al.* (1988) and Steiner *et al.* (1989), who provided the first detailed magnetostratigraphic studies of Triassic carbonates, in predominantly marine successions.

Early developments of the Triassic GPTS

The first attempts at the construction of a Triassic GPTS through the 1960s and 1970s were inevitably fragmentary, being based around nonmarine successions, which were often imprecisely dated by vertebrates and palynomorphs. Khramov (1963) was the first to attempt the construction of a Lower and Middle Triassic GPTS, based on the Vetluga successions from the Moscow Basin and existing studies from the western literature. This was later followed by attempts at a complete Triassic GPTS by McElhinney & Burek (1971), Pergament *et al.* (1971), Pechersky & Khramov (1973), and Molostovsky *et al.* (1976).

In spite of the rapid development of the GPTS for the latest Jurassic to Pleistocene, mainly through study of sea-floor linear magnetic anomalies, the absence of Triassic sea-floor largely impeded the development of a detailed Triassic GPTS until the widespread availability of SQUID magnetometers in the late 1980s. A feature that also characterizes most of the Triassic magnetostratigraphic studies and GPTS construction prior to the 1990s is the common lack of true integration with *detailed* biostratigraphies provided by the co-study of, for example, ammonoids and conodonts. It is the initial expansion of such integration in the early 1990s with studies such as Ogg & Steiner (1991) using ammonoids, and Gallet *et al.* (1992, 1993) using conodonts, that the Triassic GPTS has now been developed into such detail. In the last two decades there has been much progress, particularly in calibrating the pattern of reverse and normal magnetic field polarity changes against conodont biostratigraphies (Muttoni *et al.* 1996*a*, 2000, 2004; Gallet *et al.* 1998, 2000*a*, 2007; Channell *et al.* 2003).

The time resolution of magnetostratigraphic correlation

Correlation using magnetostratigraphic principles is at two scales. Firstly, the changing pattern of

magnetic polarity (i.e. magnetozones) over a stratigraphic interval can provide a distinctive 'bar-code' pattern for correlation. This is because magnetic field reversal is essentially a stochastic process, giving random length-durations of magnetozones (McElhinney & McFadden 2000; Lowrie & Kent 2004). The longer the fragment of the polarity bar-code, and the more constraints from other stratigraphic tools, the greater is the confidence in intersection correlation. For the Cenozoic, the maximum resolution of the GPTS is about 20–30 ka, with reversals on average every *c*. 0.22 Ma (McElhinney & McFadden 2000; Lowrie & Kent 2004). The Late Triassic appears to have a reversal rate somewhat similar to the Cenozoic, with a maximum magnetozone resolution of about 30 ka (Kent *et al.* 1995; Kent & Olsen 1999).

Secondly, correlation of the boundaries (transitions) of magnetozones provides the highest resolution of correlation. Studies on the Cenozoic suggest that time durations of magnetic field polarity transitions from reverse to normal (or vice-versa) are between 1000 to 8000 years, probably varying depending upon location and the actual magnetozone transition (McElhinney & McFadden 2000). In the Brunhes magnetochron (i.e. the normal polarity interval since 0.78 Ma: Cande & Kent 1995), the briefest evidence of pre-emptive polarity changes are geomagnetic excursions, which have a duration of less than 10,000 years (Langereis *et al.* 1997). It is probable that similar excursions existed in the Triassic, but without cm-scale studies in successions with high sedimentation rates, the prospect of using such excursions for correlation in the Triassic is remote.

The time resolution provided by magnetostratigraphic correlation is also bound up with sampling density issues, sedimentation rates and the presence of disconformities. The highest resolution is achievable from continuously deposited and expanded successions with high sedimentation rates, sampled at the smallest stratigraphic interval. For this reason, magnetostratigraphic studies can have site-selection priorities contrary to those of biostratigraphic studies, which may focus on condensed successions with high fossil recovery rates.

Stratigraphic principles of magnetostratigraphic correlation

Correlation using magnetostratigraphic normal/reverse polarity bar-code patterns relies on a number of factors related to the preserved stratigraphy and its sampling:

(a) A reasonable within-section consistency of sedimentation rate is advantageous to maintain the relative stratal (and time duration) thicknesses of magnetozones through the section. Given a detailed basin-wide sequence stratigraphy, it may be possible to estimate sedimentation rate distortions using sequence stratigraphic principles.
(b) Stratigraphic gaps can distort the magnetostratigraphic pattern, unless properly identified using biostratigraphic data, supported by appropriate sedimentology and sequence stratigraphic studies.
(c) Sections representing longer periods of time stand a better chance of providing convincing bar-code matches.
(d) Sampling resolution should be matched with sedimentation rate, and the expected number of polarity changes in a section. If sampling resolution is low, polarity changes are frequent, and sedimentation rate is also low and variable, then the recovered pattern may be a poor match to the 'real' polarity pattern. For this reason, it is not good practice to count magnetozones for correlation purposes, whereas it is much more reliable to use the dominance of polarity as a means for correlation (or use other correlation constraints), since this is not as strongly affected by sampling density and changes in sedimentation rate.

Comparison between sections with large between-section sedimentation rate differences is best accommodated by stretching or shrinking the entire magnetostratigraphic height scale linearly, using as a guide, biostratigraphic or radiometric correlation constraints in addition to the magnetostratigraphy. Using such scaling, composite timescales can be constructed in a 'pseudo-height' scale, based on principles of graphic correlation (Shaw 1964; Pälike *et al.* 2005). We here use these principles to develop the Triassic GPTS using marine sections, because with such sections there is greater chance of proving continuity using other correlation constraints. The major 'anchor points' for these composites are indicated on the diagrams (e.g. Fig. 1). We then examine the higher detail sometimes available from nonmarine sections (e.g. Newark Supergroup in the Upper Triassic). We focus primarily on the stage boundaries, because these are the only real fixed points in Triassic time, and this approach is compatible with other contributions in this book. The magnetochron couplets (i.e. each successive N–R pair) in the GPTS are labelled LT, MT and UT for the Lower, Middle and Upper Triassic, respectively.

The magnetostratigraphy of the Permian–Triassic transition

The Permian–Triassic boundary (PTB) is located at the first occurrence (FO) of the conodont *Hindeodus parvus*, in the global stratotype section and point

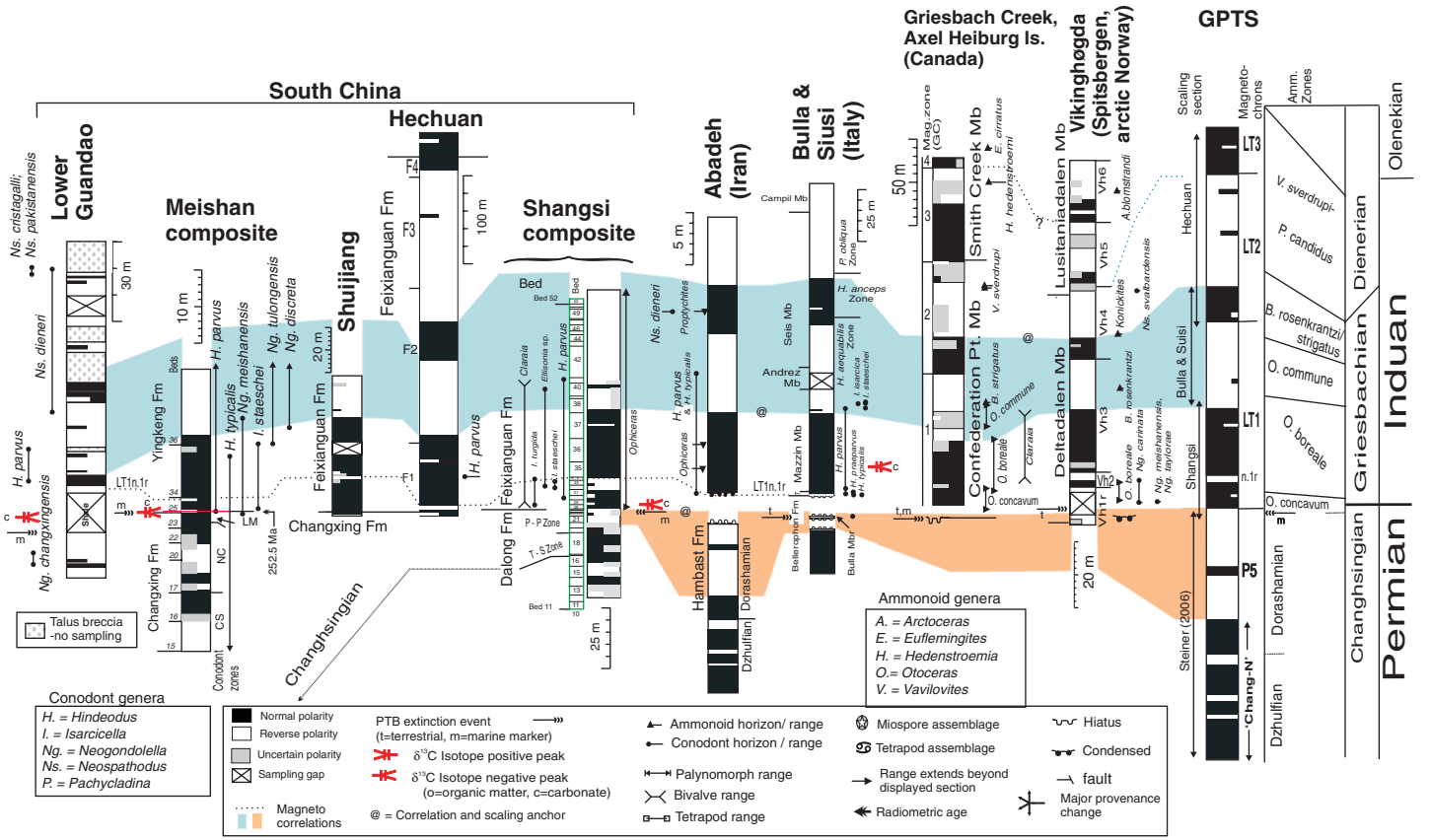

Fig. 1. Summary of the bio-magnetostratigraphy across the Permian–Triassic boundary. Section data from left to right: Lower Guandao (Payne *et al.* 2004; Lehrmann *et al.* 2006); Meishan composite (Li & Wang 1989; Yin *et al.* 2001; Zhao *et al.* 2007); Shuijiang (Chen *et al.* 1994; Heller *et al.* 1995); Hechuan (Steiner *et al.* 1989); Shangsi composite compiled from Heller *et al.* (1988), Steiner *et al.* (1989), Glen *et al.* (2009), Lai *et al.* (1996), Nicoll *et al.* (2002) and Wignall *et al.* (1995); Abadeh (Gallet *et al.* 2000*b*); Bulla & Siusi (Perri & Spalletta 1998; Scholger *et al.* 2000; Perri & Farabegoli 2003; Horacek *et al.* 2007); Griesbach Creek (Ogg & Steiner 1991; Henderson & Baud 1997; Hounslow *et al.* 2008*a*); Vikinghøgda (Hounslow *et al.* 2008*a*). South China conodont zones: CS, *Neogondolella* (*Clarkina*) *subcarinata*; NC, *Ng. changxingensis yini – Ng. changxingensis*; LM, *Hindeodus latidentatus – Ng. meishanensis*. Shangsi ammonoid zones: T–S, *Tapashanites–Shevyrevites* assemblage Zone; P–P, *Pseudotirolites–Pleuronodoceras* assemblage Zone. Conodont genus abbreviations: Ns, *Neospathodus*; Ng, *Neogondolella*. Thickness scales different for each section. Magnetozone width in the GPTS and section columns corresponds to data robustness and degree of confirmation from stratigraphically adjacent magnetostratigraphic sampling.

(GSSP) at Meishan, China (Yin *et al.* 2001) (Fig. 1). This FO follows two earlier key events in the latest Permian (i.e. in the latest Changhsingian), firstly, the marine extinction event, then slightly younger, a negative peak in $\delta^{13}C_{carb}$ (Yin *et al.* 2001; Mundil *et al.* 2004). At all other sites, the location of the PTB is based on correlation to the Meishan GSSP, using conodont, carbon isotopic, sequence stratigraphic, palynological or magnetostratigraphic data, etc. At the Shangsi section in China, the marine extinction event is at the boundary of the Dalong and Feixianguan formations (Wignall *et al.* 1995), the negative $\delta^{13}C_{carb}$ peak is between *c.* 1 to 5 m higher (see discussion in Mundil *et al.* 2004), and the first *H. parvus* is 4.5 m above the extinction event (Nicoll *et al.* 2002). At Meishan, the marine extinction event, the associated $\delta^{13}C_{carb}$ negative peak and the FO of *H. parvus* are all within a stratigraphic range of about 0.3 m (Jin *et al.* 2000; Yin *et al.* 2001, 2005). Similarly, sections in Greenland show that the $\delta^{13}C_{org}$ negative excursion is slightly younger than an initial palynofloral turnover (which is a proxy for the extinction event) to assemblages that contain miospores typical of the Triassic (Looy *et al.* 2001). In the Karoo Basin, the peak of tetrapod extinctions is synchronous with the $\delta^{13}C_{org}$ negative excursion (Ward *et al.* 2005).

Studies of $\delta^{13}C_{carb}$ over this transition in the Alps are contradictory with respect to the position of the initial isotopic decline, which is either in the upper part of the Bellerophon Fm. (Magaritz *et al.* 1988; Sephton *et al.* 2005), or in the basal Werfen Fm. (Holser *et al.* 1989), and reaches a peak at either 10–15 m or *c.* 25 m above the base of the Werfen Fm. In both cases, the most negative $\delta^{13}C_{carb}$ is younger than the FO of *H. parvus*, which is at odds with data from other marine sections.

The situation is more problematic when locating the polarity boundaries with respect to these events. In most sections where there is evidence of the latest Permian (such as at Shangsi and Guandao in China; Steiner *et al.* 1989; Lehrmann *et al.* 2006), and Abadeh in Iran (Gallet *et al.* 2000*b*), it is characterized by reverse polarity, which extends to include the late Permian extinction event itself (Glen *et al.* 2009). In the southern Italian Alps, the terrestrial extinction horizon is also located in the reverse polarity Bulla Member (Mb) (uppermost part of the Bellerophon Fm.; Scholger *et al.* 2000; Perri & Farabegoli 2003) about 0.5 m below the top (Cirilli *et al.* 1998), where there is a loss of typical late Permian miospores (e.g. *Klausipollenites schaubergeri*, *Jugasporites delsaucei*, *Nuskoisporites dulhuntyi*, *Paravesicaspora splendens*) and the introduction of forms such as *Densoisporites playfordi*, *D. nejburgii*, *Convolutispora* sp., and *Rewanispora vermiculata.* This same level also shows evidence of massive soil erosion (Sephton *et al.* 2005).

Sections such as Shuijang and Hechuan in China show a proxy for the extinction event (base of Feixanguan Fm.), as very near to the base of a normal polarity magnetozone. The magnetostratigraphy for the Meishan GSSP is anomalous with respect to other sections, in that it shows the extinction event in the middle parts of a normal magnetozone, which begins in the upper part of the Changhsingian. A reverse magnetozone in Meishan bed 27, spanning the PTB (Yin *et al.* 2001), has not been confirmed by further sampling (Yin *et al.* 2005). The most detailed and comprehensive marine-based magnetostratigraphic studies at this level are of the Shangsi section (Heller *et al.* 1988; Steiner *et al.* 1989; Glen *et al.* 2009), and place the base of a normal magnetozone (here called LT1n) 0.5 m above the base of the Feixianguan Fm. (Glen *et al.* in press), just above the extinction event and below the $\delta^{13}C_{carb}$ negative peak.

In all currently studied sections, the FO of *H. parvus* is within a normal polarity magnetozone (Fig. 1), but it also ranges into the lower parts of LT1r in the Shangsi, Abadeh and Lower Guandao sections (Fig. 1). However, the Shangsi data are different in detail from other well-dated marine sections, in that the FO of *H. parvus* (in bed 30; Nicoll *et al.* 2002) occurs below a well-defined reverse magnetozone (here equivalent of LT1n.1r, in beds 32 and 33; Fig. 1). Evidence for this magnetozone is strong at Shangsi, were it has been identified by Heller *et al.* (1988), Steiner *et al.* (1989) and Glen *et al.* (2009). There is also good evidence for a reverse magnetozone at about this level in the Deltadalen section on Svalbard (Hounslow *et al.* 2008*a*), and in S. China in the Shuijiang (*c.* 15–17 m above the base of the Feixanguan Fm.; Heller *et al.* 1995), and Hechuan sections (*c.* 3 m above the base of the Feixanguan Fm.; Steiner *et al.* 1989), although in all cases without evidence of *H. parvus*. In the Meishan GSSP, Li & Wang (1989) also detected a single reverse polarity level, some 1.5 m above the PTB (Fig. 1), which is here interpreted as probably LT1n.1r. This reverse magnetozone may also be present in the Guandao section (Fig. 1).

Yin *et al.* (2001) recognized that the range of *H. parvus* and *Otoceras boreale* overlapped, but at that time placed the boreal *Otoceras concavum* Zone in the Permian. The new detailed data of Bjerager *et al.* (2006) has demonstrated that the PTB occurs within the range of *O. concavum* in the East Greenland successions, which indicates the PTB occurs within the lowest part of magnetozone LT1n (Fig. 1). The same conclusion can be inferred in the Canadian Arctic successions (Henderson & Baud 1997), using the maximum flooding surface to infer correlation between Otto Fiord and Griesbach Creek.

In conclusion, the following succession of events and markers is associated with the marine PTB sections:

1. Initiation of a strong palynofloral turnover, corresponding to a major floral extinction event (in the late Changhsingian), located within a reverse magnetozone. This turnover appears to be coincident with extinction events in marine biota, as described by Jin *et al.* (2000*a*), Looy *et al.* (2001), Sephton *et al.* (2005) and others.
2. The base of normal magnetozone LT1n, within the latest Changhsingian.
3. A minimum in $\delta^{13}C$ representing the climax of the Late Permian extinctions and its effect on Earth systems. This level seems to approximate the major tetrapod extinction event (Ward *et al.* 2005).
4. The FO of *H. parvus* in Chinese sections, indicating the base of the Triassic, within the occurrence range of *O. concavum*.
5. The base of sub-magnetozone LT1n.1r.
6. The base of LT1r, which occurs within the occurrence ranges of *H. parvus* and the Boreal ammonoid *O. boreale* (Hounslow *et al.* 2008*a*).

The composite GPTS in Figure 1 differs from the solution of Steiner (2006), in that the equivalent of LT1n.1r is a magnetozone of half-bar width, and we specifically tie the magnetostratigraphy to other events. Steiner's (2006) magnetostratigraphic solution also has a Changhsingian part of the Meishan section in the Griesbachian and a clearly Griesbachian part of the Shangsi section in the Changhsingian, both clearly erroneous correlation solutions.

The magnetostratigraphy of the Induan–Olenekian boundary

The base of the Olenekian is provisionally defined in the Mud M04 section in India (Spiti) by the FO of *Neospathodus waageni* s.l. (Fig. 2), corresponding also to the initial increase of a positive peak in $\delta^{13}C_{carb}$ and an associated FO of the ammonoid *Rohillites rohilla* (Krystyn *et al.* 2007*b*). This isotopic peak has been dated at Guangxi, China at 251.2 ($\pm$0.2) Ma (Galfetti *et al.* 2007*a*; Fig. 2). Currently, the only section in which this boundary can be closely related to a magnetostratigraphy is West Pingdingshan, at Chaohu in China (Krystyn *et al.* 2007*b*; Sun *et al.* 2007, 2009), just below the base of normal magnetozone WP4n (Fig. 2). The magnetostratigraphy of the upper part of the West Pingdingshan section appears to bear a close correspondence to that from the Hechuan section, which however lacks significant biostratigraphy near the Induan–Olenekian boundary (Fig. 2). The Dienerian interval at Guandao is characterized by *Neospathodus dieneri* and *Ns. pakistanensis* conodont faunas and is dominated by reverse polarity, although there are sampling gaps and intervals of breccia. This probably correlates to the interval at Hechuan that includes the upper parts of the Feixianguan Fm. (Fig. 2). The *Ns. pakistanensis* conodont fauna underlying the positive peak in $\delta^{13}C_{carb}$ can be closely related to similar events at the Induan–Olenekian boundary in the proposed GSSP at Mud (Krystyn *et al.* 2007*b*).

The sections from the Sverdrup Basin and Spitsbergen appear to provide the most continuous magnetostratigraphy across the Induan–Olenekian boundary, but have a somewhat spotty ammonoid and conodont biostratigraphy and are not easily related to the proposed GSSP or sections in China. New conodont data from the Creek of Embry section on Ellesmere Island in Canada (Baud *et al.* 2008; Beatty *et al.* 2008; T. Beatty pers. comm. 2008) show *Ns. krystyni* and *Ns. kummeli* overlain by *Ns. dieneri*, suggesting that the base of magnetozone CE1r is equivalent to the base of WP3r (Fig. 2), which suggests the base of the Olenekian is within the topmost part of CE1r (i.e. LT2r). The apparent equivalent to magnetozone CE1r at the Griesbach Creek section on Axel Heiberg Island (Arctic Canada) is GC2r, in which *Vavilovites sverdrupi* occurs some 15 m below its top (Fig. 1). The Creek of Embry section displays a further *c*. 300 m before the first *Euflemingites*, indicating a rapid sedimentation rate in this section during the earliest Olenekian. Unfortunately, in this section the magnetostratigraphy over this interval is not particu-larly well defined, with many uncertain levels, but nevertheless appears to display two reverse sub-magnetozones within a normal-polarity dominated interval that probably correlates to magnetozone Vh6 at Vikinghøgda and LT4n in the composite (Fig. 2). The interval LT3n to LT4r appears to correlate to a reverse-polarity-dominated interval at Vikinghøgda, Hechuan and Gaundao (Fig. 2). Unfortunately, conodonts from strata containing *Hedenstroemia hedenstroemi* are not known from Arctic Canada, and *Ns. waageni* occurs commonly with ammonoids from the *E. romunderi* Zone (Orchard 2008). Likewise, *Ns. cristagalli* ranges from the *B. strigatus* Zone into the *V. sverdrupi* Zone (Orchard 2008), which, together with the range of this conodont at Chaohu, suggests that the Olenekian boundary is much higher in the Creek of Embry section than suggested by the magnetostratigraphy (Sun *et al.* 2009). These inconsistencies may be resolved with a more detailed bio-magnetostratigraphy from the lowest Olenekian.

The *R. rohilla* ammonoid zone at the Mud section can be correlated to the *Kashmirites densistriatus* beds at Guangxi, which lie above beds in

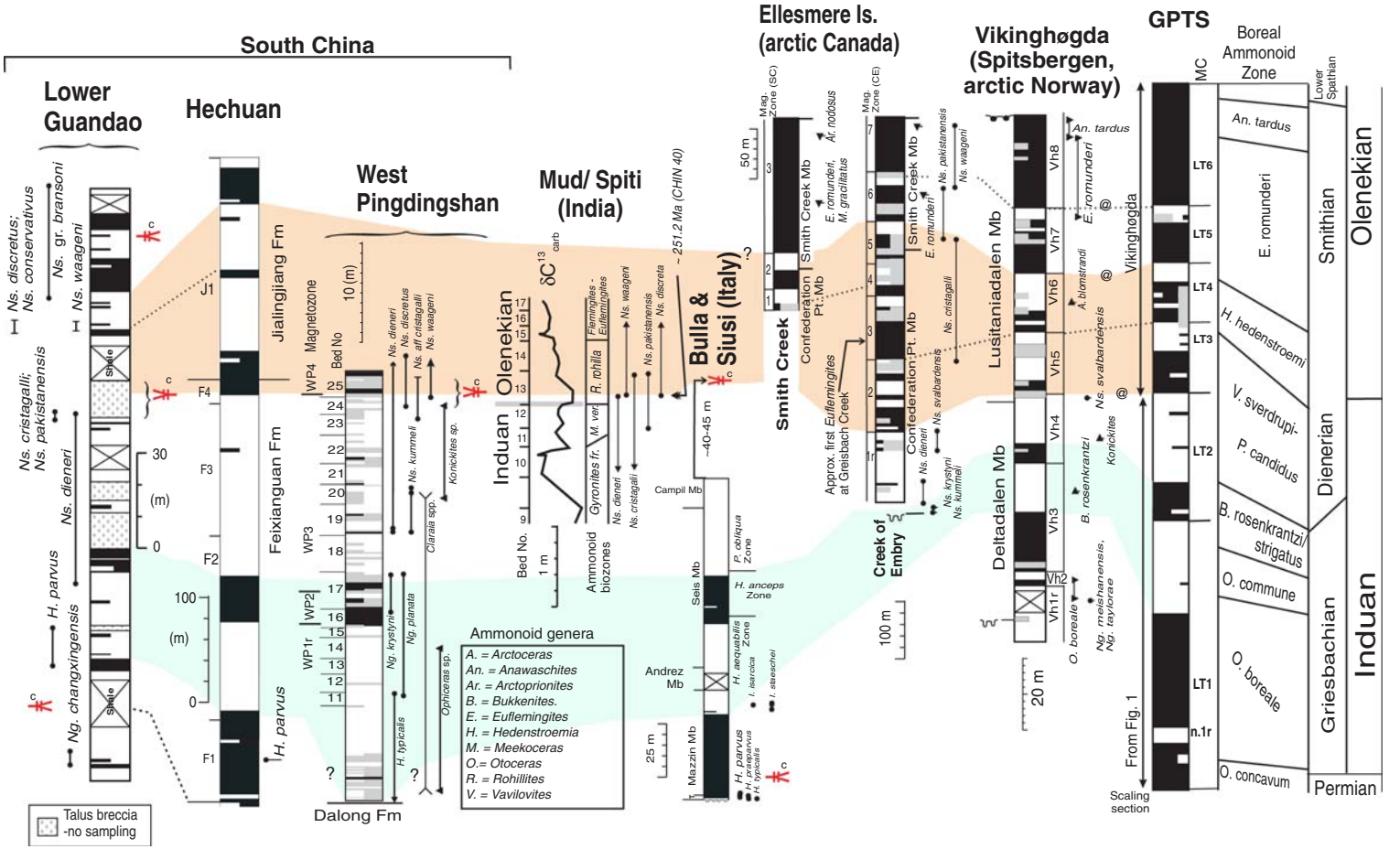

Fig. 2. Summary of the bio-magnetostratigraphy across the Induan–Olenekian boundary. Section data from left to right: Lower Guandao (Payne *et al.* 2004; Lehrmann *et al.* 2006); Hechuan (Steiner *et al.* 1989), West Pingdingshan (Sun *et al.* 2007, 2009); Mud, Spiti (Krystyn *et al.* 2007*b*); Bulla & Siusi (Scholger *et al.* 2000; Perri & Farabegoli 2003; Horacek *et al.* 2007); Ellesmere Island (Ogg & Steiner 1991; Orchard 2008; Beatty *et al.* 2008; Baud *et al.* 2008; T. Beatty pers. comm. 2008); Vikinghøgda (Hounslow *et al.* 2008*a*; Nakrem *et al.* 2008). See Figure 1 for key. Ammonoid genus abbreviations in key, others on Figure 1. Thickness scales different for each section. MC = magnetochrons.

which *H. hedenstroemi* is found (Galfetti *et al.* 2007*a*; Krystyn *et al.* 2007*b*), suggesting that the FO of *H. hedenstroemi* lies below the base of the Olenekian. This cannot be demonstrated in the Boreal sections with magnetostratigraphy, where *H. hedenstroemi* at Griesbach Creek (Fig. 1) occurs some 12 m above the top of the magnetozone GC3n (Ogg & Steiner 1991; Tozer 1994; Hounslow *et al.* 2008*a*), which is the probable equivalent of LT3n (Fig. 1). At Griesbach Creek, *Euflemingites cirratus* occurs a few metres above the top of the section measured by Ogg & Steiner (1991), an ammonoid species which does not co-occur with the zonal index *E. romunderi* in Canada (Tozer 1994), adding some support to our interpretation that magnetozone GC4n is the equivalent of LT4n, and that the first *Euflemingites* (at Griesbach Creek) occurs within LT4n (Figs 1 & 2).

In the Bulla/Siusi sections in northern Italy, the correlation (Fig. 2) of the upper-most normal magnetozone (within the Seis Mb) to West Pingdingshan is consistent with the $\delta^{13}C$ positive isotope peak, which characterizes the Induan–Olenekian boundary interval (Tong *et al.* 2007; Richoz *et al.* 2007). This positive isotopic peak occurs some 40–45 m above the top of the section sampled for magnetostratigraphy (Horacek *et al.* 2007; Posenato 2009). However, according to Kozur and Bachmann (2005), the base of the Olenekian in the Italian Bulla/Suisi sections is at the base of the *Pachycladina obliqu*a conodont Zone, at odds with both the carbon isotopic data, interpretation by others of the conodont data (Posenato 2009) and the magnetostratigraphy, which suggests instead that the *P. obliqu*a Zone in these sections begins in the base of LT2r in the Dienerian (Figs 1 & 2).

Within the normal and reverse polarity parts of magnetozone LT2, a number of sections show tentative magnetozones. Particularly significant may be those within the lower part of CE1r (Creek of Embry section), West Pingdingshan (WP3r), Gaundao and the F3 member of the Hechuan section (Fig. 2). These may indicate brief submagnetozones in LT2n and LT2r. The base of magnetozone LT2n appears to be a useful approximation of the Griesbachian–Dienerian boundary, as evident by *Ns. dieneri* and *Proptychites* sp. at this level in the Lower Guandao and Abadeh sections (Fig. 1).

Our synthesis of the Induan and Lower Olenekian magnetostratigraphy is similar to that of Steiner (2006), but differs in detail, because she tried to integrate both marine and nonmarine studies in a composite 'pattern matching' GPTS. The age assignments of Steiner (2006) are also strongly influenced by the intersection correlations and biostratigraphy presented by Ogg & Steiner (1991), which are flawed (Hounslow *et al.* 2008*a*).

Magnetostratigraphy of the Olenekian–Anisian boundary

The base of the Anisian is likely to be defined within the Dęsli Caira section in Romania, although the exact boundary is not yet decided (Grădinaru *et al.* 2007; Hounslow *et al.* 2007*a*) (Fig. 3). The boundary is here informally placed at the FO of the conodont *Chiosella timorensis*. There are many magnetostratigraphic studies through the Lower–Middle Triassic boundary interval, from both low- and high-palaeolatitude marine sections (Muttoni *et al.* 2000 and references therein; Lehrmann *et al.* 2006; Hounslow *et al.* 2007*a*, *b*), and nonmarine sections (Steiner *et al.* 1993; Nawrocki & Szulc 2000; Huang & Opdyke 2000; Hounslow & McIntosh 2003; Szurlies *et al.* 2003; Szurlies 2007; Dinarès-Turell *et al.* 2005). These studies provide independent assessment of the sequence of polarity reversals across the Olenekian–Anisian boundary and are supplemented by bio-magnetostratigraphies through the remainder of the Middle Triassic (Muttoni *et al.* 2000, 2004*a*; Szurlies 2007; Hounslow *et al.* 2008*b*).

The Spitsbergen sections have a Spathian magnetostratigraphy that is the best constrained by an ammonoid biostratigraphy (Hounslow *et al.* 2008*b*). These data suggest that the lower Spathian is dominated by normal polarity, with a single reverse magnetozone (LT6r) detected at Milne Edwardsfjellet (MF1n.2r), Vikinghøgda (Hounslow *et al.* 2008*b*), and the Creek of Embry section on Ellesmere Island (i.e. CE7r). The data from Ellesmere Island suggest that the overlying reverse magnetozone (CE8r, equivalent to LT7r) has a more substantial thickness, which Hounslow *et al.* (2008*b*) correlated with a magnetozone within the lower part of the *Keyserlingites subrobustus* Zone in the Milne Edwardsfjellet and Vikinghøgda sections. It is not possible to confirm this pattern with data from the Hechuan and Guandao sections, because age dating of the Hechuan section is poor, and the lower Guandao magnetostratigraphy has many sampling gaps over this interval. The other reliable magnetostratigraphy at about this level appears to be that from the Moenkopi Group in northern Arizona, with a *Tirolites* ammonoid fauna (indicating Spathian), that succeeds beds with *Anasibirites* and *Wasatchites* faunas indicating the late Smithian (see discussion later; Fig. 4).

The uppermost Olenekian is characterized by a reverse magnetozone LT9r, which can be correlated between sections at Kçira (Muttoni *et al.* 1996*a*), Chios (Muttoni *et al.* 1995), Dęsli Caira (Grădinaru *et al.* 2007), Guandao (Lehrmann *et al.* 2006; Orchard *et al.* 2007), and Milne Edwardsfjellet (Hounslow *et al.* 2008*b*). Equivalents of magnetozone LT9r also appear to be present in the Hechuan section, if the conodonts *Neospathodus*

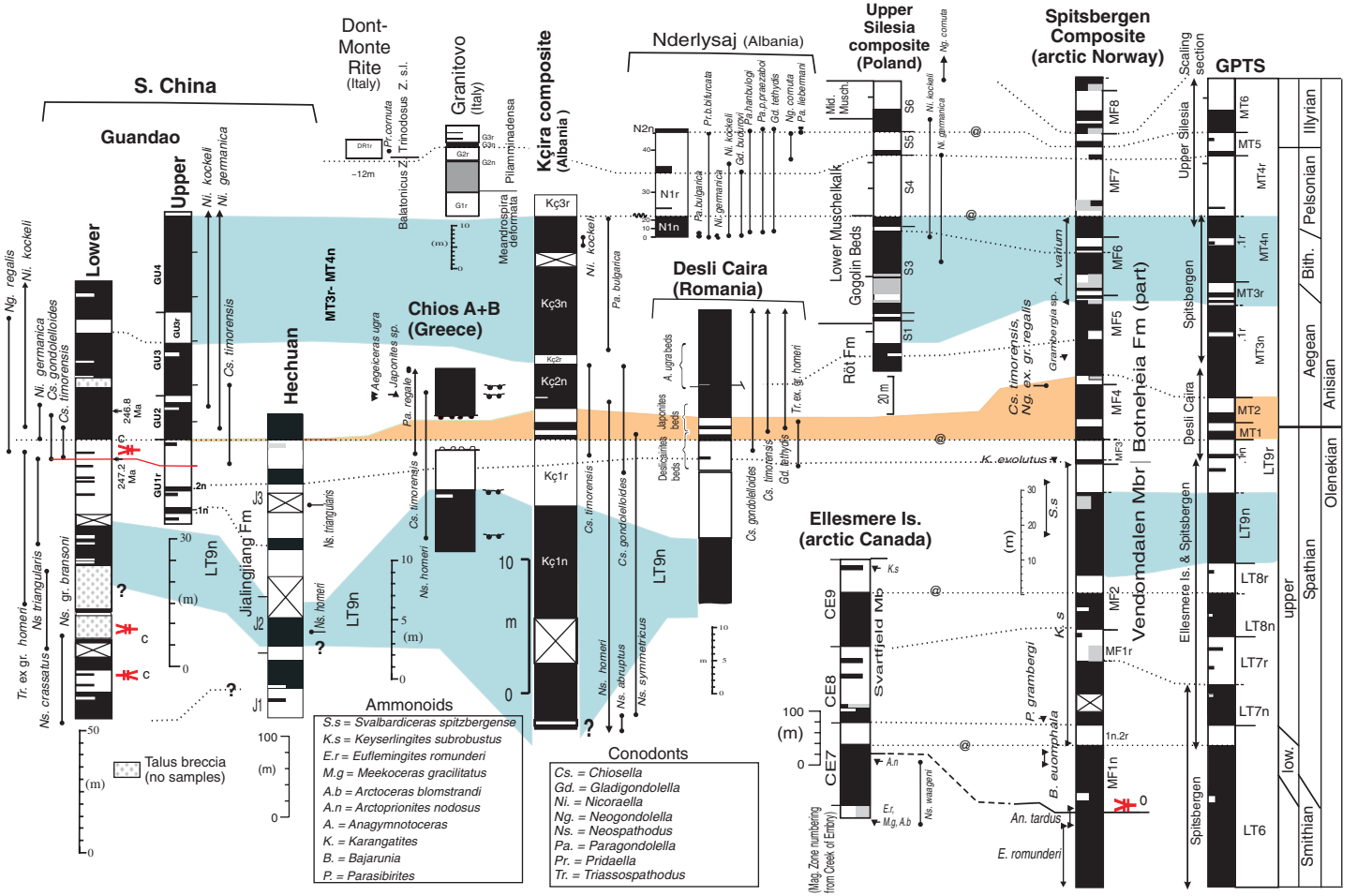

Fig. 3. Summary of the bio-magnetostratigraphy across the Olenekian–Anisian boundary. Section data from left to right: Guandao (Lehrmann *et al.* 2006; Orchard *et al.* 2007); Hechuan (Steiner *et al.* 1989); Chios (Muttoni *et al.* 1995); Dont-Monte Rite and Nderlysaj (Muttoni *et al.* 1998); Granitovo (Muttoni *et al.* 2000); Kçira (Muttoni *et al.* 1996*a*); Dęsli Caira (Grădinaru *et al.* 2007). Ellesmere Island composite is from the Smith Creek and Creek of Embry sections of Ogg & Steiner (1991) and Orchard (2008). Upper Silesia composite (Nawrocki 1997; Nawrocki & Szulc 2000); Spitsbergen composite (Hounslow *et al.* 2008*a*, *b*; Galfetti *et al.* 2007*b*). The base Anisian used is the first occurrence of *Cs. timorensis* in the Dęsli Caira section (Grădinaru *et al.* 2007). Thickness scales different for each section. See Figure 1 for key. Ammonoid genus abbreviations from Figure 2 and key.

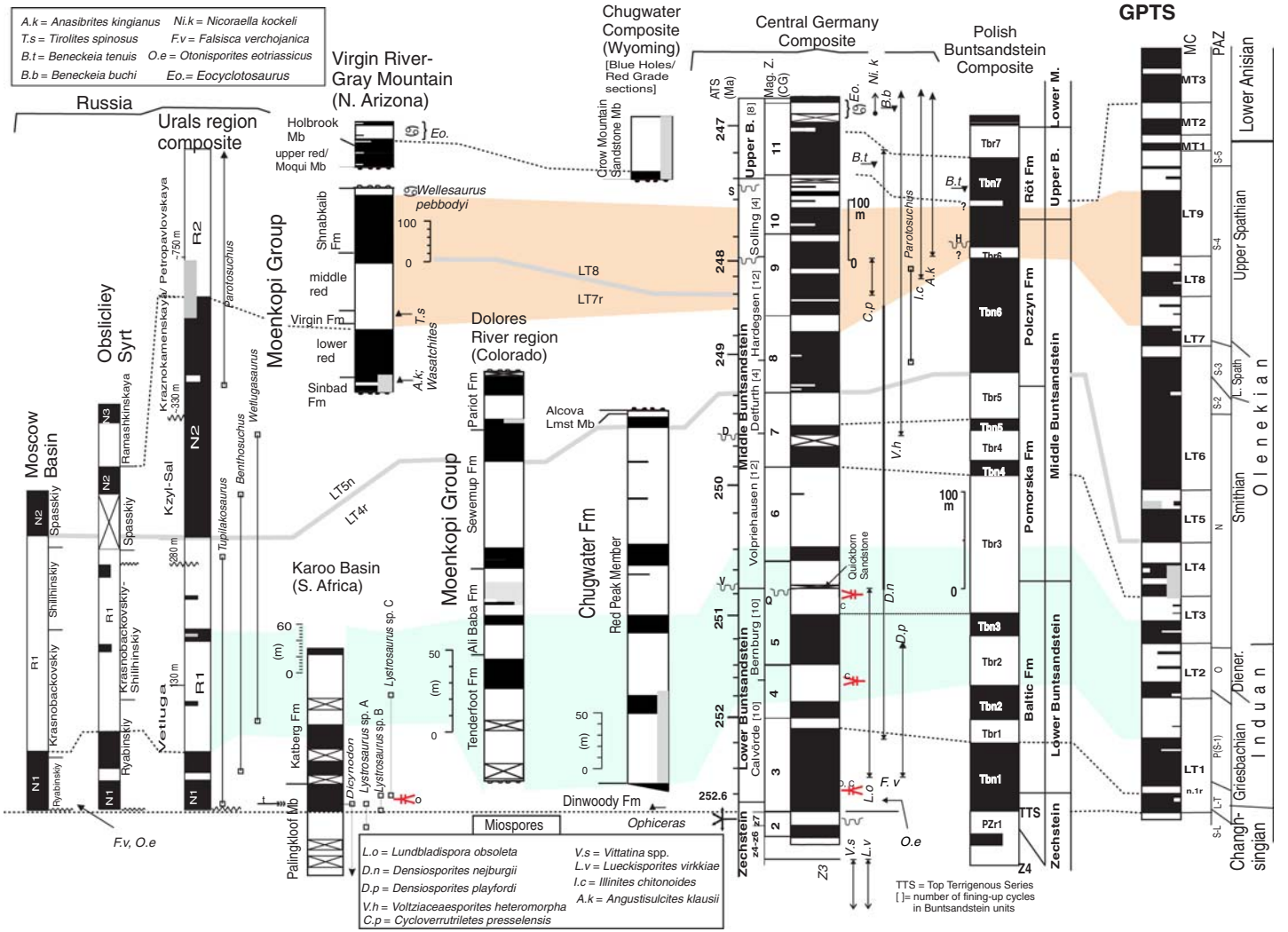

Fig. 4. Correlation between the magnetostratigraphy of non-marine Lower Triassic sections and the marine GPTS. Section data from left to right: Russia–columns left to right from Figures 16, 29 and 14 of Molostovsky (1983), vertebrate data from Figure 35 of Molostovsky (1983), two left columns have no vertical scale; Karoo Basin (Ward *et al.* 2005; Steiner *et al.* 2003); Virgin River–Gray Mountain (Bissell 1973; Steiner *et al.* 1993; Lucas *et al.* 2007*a*, *b*); Dolores River (Helsley 1969; Helsley & Steiner 1974); Chugwater composite (Boyd & Maughan 1973; Shive *et al.* 1984; Steiner 2006); Central German composite (Szurlies 2007; Hounslow *et al.* 2007*b*; Heite *et al.* 2005, 2006; Heunisch 1999; C. Huenisch pers. comm.); Polish Buntsandstein composite (Nawrocki 1997; Szurlies 2007). Thickness scales different for each section except for Moscow Basin and Obslicliey Syrt which have no scale. See Figure 1 for key. PAZ = Boreal miospore zonation (Hounslow *et al.* 2008*b*). MC = magnetochrons.

triangularis and *N. homeri* are used to constrain the correlation with the Guandao sections (Fig. 3). Reverse magnetozone LT9r has at least one normal submagnetozone (LT9r.1n), found at Milne Edwardsfjellet, Dęsli Caira and upper Guandao. There is some evidence of a second normal polarity submagnetozone within LT9r in the upper Guandao (i.e. GU1r.1n) and Hechuan sections, although the magnetostratigraphic data from both Guandao sections are 'noisy' and contain many 'half-bar' tentative submagnetozones. Based only on the match of magnetostratigraphic polarity pattern, Steiner (2006) suggested this interval (i.e. J3 interval of the Jialingjiang Fm.; Fig. 3) at Hechuan to be early Spathian, which is not supported by the presence of late Spathian conodont faunas.

Magnetochrons MT1 and MT2 characterise the Olenekian–Anisian transition and can be confidently correlated between Kçira, Dęsli Caira, and the Spitsbergen composite section (Fig. 3). The reverse and normal parts of these magnetochrons appear to vary somewhat in relative thickness, probably due to sedimentation rate and/or sampling density differences in the sections near the Olenekian–Anisian boundary (Fig. 3). Magnetochrons MT1 and MT2 were not detected at Chios due to faulting and the presence of a hiatus at the top of LT9r (Muttoni *et al.* 1996*a*). A predominantly normal polarity interval (MT3n to MT4n; Fig. 3) succeeded by a predominantly reverse polarity interval (MT4r to MT6r) are present in the Anisian, up to the Pelsonian and Illyrian substages. This pattern is observed at Kçira (Muttoni *et al.* 1996*a*), the Upper Silesia sections in Poland (Nawrocki & Szulc 2000; Nawrocki 1997), the Albanian Nderlysaj section, the Dont-Monte Rite section from the southern Italian Alps (Muttoni *et al.* 1998), as well as the Granitovo section from Bulgaria (Muttoni *et al.* 2000).

The sections at Guandao and Hechuan are difficult to relate to the Kçira and Dęsli Caira sections at the base of the Anisian, because MT1 and MT2 appear to be missing in the Chinese sections where MT3n (of Bithynian age, indicated by *Nicoraella germanica*) rests directly on LT9r (Fig. 3). The FO of *Ch. timorensis* also appears to be diachronous relative to the magnetostratigraphy (Hounslow *et al.* 2007*b*). The original correlation at Guandao proposed by Lerhmann *et al.* (2006) suggested that GU2n is the equivalent of MT4n (Fig. 3), a correlation that is driven by the conodont biostratigraphy but that largely ignores the magnetostratigraphy. They also suggested that submagnetozones GU1r.1n and GU1r.2n are the equivalent of MT1n and MT2n; this is only likely if order of magnitude fluctuations (on a metre to 10 m scale) in the sedimentation rate occurred, which is not evident in the lithology of these sections (cf. Lehrmann *et al.* 2006; Orchard *et al.* 2007). The problems of correlating Guandao to other sections also relate to the fact that *Nicoraella kockeli* and *Ni. germanica* appear very low in the section compared to the biomagnetostratigraphy in other sections. Both these conodonts appear to first occur high up in MT4n at Kçira and in the Upper Silesia composite section (Muttoni *et al.* 1996*a*; Nawrocki & Szulc 2000; Szurlies 2007).

Magnetostratigraphy of the nonmarine Lower Triassic

There is a close correspondence between the magnetostratigraphy of Lower Triassic marine successions and that from nonmarine successions, although correlation details are often debatable without other constraining stratigraphic data (Steiner 2006; Szurlies *et al.* 2003; Szurlies 2007; Fig. 4).

The extinction events in the latest Permian are well constrained in the Karoo Basin (South Africa) and probably the German Buntsandstein, by a negative $\delta^{13}C_{org}$ peak within what appears to be the lower part of the equivalent of LT1n (Fig. 4). In the Karoo Basin, constraint is also provided by the vertebrate extinction event indicated by the last occurrence of *Dicynodon* (Ward *et al.* 2005). In contrast to the marine extinction event, the tetrapod turnover is in the lowest part of LT1n rather than in the underlying reverse magnetozone. In the Buntsandstein successions of Germany and Poland, the terrestrial extinction event is not well marked; typically late Permian palynomorphs such as *Lueckisporites* sp. and *Vittatina* sp. are separated from typically Triassic forms such as *Lundbladispora* and *Densoisporites* by a barren interval, covering the Z4–Z7 part of the Zechstein and lowest part of the Lower Buntsandstein (Fijalkowska 1995; Heunisch 1999; Yaroshenko & Lozovsky 2004). The correlated proxy for the PTB in the Buntsandstein is the base of the *Falsisca verchojanica* conchostracan zone, coincident with a negative carbon isotopic peak (Kozur & Bachmann 2005). It may be that the major sediment provenance change in the Z7 cycle of the Zechstein (Hiete *et al.* 2005, 2006) is a proxy for the latest Permian extinction turnover (Fig. 4), in that the terrestrial extinction event may have radically affected sediment transport systems, through a decline in sediment trapping by vegetation loss (cf. Sephton *et al.* 2005).

Magnetozone LT1n is also apparent in the multiple-section data from the Moscow Basin and the Urals region (Molostovsky 1983, 1996; Taylor *et al.* 2009; Fig. 4). In the Wordie Creek Formation in Greenland, the tetrapods *Tupilakosaurus, Wetlugasaurus* and *Luzocephalus* co-occur with ammonoids that range in age from Griesbachian to early

Dienerian (Lozovsky 1998; Lucas 1999). Hence, the occurrence of these tetrapods in the Russian sections (shown under Urals composite in Fig. 4; Molostovsky 1983), allows an approximate correlation to the marine substages. The lowest parts of the Russian Vetluga successions also appear to preserve the Permian–Triassic transitional palynoflora that occurs below the PTB at other locations (Krassilov *et al.* 1999; Yaroshenko 2005), which appears to particularly characterise the lower part of magnetozone LT1n (Hounslow *et al.* 2008*a*; Metcalfe *et al.* 2009). In addition, Russian sections at Blyumental/Kou-Su, Chesnokovka and Buzuluk–Grchevka (three of the six sections contributing to the Urals composite; Molostovsky 1983), Boyevaya Gora, Tuyembetka (Taylor *et al.* 2009) show the equivalent of LT1n.1r within the LT1n magnetozone (Fig. 4).

Overlying magnetozone LT1n in marine sections is a mid Griesbachian to mid Smithian reverse-polarity dominated interval (LT1r to LT4r; Figs 1 & 2), which has clear parallels in the sections from Russia (Molostovsky 1983, 1996), the lower three-quarters of the Moenkopi Group in Colorado and the Chugwater Formation in Wyoming (Fig. 4). For many years the Russian composite magnetostratigraphy through this dominantly reverse polarity interval excluded several tentative short-duration normal polarity intervals (Molostovsky 1983; Lozovsky & Molostovsky 1993) detected in sections such as the Sosnovyiy/Vetlyanovskiy and Blyumental/Koya-Su gorges (Molostovsky 1983) and Sarysu (Khramov 1987), but these are now included (Molostovsky 1996). This uncertainty in part reflects the low palaeomagnetic sampling density used in some of these Russian sections and the common lack of proper demagnetisation.

It is debateable where the LT1r–LT4r reverse-polarity-dominated interval begins in the German and Polish Buntsandstein sections. Szurlies (2007) has suggested that CG3r/Tbr1 is the equivalent of LT1r (and CG5n/Tbn3 = LT3n), a correlation that is strongly influenced by the debateable age assignments of the Buntsandstein conchostracan fauna outlined by Kozur (1999) and Kozur and Bachmann (2005); particularly, the placement of the base of the Olenekian (Posenato 2009). The primary means of locating the Olenekian in the Buntsandstein is the stratigraphically 'close' occurrence of *M. truempyi* with the Olenekian ammonoid *Flemingites flemingianus* in Madagascar (Kozur & Bachmann 2005), suggesting that *M. truempyi* is indicative of the Olenekian. Stratigraphic 'closeness' is here not a strong case for dating in ill-documented successions fluctuating from marine to non-marine conditions. However, support for the correlations of Szurlies (2007) comes from Galfetti *et al.* (2007*a*), who suggest a duration of *c*. 1.4 Ma for the Induan, which is similar to the *c*. 1.2 Ma duration based on cyclostratigraphy, from the FO of *F. verchojanica* to the base of magnetozone CG5n (correlated to the base of LT3n by Szurlies 2007).

However, a number of problems remain with the correlations of Szurlies (2007). Firstly the cyclostratigraphy from the Calvörde Fm. suggests that CG3r is exceptionally brief at some *c*. 50 ka when other sections show a longer relative duration, and an interval occupied by some *c*. 1.5 ammonoid zones (Figs 1 & 4). Secondly the dominance of normal polarity (i.e. interval CG3n/Tbn1 to CG4n/Tbn2) in the Calvörde Fm. is more compatible with this interval being equivalent to LT1n (Fig. 4). Thirdly, others have determined different numbers of cycles in the units of the Buntsandstein (Geluk & Röhling 1999), which may reflect the non-basin centre focus of some of the sections of Szurlies (2007). For these reasons an alternative, more likely correlation, is suggested in Figure 4.

The upper boundary of the reverse-polarity dominated interval from LT1r to LT4r probably represents the top of GC7r/Tbr5 in the Buntsandstein and an equivalent level in other sections (Fig. 4). Alternatively, Szurlies (2007) has correlated LT5n with GC7n which seems less likely, considering that normal polarity dominates from LT5n in Boreal sections (e.g. Fig. 2), and LT4n is most likely correlated to the Tbn4–Tbn5 interval in the Polish Middle Buntsandstein, which Szurlies (2007) has correlated to CG7n. Unfortunately, there appears to be no useful palynology from the Lower Buntsandstein, Volpriehausen or Detfurth formations to confirm or deny these two sets of proposed correlations (C. Heunisch, pers. comm. 2008; Fig. 4).

The normal-polarity-dominated interval from LT5n to LT9n has clear parallels in the normal-polarity-dominated upper parts of the Middle Buntsandstein (Fig. 4). However, a confident match in the relative thicknesses of the three reverse magnetozones between the GPTS and the central German Buntsandstein composite is not visually convincing. The thickest reverse magnetozone in the marine composite is LT7r from the Boreal sections (Figs 3 & 4), which either represents magnetozone GC8r or GC9r. Similarly, magnetozone LT7r appears equivalent to the reverse magnetozone spanning most of the 'middle red' and Virgin Formation in the northern Arizona composite. The ammonoids *Anasibrites kingianus* and *Wasatchites* sp. from the Sinbad Fm. of the Moenkopi Group in Utah indicate the upper Smithian (Lucas *et al.* 2007*b*). However, the magnetostratigraphy for the Sinbad Formation in the Virgin River-Gray Mountain composite (Fig. 4) is derived from a thinner succession of the Sinbad Formation at Lees Ferry, farther south in Arizona (Steiner *et al.* 1993), so it

is not clear that the ammonoids and magnetostratigraphy represent exactly the same levels. The ammonoid *Tirolites spinosus* collected from low in the Virgin Formation near the Utah–Arizona border (Bissell 1973) is good evidence of the Spathian.

Like the Moenkopi Group in northern Arizona, sections from the Urals appear to display a particularly thick representation of LT7r. In the Russian sections, the correlation is supported by the co-occurrence of the tetrapod *Parotosuchus* with the Spathian ammonoid *Tirolites cassianus*, within the Bogdinskaya Member at Bolshoye Bogdo Mountain, in the Cis–Caspian depression (Molostovsky 1983, 1996; Molostovsky *et al.* 1998). Evidently, the Spathian displays particularly dramatic interregional changes in sedimentation rates that are probably the reason for such large variations in the relative thickness of these reverse magnetozones.

Szurlies (2007) has outlined the reasoning for correlating the German Buntsandstein magnetozone GC10r to the equivalent of LT9r in the Kçira section. The Anisian ammonoids *Beneckeia tenuis*, *B. buchi*, and *Balatonites ottonis* and the conodont *Nicoraella kockeli* occur in the Upper Buntsandstein and provide reliable biostratigraphic ties to the marine Middle Triassic (Fig. 4). This is supported by the presence of *Stellapollenites thiergartii* in a miospore assemblage from the Upper Buntsandstein (Visscher *et al.* 1993; Heunisch 1999). In addition, the FO of *Illinites chitonoides*, within the upper part of the Hardegsen Fm., has an equivalent FO in the Svalis-4 palynostratigraphic assemblage zone of Vigran *et al.* (1998). In the Vikinghøgda section, this FO is within the lower part of LT9n (Mørk *et al.* 1999; Hounslow *et al.* 2008*a*; Figs 3 & 4).

Anisian–Ladinian and Ladinian–Carnian boundaries

The magnetostratigraphy and biostratigraphy of the Anisian–Ladinian boundary successions from the Tethyan marine realm have received considerable attention in recent years (Fig. 5). The first attempts at magnetostratigraphy were carried out in the latest Anisian Prezzo Limestone and Buchenstein Beds in the Southern Italian Alps, which are largely overprinted by excessive heating, caused by the Late Eocene–Early Oligocene Adamello batholith (Muttoni & Kent 1994). Hints of primary magnetic components that survived this overprinting were tentatively isolated and assigned to a latest Anisian interval of normal polarity with a duration of perhaps one million years and spanning the Trinodosus Zone and most of the overlying *Lardaroceras*-bearing beds (Muttoni & Kent 1994 and references therein). Subsequent analyses of coeval sections from the Southern Alps (Muttoni, unpublished data) revealed, however, that these magnetic components may in fact be pre-folding remagnetizations of about Late Cretaceous age. Attention was therefore paid to the island of Hydra (Greece) where Angiolini *et al.* (1992) identified the Anisian–Ladinian boundary in the 24-m-thick Aghia Triada section, from the nodular, reddish Han-Bulog Limestone. The first results (Muttoni *et al.* 1994) yielded a consistent magnetostratigraphic pattern relating to a late Anisian–Ladinian conodont biostratigraphy, in which the FO of *Pridaella trammeri* (= *Gondolella trammeri*, = *Paragondolella trammen*) was used as a proxy of the Anisian–Ladinian boundary, results which were refined by Muttoni *et al.* (1997, 1998) (Fig. 5). Confirmation of the Aghia Triada results were sought in the coeval 60-m-thick Vlichos section on Hydra (Muttoni *et al.* 1997, 1998, 2000), but there tectonic complexities disrupted the original stratigraphic continuity, confirmed later by field inspection (GM), and the Vlichos data are therefore excluded from this compilation.

In the late 1990s, attention moved back to the Alps, and specifically to the Dolomites in Italy and the Northern Calcareous Alps in Austria. Magnetostratigraphic investigations on biostratigraphically-dated limestones and radiometrically-dated tuffs in the Buchenstein Beds from the Dolomites started with the Anisian–Ladinian boundary interval in the Frötschbach section (Muttoni *et al.* 1996, 1997), and were followed by parallel studies on the nearby coeval Pedraces and Belvedere sections (Brack & Muttoni 2000). A satisfactory magnetostratigraphic correlation was obtained on laterally traceable limestone and volcaniclastic intervals, showing the high degree of reproducibility of the magnetic polarity fingerprint through the Anisian–Ladinian boundary interval, throughout much of the Buchenstein Basin of the Dolomites (Fig. 5). In the Northern Calcareous Alps, Austria, Gallet *et al.* (1998) produced a magnetostratigraphy from four coeval sections (Mendlingbach 1 and 2, and Gamsstein East and West), which again showed a consistent polarity pattern across the Anisian–Ladinian boundary interval constrained by conodont biostratigraphy (Fig. 5).

A breakthrough study was carried out on the *c.* 110 m-long Seceda core, drilled by the Geological Survey of Bolzano in 1998 at Mount Seceda in the northwestern Dolomites (Brack *et al.* 2000). With over 90% recovery, this core offered a unique opportunity to reconstruct, in stratigraphic continuity, a portion of the Middle Triassic pattern of polarity reversals (Muttoni *et al.* 2004*a*). The Seceda core spans a complete succession of Buchenstein Beds with limestone and associated 'Pietra Verde' volcaniclastic layers, which were correlated to the nearby Seceda outcrop section with associated radiometric

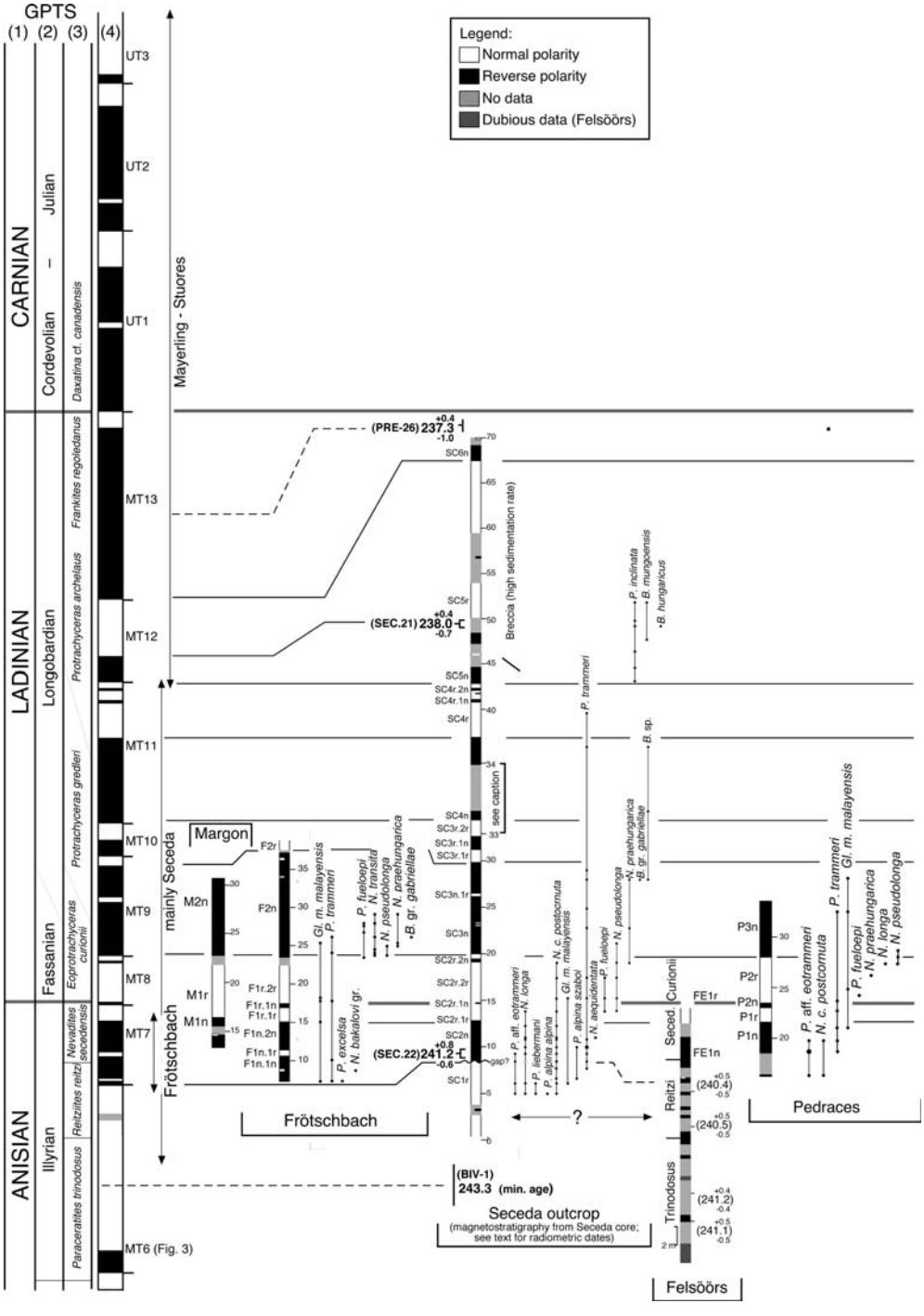

Fig. 5. Summary of the bio-magnetostratigraphy across the Anisian–Ladinian and the Ladinian–Carnian boundary. Section data from left to right: Margon–Val Gola (Gialanella *et al.* 2001 reinterpreted by Brack *et al.* 2001), Frötschbach (Muttoni *et al.* 1996*b*, 1997), Seceda (Muttoni *et al.* 2004*a*), Felsöörs (Márton *et al.* 1997; Vörös *et al.*

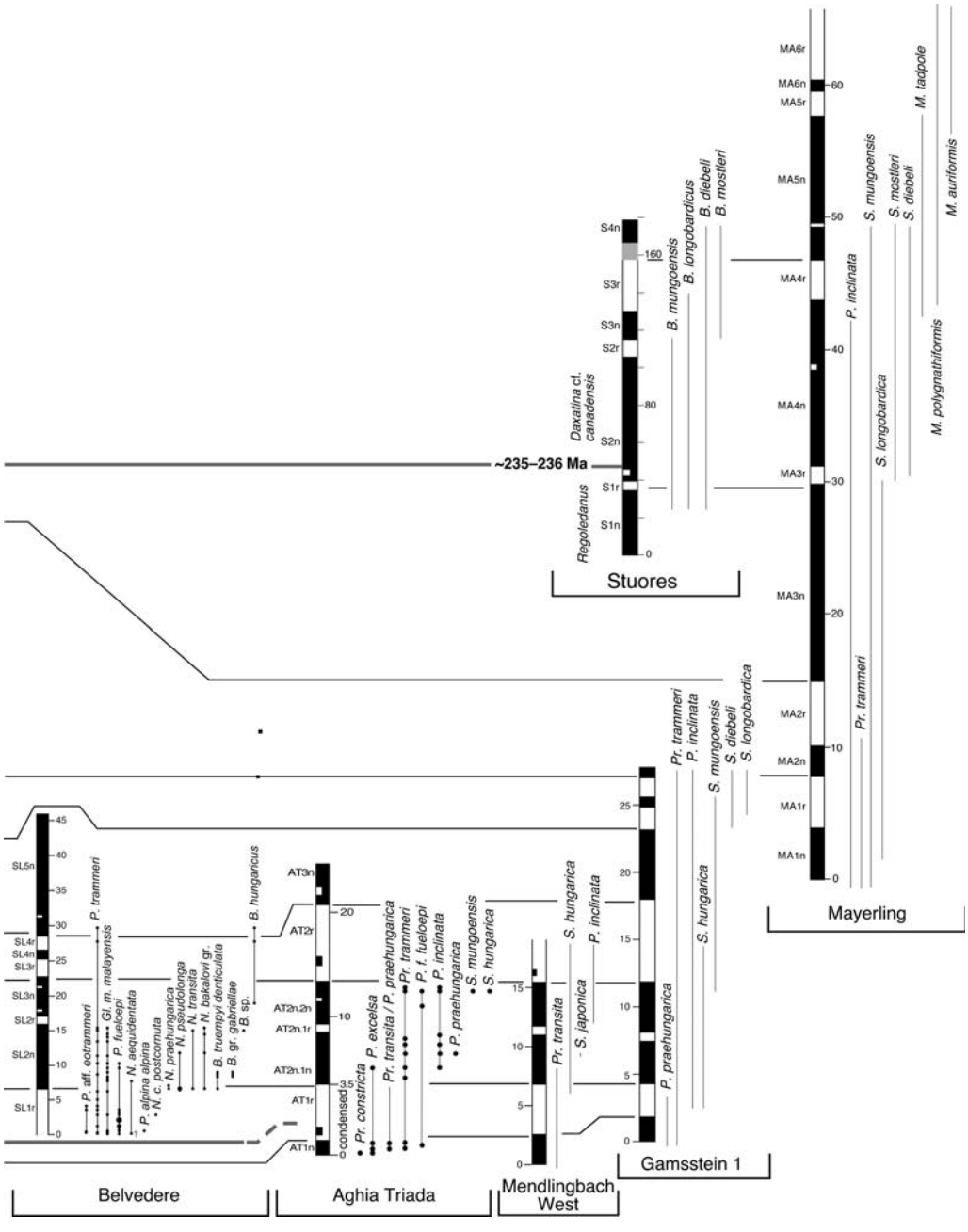

Fig. 5. (*Continued*) 2003), Pedraces and Belvedere (Brack & Muttoni 2000), Aghia Triada (Muttoni *et al.* 1998 and references therein), Mendlingbach West, Gamsstein 1, Mayerling (Gallet *et al.* 1998), and Stuores (Broglio Loriga *et al.* 1999). Stratigraphic depth of sections expressed in metres. In left panel: (1) Middle Triassic stages, (2) Middle Triassic sub-stages, (3) ammonoid zonation and (4) composite magnetostratigraphic sequence arranged in magnetochrons MT6 to UT3. Thickness scales different for each section. See Figure 1 for key. Conodont genera: B., *Budurovignathus*; Gl., *Gladigondolella*; M., *Metapolygnathus*; N., *Neogondolella*; P., *Paragondolella*; Pr., *Pridaella*; S., *Sephardiella.* [for Frötschbach, Seceda, Pedraces, and Belvedere, see compilation in Muttoni *et al.* (2004*a*); for Aghia Triada, Mendlingbach West, Gamsstein 1, and Mayerling, see compilation and notes in Muttoni *et al.* (2000); for Stuores, see Broglio Loriga *et al.* (1999)].

and biostratigraphic age data. Two ash layers located in the 'Lower Pietra Verde' and 'Upper Pietra Verde' intervals in the Seceda outcrop section yielded U–Pb ages of 241.2 (+0.8–0.6) Ma (SEC.22) and 238.0 (+0.4–0.7) Ma (SEC.21), respectively (Fig. 5; Mundil *et al.* 1996; Brack *et al.* 1996; updated by Brack *et al.* 2007), indicating an average sediment accumulation rate of *c.* 10 m/ma. More recently, Brack *et al.* (2007) obtained a new radiometric age estimate (BIV-1) from the Upper Anisian Bivera Fm. at Monte Bivera (Trinodosus Zone) based on 12 individual zircon ages ranging from 243.3 Ma to 241.6 Ma. Because of Pb loss and the mild leaching step, Brack *et al.* (2007) interpreted the age of 243.3 Ma to be the minimum age for sample BIV-1, which should fall just below the base of the Seceda magnetostratigraphic sequence within the Trinodosus Zone (Fig. 5).

Magnetostratigraphic data from Seceda were correlated with data from the coeval Frötschbach, Pedraces, and Belvedere sections, as well as Margon-Val Gola from Trentino (Gialanella *et al.* 2001; reinterpreted by Brack *et al.* 2001), and a satisfactory correlation was obtained (Fig. 5). The magnetozone interval SC2n–SC3n at Seceda corresponds with F1n–F2n at Frötschbach, P1n–P3n at Pedraces, SL1r–SL2n at Belvedere and M1n–M2n at Margon–Val Gola, and with similar patterns at Aghia Triada, Mendlingbach West, and Gamsstein 1. The magnetostratigraphic data from the Felsöörs section, Hungary (Márton *et al.* 1997; Vörös *et al.* 2003) show normal polarity through the F1n magnetozone ranging through the Reitzi Zone, whereas at Seceda the same ammonoid zone is found reverse in magnetozone Sc1r (correlated to Seceda following Brack *et al.* 2005; Fig. 5). However, the Felsöörs section contains major sampling gaps due to thick tuff layers that mostly did not yield samples. Also, in the sampled layers some palaeomagnetic data yielded dubious directions, with in two cases normal and reverse polarity reported from the same level (limestone bed 99B and tuff layer between limestone beds 101 and 102; Fig. 5; Márton *et al.* 1997). These dual-polarity problems presumably indicate the existence at Felsöörs of unresolved normal polarity overprints; therefore, we maintain SC2r as the main late Anisian reverse polarity zone corresponding to MT6r in the GPTS (Fig. 5). Support for this stance comes from the nonmarine studies in the Anisian, which suggest additional detail in MT6r, which is not seen in any marine section over this interval (see below; Fig. 6).

The magnetostratigraphic correlations between Seceda, Frötschbach, Pedraces, Belvedere, Margon-Val Gola, Aghia Triada, Mendlingbach West, and Gamsstein 1 allow the generation of a reference magnetostratigraphy with the U–Pb dates from Seceda and Monte Bivera and the ancestor–descendant faunal associations of paragondolellids, neogondolellids (conodonts) and ammonoids, present in different degrees of preservation, in all correlated sections from the Dolomites. This augments the numerical and biostratigraphic definition of the Anisian–Ladinian GSSP, at the FO of *Eoprotrachyceras curionii* (base of the *E. curionii* Zone), 5 m above the base of the Buchenstein Beds in the Bagolino section of northern Italy (Brack *et al.* 2005). This level can been traced to metre level 83.7 in the Seceda core corresponding to metre level 14.7 in the Seceda outcrop section, very close to the base of reversal SC2r.2r and *c.* 5 m above the level with a U–Pb age of 241.2 (+0.8–0.6) Ma (Muttoni *et al.* 2004*a*; Brack *et al.* 2005; Fig. 5).

The magnetostratigraphy of the Ladinian–Carnian boundary interval has not been as extensively studied as the Anisian–Ladinian boundary. Gallet *et al.* (1998) presented the magnetobiostratigraphy of the Mayerling pelagic limestone section from the Northern Calcareous Alps, which contains a rich conodont fauna encompassing the uppermost Anisian to Lower Carnian. The >60 m-thick Mayerling section, with 14 well-defined polarity intervals spanning a succession of age-diagnostic conodont events, is currently the most continuous marine section studied through the Ladinian–Carnian boundary interval (Fig. 5). The 160 m-thick Stuores section in the Dolomites, with higher sediment accumulation rates, covers a shorter time interval compared to Mayerling and has been extensively studied for biostratigraphy and magnetostratigraphy (Broglio Loriga *et al.* 1999). Stuores is the ratified GSSP for the base of the Carnian, with the FO of the ammonoid *Daxatina canadensis* as the basal Carnian marker (Mietto *et al.* 2007), with a succession of polarity reversals that can confidently be correlated to Mayerling (Broglio Loriga *et al.* 1999).

The only other section studied for magnetostratigraphy across the Ladinian–Carnian boundary is from Spitsbergen (Arctic Norway), in which a large part of the late Ladinian is missing near the boundary (Hounslow *et al.* 2007*a*). The boundary interval is dated by sporadic occurrences of conodonts and ammonoids. The magnetostratigraphy confirms that the correlated base of the Carnian occurs within the stratigraphic gap, below the traditional Boreal Carnian (at the base of the *Stolleyites tenuis* ammonoid biozone).

Age calibration of the Middle Triassic GPTS

According to Hinnov & Goldhammer (1991) and Preto *et al.* (2001) the Latemar carbonate platform

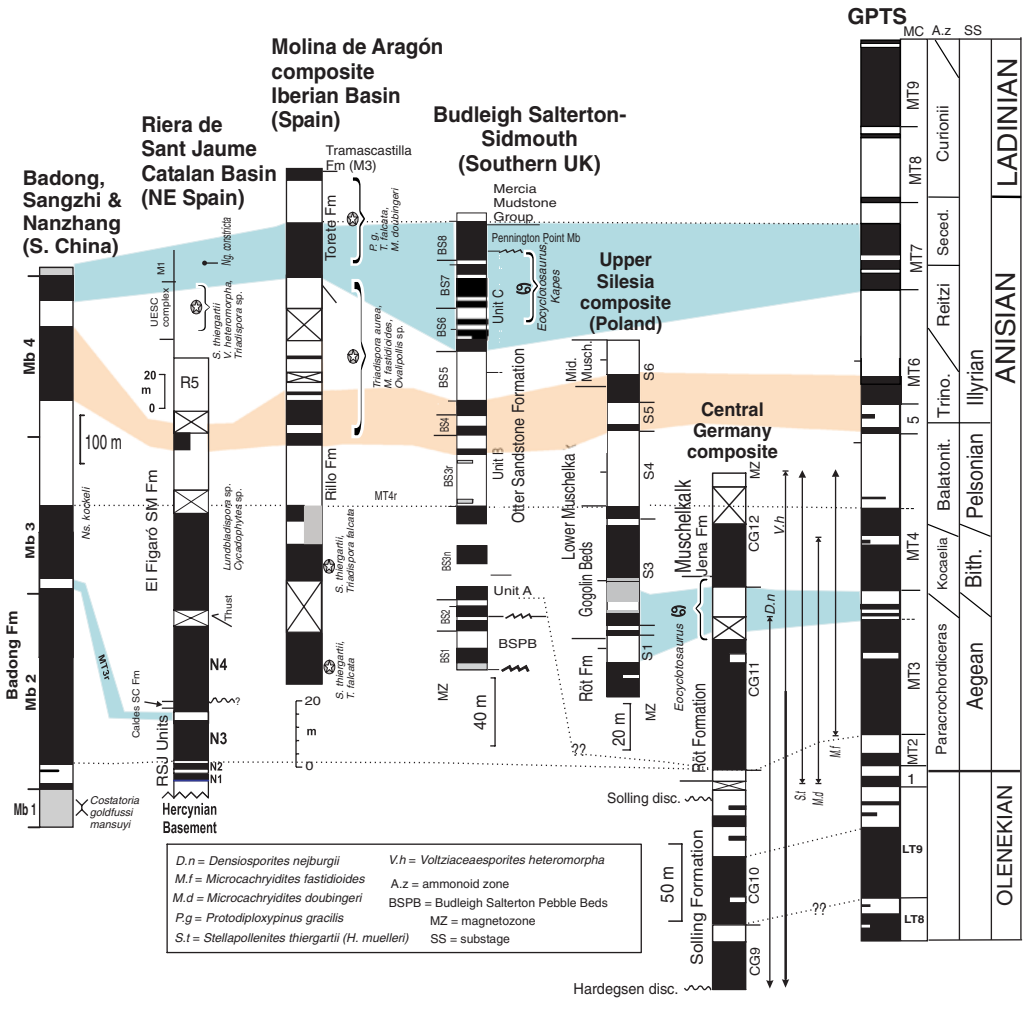

Fig. 6. Summary of the bio-magnetostratigraphy from non-marine Middle Triassic sections, and possible correlations to the marine bio-magnetostratigraphy. Section data from left to right: Badong, Sangzhi and Nanzhang (Huang & Opdyke 2000); Riera de Sant Jaume (Arche *et al.* 2004; Dinarès-Turrell *et al.* 2005); Molina de Aragòn (Rey *et al.* 1996; Arche *et al.* 2004; Dinarès-Turrell *et al.* 2005); Budleigh Salterton-Sidmouth (Benton 1997; Hounslow & McIntosh 2003); Upper Silesia (Nawrocki & Szulc 2000; Nawrocki 1997); Central Germany (Heunisch 1999; Szurlies 2007; Hounslow *et al.* 2007*b*, C. Heunisch, pers. comm. 2008). Thickness scales different for each section. See Figure 1 for key. GPTS column from Figures 3 and 5.

in the Dolomites, which has a platform interior characterized by a *c*. 470 m-thick lagoonal succession consisting of *c*. 600 shallowing-upward cycles can be attributed to a 9–12 Ma record of precessional forcing of sea level change. However, U–Pb dating of zircons from volcaniclastic layers within the Latemar succession (from top to bottom: LAT–32, 241.7 $+1.5/-0.7$, Mundil *et al.* 2003; LAT-30: 241.2 $+0.7/-0.6$, Mundil *et al.* 2003; re-dated to 242.8 $\pm$ 0.2 Ma, Brack *et al.* 2007; LAT-31: 242.6 $\pm$ 0.7 Ma, Mundil *et al.* 2003), and the correlative basinal Buchenstein Beds (SEC.22, SEC.21; see above) suggests that the Latemar cycles only span at most a few million years (Brack *et al.* 1996; Mundil *et al.* 1996, 2003). Similarly, Kent *et al.* (2004) showed that most of the Latemar succession is of normal magnetic polarity, which together with biostratigraphic and lithostratigraphic correlations between beds in the adjacent Buchenstein Basin, suggested that the bulk of the Latemar platform deposition was coeval with magnetozone SC2n at Seceda

(MT7n in GPTS; Fig. 5). Kent and coworkers therefore concluded that magnetozone SC2n (at Seceda) and the time-equivalent Latemar deposition, in fact, had a duration an order of magnitude less (*c*. 1 Ma). Therefore, straightforward interpretation of the U–Pb age model for Buchenstein deposition, and the magnetostratigraphy through the Secedensis Zone are internally consistent, and opposed to the cyclostratigraphic analyses of the Latemar succession by Hinnov & Goldhammer (1991) and Preto *et al.* (2001). We, therefore, like Kent *et al.* (2006), abandon the long duration hypothesis for the Latemar succession based on cycle counting, accepting U–Pb zircon dates as the main constraints on the duration of the Middle Triassic.

Like the problematic magnetostratigraphy from the Felsöörs section, the multigrain U–Pb-zircon ages of Pálfy *et al.* (2003) are distinctly too young compared to the radiometric age data from the Dolomites. As reported by Brack *et al.* (2005), these ages overlap within error with respect to SEC22 from Seceda. The younger mean values of the seemingly stratigraphically older layers at Felsöörs may be due to the (unresolved) contribution from grains affected by lead loss.

Robust age constraints on the composite Middle Triassic GPTS are based on the U–Pb age data of BIV-1 (minimum age of 243.3 Ma) from the Trinodosus Zone at Monte Bivera, and SEC.22 (241.2 +0.8–0.6 Ma) and SEC.21 (238.0 +0.4–0.7 Ma) from the Buchenstein Beds as discussed above, with the 241.2 Ma age closely associated with the Anisian–Ladinian boundary at the base of the Curionii Zone (Brack *et al.* 2005). A Ladinian–Carnian boundary at *c*. 235 Ma (Brack *et al.* 2005) to *c*. 236 Ma (Fig. 5) is derived from U–Pb data and field observation from the upper Ladinian granites at Predazzo in the Southern Alps. This intrusion, dated at 237.3 (+0.4/−1.0) Ma (sample PRE-26, Fig. 5; Brack *et al.* 1996), post-dates the Ladinian Buchenstein Beds in which the youngest U-Pb age is 238.0 (+0.4/−0.7) (Mundil *et al.* 1996), and pre-dates sediments of the Wengen Volcanosedimentary Group (S. Cassiano Formation), which toward its top contains the Ladinian–Carnian boundary at Stuores (Broglio Loriga *et al.* 1999). Therefore, the Ladinian–Carnian boundary should be just a few Ma younger than *c*. 237 Ma (i.e. *c*. 235–236 Ma; Fig. 5). With a Ladinian–Carnian boundary at *c*. 235.5 Ma and an Anisian–Ladinian boundary at *c*. 241 Ma, the Ladinian Stage is *c*. 5.5 my duration. The composite sequence of magnetic polarity reversals outlined here encompasses 34 magnetozones spanning the late Anisian–early Carnian that are arranged in a sequence of magnetochrons from MT6 to UT3 (Fig. 5).

Magnetostratigraphy of the nonmarine Middle Triassic

As with the Lower Triassic, a substantial number of studies of the Anisian have been made in nonmarine successions (Fig. 6). The generally distinctive character of the Anisian, with a lower part dominated by normal polarity followed by dominantly reverse polarity in the mid Anisian, generally allows for a confident correlation with the Middle Triassic GPTS (Fig. 6); correlations largely follow those used by the original authors. Magnetochrons MT1 and MT2 are probably present in the Riera de Sant Jaume section (Catalan Basin), and the Middle–Upper Buntsandstein boundary interval (uppermost Solling Fm. to lowermost Röt Fm.) from the Germanic Basin (Fig. 6; Dinarés-Turell *et al.* 2005; Szurlies 2007). One of the features at this level, which supports the central German Basin magnetostratigraphic correlation in Figure 6, is the appearance of *Triadispora* sp., which in the Milne Edwardsfjellet section is consistently present from magnetochron MT2 (Hounslow *et al.* 2008*b*), the approximate correlative level at which this pollen becomes common to abundant in the German Upper Buntsandstein. Magnetochron MT2 also appears to have been detected by Huang & Opdyke (2000) in the Badong Fm. in South China (Fig. 6). Correlations to the GPTS from the Upper Silesia (Poland) and the central Germany composites, over the magnetochron interval MT3 and MT4, are constrained by a variety of ammonoid, conodont, and basin-wide borehole geophysical log data (Kozur 1999; Szurlies 2007).

Studies in the Catalan and Iberian basins can be correlated to the Triassic GPTS, and are largely constrained by a fragmentary palynostratigraphy at the formation level, a regional lithostratigraphy, and overlying marine sediments (Muschelkalk facies) that have generally better

Fig. 7. Summary of the bio-magnetostratigraphy across the Carnian–Norian boundary. Section data from left to right: Guri Zi (Muttoni *et al.* 2005); Pizzo Mondello (Muttoni *et al.* 2004*b*); Silická Brezová (Channell *et al.* 2003); Bolücektasi Tepe (Gallet *et al.* 1992, 2000*a*); Kavaalani (Gallet *et al.* 2000*a*). Stratigraphic thickness of sections in meters. In right panel, composite GPTS arranged in magnetochrons UT19 to UT14 with indication of the position of the conodont-based Carnian–Norian boundary (provisionally placed at the FOs of *Metapolygnathus echinatus* and *M. parvus* at Pizzo Mondello; Nicora *et al.* 2007) and U–Pb radiometric age estimate of magnetochron UT10n from Furin *et al.* (2006). Thickness scales different for each section. See Figures 1 and 5 for key.

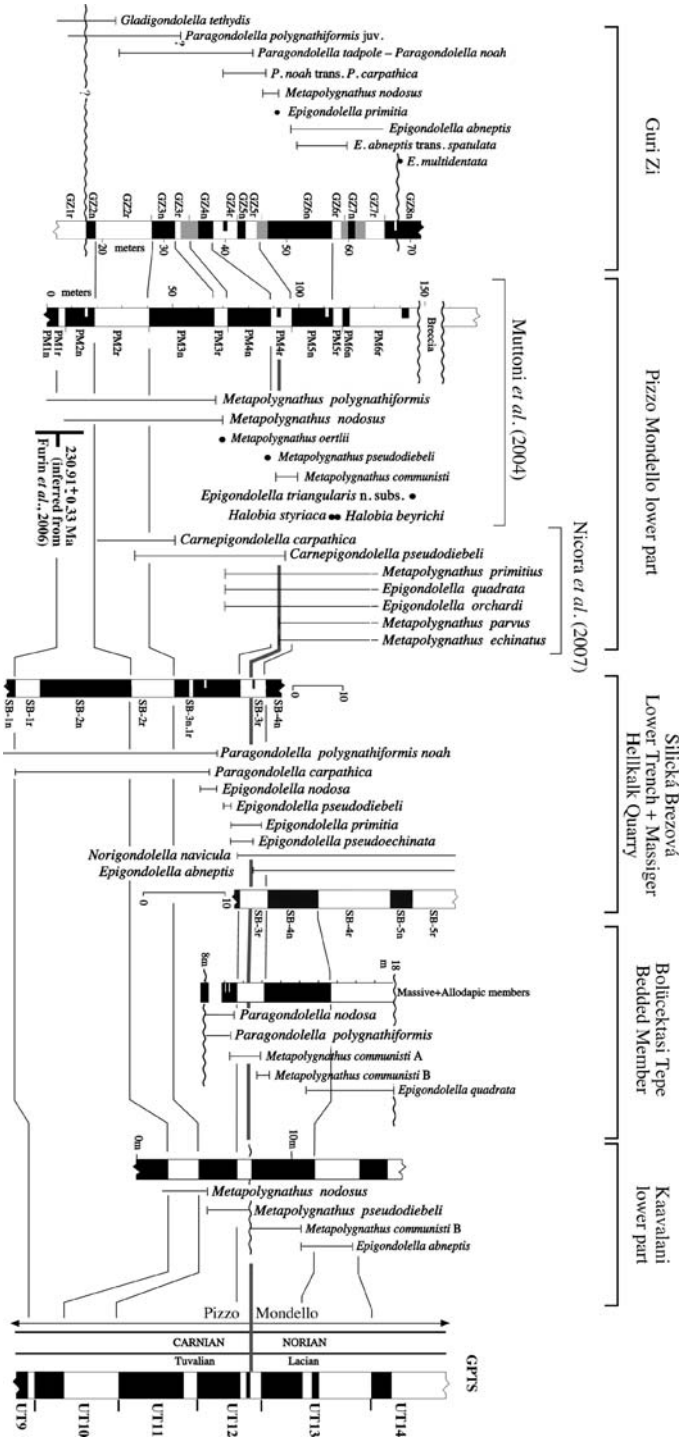

Fig. 7. *Continued*.

age control in the Ladinian (Arche *et al.* 2004; Dinarés-Turell *et al.* 2005). Those for the Otter Sandstone Fm. in the Budleigh Salterton to Sidmouth section (UK) are age constrained by tetrapods, including *Kapes* and *Eocyclotosaurus*, which indicate the Anisian Perovkan land-vertebrate faunachron (Benton 1997; Hounslow & McIntosh 2003). There are indications from the sections at Molina de Aragon and Budleigh Salterton-Sidmouth that the magnetostratigraphic pattern may contain additional short normal magnetozones over the MT4r to MT6r interval that have not been well characterised in the marine sections shown in Figure 5. The character of the polarity pattern during magnetochrons MT5n–MT6r may therefore be better represented by data from these non-marine sections.

Carnian–Norian boundary

Candidate sections for defining the base Norian GSSP are Black Bear Ridge (Williston Lake, British Columbia, Canada; e.g. Orchard *et al.* 2001, 2007) and Pizzo Mondello (Sicily, Italy; Muttoni *et al.* 2004*b*; Nicora *et al.* 2007). Proposed guide forms for the base of the Norian are favoured as the FO of *Metapolygnathus echinatus* at Black Bear Ridge (Orchard 2007) or the FO of *M. echinatus* and *Metapolygnathus parvus* at Pizzo Mondello (Nicora *et al.* 2007).

Integrated magnetostratigraphic and biostratigraphic studies across the Carnian–Norian boundary in the marine realm started in the early 1990s with the pioneering work of Gallet *et al.* (1992) on the 73 m thick, upper Carnian–upper Norian Bolücektasi Tepe section in Turkey. The basal bedded limestone member, 10 m thick in this section, yielded a sequence of polarity reversals covering the stratigraphic range of *Metapolygnathus communisti*, which was used by these authors as a proxy for the base Norian (Fig. 7). Nearly 10 years lapsed until the broadly coeval, *c*. 55 m-thick, Kavaalani section, in Turkey, was published (Gallet *et al.* 2000*a*). In its basal 10 m, this section extends through the Carnian–Norian boundary interval and has age diagnostic conodonts that can be correlated to the Bolücektasi Tepe section (Fig. 7). A magnetostratigraphic investigation of Middle and Upper Triassic fossiliferous limestones cropping out around Williston Lake in British Columbia (Canada), particularly at Black Bear Ridge, was attempted but the strata were found to be remagnetized during the early stages of Laramide folding in the Cretaceous (Muttoni *et al.* 2001*a*). The first magnetostratigraphic and biostratigraphic study of an expanded (*c*. 150 m-thick) Carnian–Norian boundary section at Pizzo Mondello in Sicily was published by Muttoni *et al.* (2001*b*). Muttoni *et al.* (2004*b*) refined these initial findings, focusing primarily on the distribution of *Metapolygnathus communisti* and additional key species for the definition of the boundary (Fig. 7), and extended the analysis upwards through an additional *c*. 280 m of strata previously attributed to the late Norian by Gullo (1996). In a recent re-analysis of the Pizzo Mondello section (after Muttoni *et al.* 2004*b*), Nicora *et al.* (2007) established the FOs of *Metapolygnathus echinatus* and *M. parvus* in sample NA36, 8 m above *Gonionotites maurolicoi* and 7 m below a Norian radiolarian assemblage, with the conodont marker considered as suitable to define the base of the Norian Stage.

The Silická Brezová section, Slovakia is a composite compiled from seven separate but partially overlapping sections correlated by means of lithostratigraphic marker beds, biostratigraphy and magnetostratigraphy, and straddling *c*. 120 m of upper Carnian–upper Norian strata (Channell *et al.* 2003). Magnetostratigraphic and biostratigraphic data through the Carnian–Norian boundary were obtained from the Lower Trench, and Massiger Hellkalk Quarry sections (boundary used by these authors at FO of *Norigondolella navicula:* Fig. 7). Similarly, a magnetostratigraphy and conodont biostratigraphy through the Carnian–Norian boundary interval was obtained from the 70 m-thick limestone section at Guri Zi in northern Albania (Muttoni *et al.* 2005), with the boundary placed between the LO of *Metapolygnathus nodosus* (= *Epigondolella nodosa*) and the FO of *Epigondolella abneptis*.

All these sections through the Carnian–Norian boundary interval contain a similar assemblage of conodonts within a framework of broadly correlative magnetozones (Fig. 7), although Guri Zi is affected by variations in sediment accumulation rates associated with turbiditic deposition of calcarenites (Muttoni *et al.* 2005). These biomagnetostratigraphies define a sequence of 16 magnetozones (organized in magnetochrons UT9 to UT14) of late Carnian (Tuvalian) to early Norian (Lacian) age, with the Carnian–Norian boundary provisionally placed at the FOs of *Metapolygnathus echinatus* and *M. parvus* at Pizzo Mondello (Nicora *et al.* 2007) (Fig. 7).

A U–Pb zircon date of 230.91 $\pm$ 0.33 Ma from late Carnian limestones in southern Italy (Furin *et al.* 2006; Fig. 7), are tentatively correlated with the lower part of the Silická Brezová and Pizzo Mondello sections using a constraining conodont biostratigraphy (Fig. 7). A consensus (detailed below) has been reached for correlating the conodont-based Carnian–Norian boundary interval into the Newark Supergroup astrochronological polarity timescale (APTS) (Kent *et al.* 1995; Kent

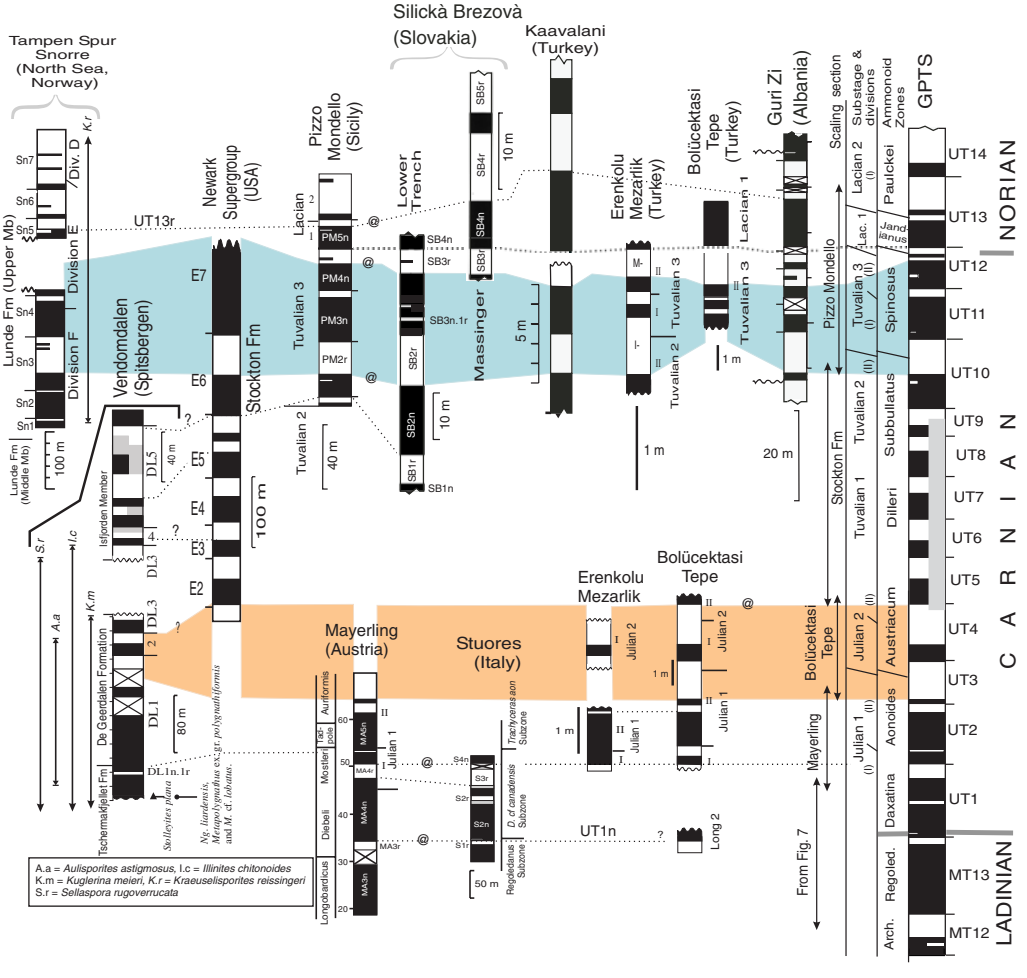

Fig. 8. Summary magnetic polarity pattern for the Carnian. Section data from left to right: Tampen Spur, Snorre (Nystuen *et al.* 1989; Eide 1989; Bayer & Lundschien 1998); Vendomdalen (Hounslow *et al.* 2008*b*); Newark Supergroup (Kent *et al.* 1995; Le Tourneau 1999); Pizzo Mondello (Muttoni *et al.* 2004*b*); Mayerling (Gallet *et al.* 1998), Silická Brezová (Channell *et al.* 2003); Stuores (Broglio Loriga *et al.* 1999); Kavaalani (Gallet *et al.* 2000*a*); Erenkolu Mezarlik and Bolücektasi Tepe (Gallet *et al.* 1992, 2000*a*); Guri Zi (Muttoni *et al.* 2005). Julian, Tuvalian Lacian are substages and their subdivisions detailed in Gallet *et al.* (1992) and Krystyn *et al.* (2002). Thickness scales different for each section. See Figures 1 and 3 for key.

& Olsen 1999; Olsen & Kent 1999), suggesting that the Carnian–Norian boundary falls within the interval *c*. 227–228 Ma (Muttoni *et al.* 2004*b*).

The Carnian GPTS

The Carnian GPTS is in part built by extending those sections which cover the Ladinian–Carnian and Carnian–Norian boundary intervals, and using additional sections which are less well-dated (Fig. 8). The upwards extension from the Ladinian–Carnian boundary is largely achieved using the Bolücektasi Tepe section (Gallet *et al.* 1992; Gallet *et al.* 2002*a*), which appears to correlate approximately to the palynologically-dated lower Carnian section from the De Geerdalen Fm. in Spitsbergen (Hounslow *et al.* 2007*a*). These Spitsbergen sections may extend upwards into the middle or upper Carnian in the overlying Isfjorden Member (Fig. 8), but the palynological data is not sufficiently clear to confidently distinguish Carnian from Norian (Hounslow *et al.* 2007*a*).

Likewise, the polarity pattern from the Carnian–Norian boundary can be extended down into UT9 (i.e. equivalent to SB1n) using the Lower Trench

section at Silická Brezová (Fig. 8). The nonmarine sections from the Stockton Fm. (Newark Supergroup: Kent *et al.* 1995), and the Upper Lunde Fm. E/F divisions at Snorre (Bayer & Lundschien 1998) can be confidently matched to those marine sections from the boundary interval (Muttoni *et al.* 2004*b*). The Snorre composite through the Upper Lunde Fm. E and F divisions is placed in the upper Carnian, since the FO of *Kraeuselisporites reissingeri* (associated with *Ovalipollis pseudoalatus* in the Snorre assemblages; Eide 1989) is in the Tuvalian (Roghi 2004). In the Snorre area the *K. reissingeri* assemblage overlies more diverse assemblages in the lowest part of the Upper Lunde and Middle Lunde (Eide 1989; Nystuen *et al.* 1989) containing *Enzonalasporites vigens*, *Granuloperculatipollis rudis*, *Triadispora obscura* and *O. pseudoalatus*, amongst others. Comparison to ammonoid-dated sections from the Alps (Roghi 2004) suggests these assemblages are approximately Tuvalian in age, supporting the suggested magnetostratigraphic correlation.

The magnetostratigraphic match of the Stockton Fm. to the marine sections suggests that magnetochrons E2 to E5 probably extend into the Dilleri Zone (Tuvalian–1; Fig. 8). These correlations are weakly supported by the polarity pattern from the Spitsbergen Isfjorden Mb, in which magnetozone interval DL4 to DL5 appears to approximately match the Stockton Fm. E3 to E5 magnetozones (Fig. 8). Supporting data to confirm these correlations (or any other) in the middle Carnian are absent, and for this reason, the magnetochron UT5 to UT9 interval is displayed as half grey to reflect this.

The Norian GPTS

The correlation of marine sections to the Newark APTS suggests that the Norian is the longest stage in the Triassic and as such merits special attention in terms of its magnetic polarity pattern. Key marine sections for the construction of a Norian GPTS are Bolücektasi Tepe, Kavaalani and Kavur Tepe from Turkey (Gallet *et al.* 1992, 1993, 2000*a*), Scheiblkogel, Austria (Gallet *et al.* 1996), Silická Brezová, Slovakia (Channell *et al.* 2003), and Pizzo Mondello, Sicily (Muttoni *et al.* 2004*b*). The GPTS and biostratigraphically-constrained polarity succession through the Norian has been much debated, and different solutions proposed by Krystyn *et al.* (2002); Channell *et al.* (2003), Hounslow *et al.* (2004), Muttoni *et al.* (2004*b*) and Gallet *et al.* (2007).

Bolücektasi Tepe, Kavur Tepe, Scheiblkogel, and Kavaalani were correlated by Krystyn *et al.* (2002) by fitting magnetic polarity zones into a correlation scheme based on conodont zonations. These conodont zonations (shown in Fig. 9) are related to age, largely through co-linked studies of ammonoids and conodonts in Timor (Indonesia) and some other Tethyan locations (Krystyn *et al.* 2002). This biozone framework was used to construct a composite sequence of magnetic polarity reversals, scaled to equal conodont biozone duration, tied to the numerical calibrations of the Upper Triassic stages of Gradstein *et al.* (1994). Subsequently, Gallet *et al.* (2003) used the same composite succession with updated (and more appropriate) numerical constraints, to construct a tentative uppermost Carnian–Norian biozone-scaled GPTS.

Muttoni *et al.* (2004*b*) attempted to construct the uppermost Carnian–Norian magnetic polarity reversal pattern by adopting the 430 m-thick Pizzo Mondello section as a reference section that was correlated to the *c.* 140 m composite stratigraphy of the Silická Brezová section. The Muttoni *et al.* (2004*b*) solution resulted in a somewhat lower number of Norian normal and reverse polarity zones (20) compared to Krystyn *et al.* (2002) (25), or the even higher number (31) that arises if the new Sevatian to Rhaetian data of Gallet *et al.* (2007) are taken into account. This discrepancy arose from the different procedures adopted for correlation, and the differing recognition of missing time in the sections. For example, Muttoni *et al.* (2004*b*) attempted to establish statistical correlations by using magnetostratigraphic fingerprints in a one-to-one magnetozone matching approach, assuming, as a first order approximation, that stratigraphic thickness is a linear function of time. Priority was given to expanded and lithologically homogeneous sections such as Pizzo Mondello that tend to minimize the problematic occurrence of stratigraphic or fault gaps (although high

Fig. 9. Summary magnetic polarity pattern for the Norian, based on inter-section correlation. Relative thickness of magnetozones determined by the correlation grid (horizontal lines), with the scale provided by the appropriate section indicated on the right (see text for details). Section data from left to right: Scheiblkogel (Gallet *et al.* 1996); Kavur Tepe (Gallet *et al.* 1993, 2000*a*); Pizzo Mondello (Muttoni *et al.* 2004*b*); Kavaalani (Gallet *et al.* 2000*a*); Silická Brezová (Channell *et al.* 2003); Bolücektasi (Gallet *et al.* 1992, 2000*a*). Thickness scales different for each section. See Figure 1 for key. Conodont zonation and sub-stage divisions of Gallet *et al.* (1992, 2000*a*) and Krystyn *et al.* (2002). Substage divisions: Tu–3 = Tuvalian–3; La–1, La–2, La–3 = Lacian 1, 2 and 3; Al–1, Al–2, Al–3 = Alaunian 1, 2 and 3; Sev–1, Sev–2 = Sevatian 1 and 2. C.bZ = conodont biozone. Conodont biozonation on the Silická Brezová column from Channell *et al.* (2003). Sections segmented according to the hiatus and faulting information given by authors.

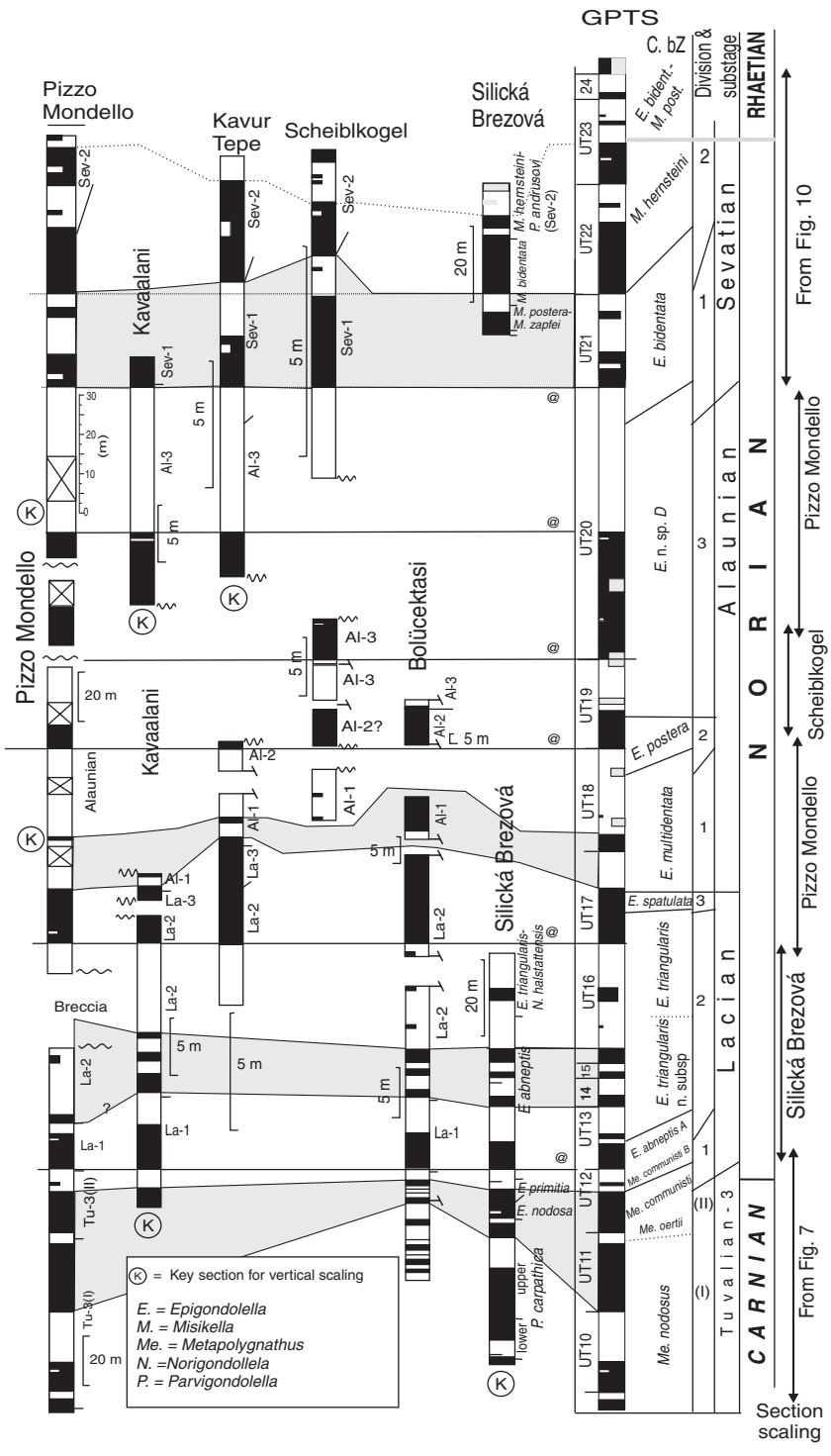

Fig. 9. *Continued*.

accumulation rate is no guarantee of completeness). However, these sections, with high accumulation rates, tend to be less fossil-rich than condensed sections with lower accumulation rates, so biostratigraphic completeness cannot be demonstrated. Fossiliferous sections were preferred by Krystyn *et al.* (2002) using first-order correlation by matching key conodont ranges from individual sections, allowing a multiple-section composite to be constructed. However, these fossiliferous sections are frequently condensed with stratigraphic gaps (indicated by hardgrounds) and faults, which need to be included in the correlation modelling. For example, the middle Norian (Alaunian) part of the composite bio-magnetobiostratigraphic sequence of Krystyn *et al.* (2002) has been constructed by piecing together magnetozones from individual sections segmented by hiatus and fault gaps.

The GPTS equal-duration biozone concept (Krystyn *et al.* 2002; Gallet *et al.* 2003) has restricted value for marine to nonmarine correlations, which has in part lead to the continuing debate about the Norian. Instead of utilising the equal-duration biozone concept, we use an approach that consists of constructing a composite bio-magnetostratigraphy (Fig. 9), scaled to section thickness, using the following principles:

- Data from the thickest sections is used to scale the composite, because such sections are likely to provide the best magnetostratigraphic detail.
- A magnetostratigraphic correlation grid is constructed, based on the correlation between section magnetozones, guided by the biostratigraphic framework.
- The correlation grid constrains the amount of vertical stretching which can be applied to the section data, and provides limits on the relative thickness of the magnetozones in the composite, by minimising the amount of missing section at stratigraphic or fault gaps.
- Section repetition across faults is only detectable by the conodont biozone framework (some details in Krystyn *et al.* 2002), which for most of these Norian sections, has only been published in summary form.

If sedimentation rates were constant in each section, but differed between sections, vertical stretching of scales would produce a perfect horizontal correlation grid, but since sedimentation rates tend to vary within sections, the correlation grid lines can be inclined (e.g. see magnetozone UT17r in Fig. 9). In addition, a limited number of anchor correlation lines exist, which constrain the amount of vertical stretch (shown as '@' in Fig. 9). This process is similar to that used in constructing spliced-core composite sections, typically used on IODP cores (Pälike *et al.* 2005), which are based on the principles of graphic correlation (Shaw 1964).

The least constrained part of this procedure centres on the disconformities and faulted-boundaries that fragment the section magnetostratigraphy (Fig. 9). The most parsimonious solution is one that minimises the likely missing intervals (Shaw 1964; Edwards 1989). The best constrained parts of the GPTS composite are in the lower Norian, where sections, without apparent breaks, provide good inter-section relative thickness constraints (Fig. 9). The Norian–Rhaetian boundary interval is also well constrained, although some problems remain (see Fig. 10 and later). The Pizzo Mondello section is particularly important for scaling the entire Norian composite. The least constrained part of the GPTS is in the middle Norian (Alaunian), where the composite magnetozones UT18 and UT19 are not well constrained in relative thickness. For example, UT19n is only constrained in the incomplete data at Pizzo Mondello, and UT19r is only constrained in the lower part of the fragmented Scheiblkogel section (Fig. 9). Similarly, the Alaunian-1 part of the Bolücektasi Tepe section may represent a younger sub-magnetozone in UT18r, rather than being equivalent to UT18n. Likewise, the relative thickness of UT20n depends much on the amount missing and unsampled at Pizzo Mondello. The solution presented is similar to the 'equal biozone' GPTS of Gallet *et al.* (2007) but scaled to section thickness. This difference is particularly noticeable for the Lacian-3 interval whose only thickness constraint is *c.* 2 m of strata at the Kavur Tepe section (Fig. 9).

The Norian–Rhaetian boundary

The GSSP section for the base of the Rhaetian is likely to be in Austria in the Steinbergkogel section A, at the FO of *Misikella posthernsteini* (Krystyn *et al.* 2007*a*). The conodont biostratigraphy, palynology and magnetostratigraphy of this and nearby sections have been studied in detail (Krystyn *et al.* 2007*a*). These demonstrate the similarity in conodont ranges and magnetostratigraphy of the Steinbergkogel sections, and previously published magnetostratigraphic data from Scheiblkogel (Austria), Pizzo Mondello (Sicily), Silická Brezová (Slovakia) and the Bolücektasi Tepe, Kavaalani, Kavur Tepe and Oyuklu sections in Turkey (Fig. 10). Overall, there is good agreement between the various magnetostratigraphies and biostratigraphies from the sections covering the Norian–Rhaetian boundary interval (Fig. 10). The Pizzo Mondello section has the largest sedimentation rate and most detailed magnetostratigraphy in the latest Norian, Steinbergkogel provides

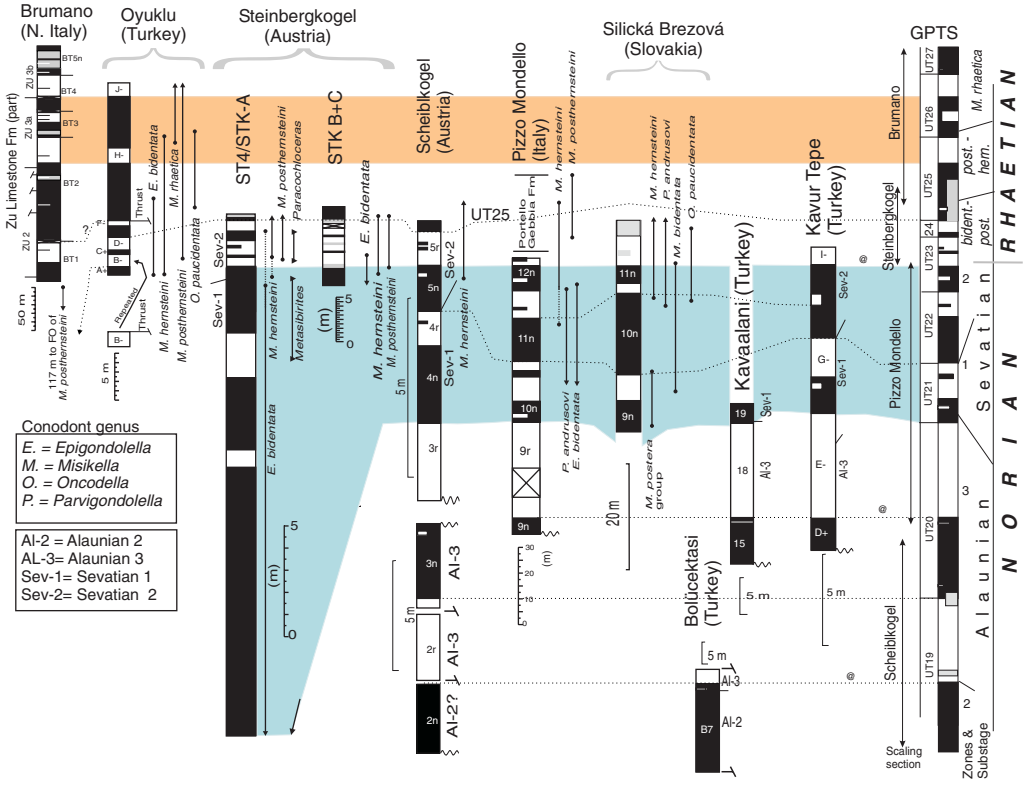

Fig. 10. Summary magnetostratigraphy of the Norian–Rhaetian boundary. Section data from left to right: Brumano (Muttoni *et al.* 2010); Oyuklu (Gallet *et al.* 2007); Steinberkogel (Krystyn *et al.* 2007*a*); Scheiblkogel (Gallet *et al.* 1996); Pizzo Mondello (Muttoni *et al.* 2004*b*); Silická Brezová (Channell *et al.* 2003); Bolücektasi (Gallet *et al.* 1992, 2000); Kavaalani (Gallet *et al.* 2000*a*); Kavur Tepe (Gallet *et al.* 1993, 2000*a*). Sections segmented according to the hiatus and faulting information given by authors. Thickness scales different for each section. See Figure 1 for key.

the most detail in the earliest Rhaetian, and Brumano (Italy) in the remainder of the Rhaetian (Muttoni *et al.* 2010).

An important constraint in these correlations near the Norian–Rhaetian boundary is the FO of *Misikella hernsteini* (i.e. base of Sevatian 2) in normal magnetozone UT22n in most sections. At Pizzo Modello, this is in PM11n, whereas at Steinbergkogel this event appears to be slightly higher (Fig. 10). A second constraint is the relatively thick reverse magnetozone in the uppermost Alaunian (i.e. in *Epigondolella* n. sp *D* Zone, Alaunian 3) at Kavur Tepe (E−), Kavaalani (K18), and Pizzo Mondello (PM9r), which confidently defines the magnetozone UT20r in the GPTS (Figs 9 & 10). The solution for the Silická Brezová to Pizzo Mondello correlation (Fig. 10) is that used by Gallet *et al.* (2007) and Muttoni *et al.* (2004*b*).

Channell *et al.* (2003) originally suggested correlating magnetozones SB9n at Silická Brezová with 3n at Scheiblkogel, B7n at Bolüceltasi Tepe, KV15 at Kavaalani, and D+ at Kavur Tepe (Fig. 10). These correlations seem less likely, because they would require: (a) substantial within-section changes in the sedimentation rate at the Silická Brezová section; (b) absence of reverse magnetozones within SB10n in the Silická Brezová upper trench section (which was densely sampled); and (c) because it violates the biostratigraphic age constraints at Bolücektasi Tepe. Signs of condensation are however seen in the lower part of the Silická Brezová upper trench section, where it is most reddened and clasts (possibly reworked) occur in the lowest 5 m (Channell *et al.* 2003).

An alternative correlation solution for Scheiblkogel is to correlate magnetozones 4n with PM11n at Pizzo Mondello and the underlying 3r with PM10r, because there is no direct evidence of the Alaunian 3 zone at Scheiblkogel (Fig. 10; Gallet *et al.* 1996). However, the correlation in Figure 10 is compatible with the data from Kavur Tepe in which *Epigondolella* (= *Mockina*) *bidentata*

ranges into the E− magnetozone, suggesting that the base of the Sevatian 1 zone (*E. bidentata* biozone) extends into the top of UT20r (Figs 9–10).

The Oyuklu section is complicated by a thrust near the base of the section, which repeats the overlying B− magnetozone within the occurrence range of *E. bidentata* and *M. hernsteini*. Gallet *et al.* (2007) correlated magnetozone PM12n at Pizzo Mondello with magnetozone E+ in the Oyuklu section (Fig. 10), but a more likely correlation is with A+ at Oyuklu (Fig. 10). This solution is more compatible with the FO of *M. posthernsteini* that occurs within the B− magnetozone at Oyuklu and within the Portella Gebbia Fm. (above the Cherty Limestone and magnetostratigraphy) at Pizzo Mondello (Gullo 1996; Fig. 10). The solution of Gallet *et al.* (2007) would have placed the correlated FO of *M. posthernsteini* within PM11r at Pizzo Mondello, which is incompatible with the biostratigraphy.

Magnetozone UT25n in the composite GPTS is poorly represented in the section data (Fig. 10); its base appears to be represented in the Steinbergkogel and Oyuklu sections (i.e. E+ at Oyuklu) and the upper part at Brumano (BT1 to BT2n) and Oyuklu (G+). The mid parts of UT25n appear to be represented at Brumano and Oyuklu, but the most continuous record in the Oyuklu section is disrupted by a thrust that forms the upper boundary to the apparent reverse sub-magnetozone (equivalent to BT1r? in the Brumano section) within UT25n. A section with a more complete magnetostratigraphy over this interval would improve the polarity pattern within magnetochron UT25n.

Norian–Rhaetian nonmarine studies and correlations to Tethyan sections

The most important nonmarine magnetozone succession through the Norian is from the Newark Supergroup (Kent *et al.* 1995; Fig. 11). The magnetostratigraphy through the Lockatong Fm. of the Newark Supergroup is confirmed by studies from the Dan River–Danville basins in the eastern USA (Kent & Olsen 1997; Fig. 11). The magnetostratigraphy through the Chinle Group of the southwestern USA (Molina-Garza *et al.* 1996) is of insufficient sampling resolution to confirm the Newark Supergroup magnetostratigraphy, but appears to confirm the general reverse polarity character of the E8r to E12r and E17r to E20r intervals (Fig. 11). The polarity pattern through the lower and middle parts of the Passaic Fm. is confirmed by data from the Fundy Basin (Kent & Olsen 2000), St Audrie's Bay (Hounslow *et al.* 2004) and the Lunde and Lewis formations in the northern North Sea (Hounslow *et al.* 1995; Bayer & Lundschien 1998; Bergan 2005; Fig. 11). The dominantly reverse polarity interval E18r to E20r in the Newark Supergroup is confirmed by data from the Fundy Basin, the Chinle Group, St Audries Bay and the Upper Lunde Fm. (Kent & Olsen 2000; Molina-Garza *et al.* 1996; Hounslow *et al.* 2004; Bergan 2005; M. Bergan pers. comm. 2008). Likewise, the collection of poorly-dated UK and Norwegian non-marine sections and cored intervals appears to confirm the general character of the E14r to E18n interval from the Newark Supergroup (Fig. 11). The polarity character of the E13 to E14 interval is so far not strongly supported by data from any area outside the eastern USA.

The correlation of the Newark Supergroup magnetostratigraphy to the numerous Norian–Rhaetian marine sections has attracted considerable debate, with alternative solutions offered by Gallet *et al.* (1993, 2000*a*, 2007), Krystyn *et al.* (2002), Channell *et al.* (2003), Muttoni *et al.* (2004*b*, 2010) and Hounslow *et al.* (2004). The fundamental reason for such continued debate is the absence of any strong supporting biostratigraphic information that allows detailed correlation of the Newark Supergroup with successions outside the eastern USA. Palynofloral zonations and land-vertebrate faunachrons provide mostly ambiguous, low resolution correlations (Cornet 1993; Fowell & Olsen 1993; Lucas & Tanner 2007). Correlations are also hampered by the somewhat ambiguous middle Norian magnetostratigraphy from the marine sections, which are fragmented by disconformities and faulting (e.g. Fig. 9). These debates have focused on two issues, firstly the location of the Carnian–Norian boundary in the Newark Supergroup and secondly the position and extent of the Rhaetian in the Newark Supergroup APTS.

The Carnian–Norian boundary in the Newark Supergroup

Muttoni *et al.* (2001*b*) sought a match of the magnetozone patterns across the conodont-based Carnian–Norian boundary at Pizzo Mondello and the palynology-based Carnian–Norian boundary in the Newark Supergroup, which suggested a correlative Carnian–Norian boundary within Newark magnetozones E14n–E16n and hence above the palynological Carnian–Norian boundary as originally placed, within Newark magnetozone *c*. E13 (Kent *et al.* 1995). Krystyn *et al.* (2002) used data from Bolücektasi Tepe, Kavur Tepe, Scheiblkogel and Kavaalani to construct an equal biozone upper Carnian–upper Norian composite which was then correlated to Newark Supergroup magnetozones E3–E22 with the Carnian–Norian boundary placed in magnetozone E7 (Fig. 8), using only pattern matching criteria. Channell *et al.* (2003)

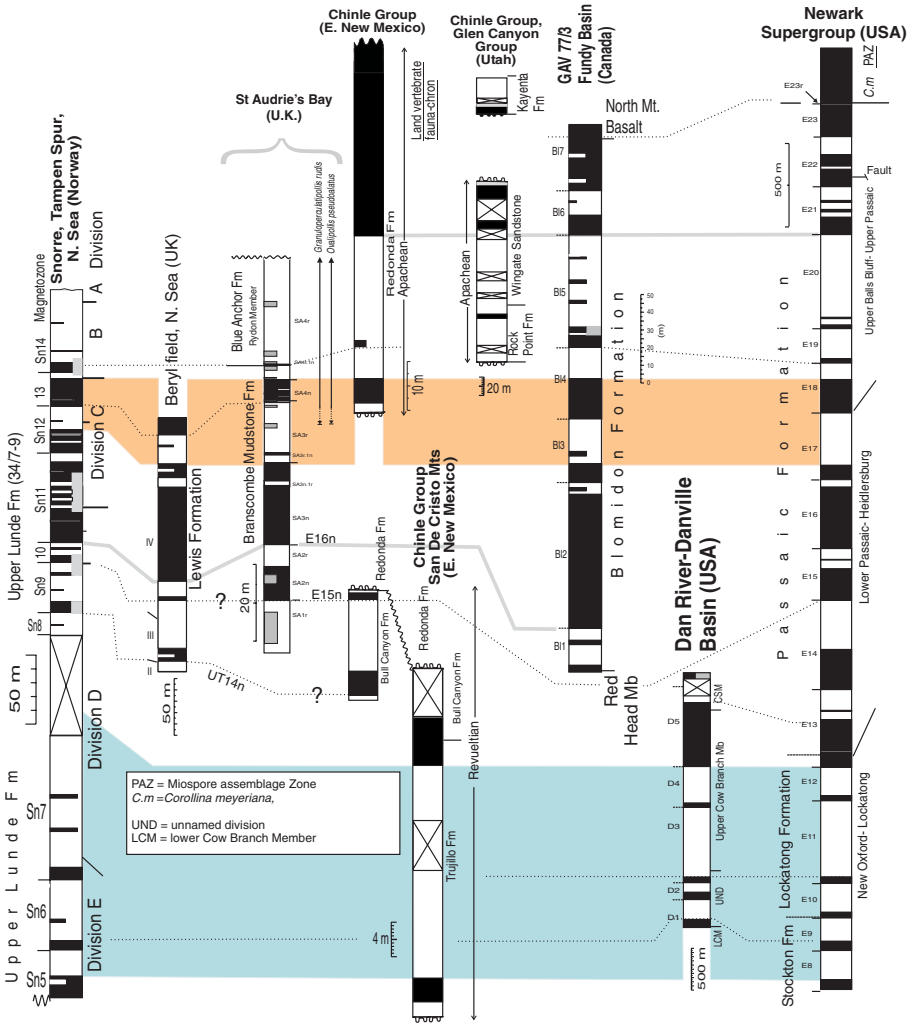

Fig. 11. Summary of non-marine magnetostratigraphic studies of the Norian–Rhaetian. Section data from left to right: Snorre, Tampen Spur (Nystuen *et al.* 1989; Bayer & Lundschien 1998; Bergan 2005; M. Bergan, pers. comm. 2008); Lewis Fm., Beryl area (Hounslow *et al.* 1995; Bond 1997); St Audrie's Bay (Hounslow *et al.* 2004); Chinle group (Reeve & Helsley 1972; Molina-Garza *et al.* 1996; Lucas 1999); Fundy Basin (Kent & Olsen 2000); Dan River-Danville basins (Kent & Olsen 1997); Newark Supergroup, Newark Basin (Kent *et al.* 1995). Thickness scales different for each section. See Figure 1 for key.

reached similar conclusions regarding the magnetostratigraphic position of the Carnian–Norian boundary in the Newark Supergroup, using a supporting argument based around the vertebrate *Paleorhinus*. Muttoni *et al.* (2004*b*) attempted a correlation using a correlation-coefficient-based statistical approach, relating the thickness of Pizzo Mondello magnetozones to the duration of the correlative Newark Supergroup magnetozones, for each of the 16 possible relations. From a statistical standpoint their option #2 was the most robust and indicated the position of the Carnian–Norian boundary in magnetozone E7 (Fig. 8), similar to that proposal by Krystyn *et al.* (2002) and Channell *et al.* (2003), a correlation solution for the Lockatong Fm. and upper parts of the Stockton Fm. that is now generally accepted (Figs 8 and 12).

Location of the Norian–Rhaetian boundary in the Newark Supergroup

Broadly there have been three proposed correlation options, which place the conodont-defined

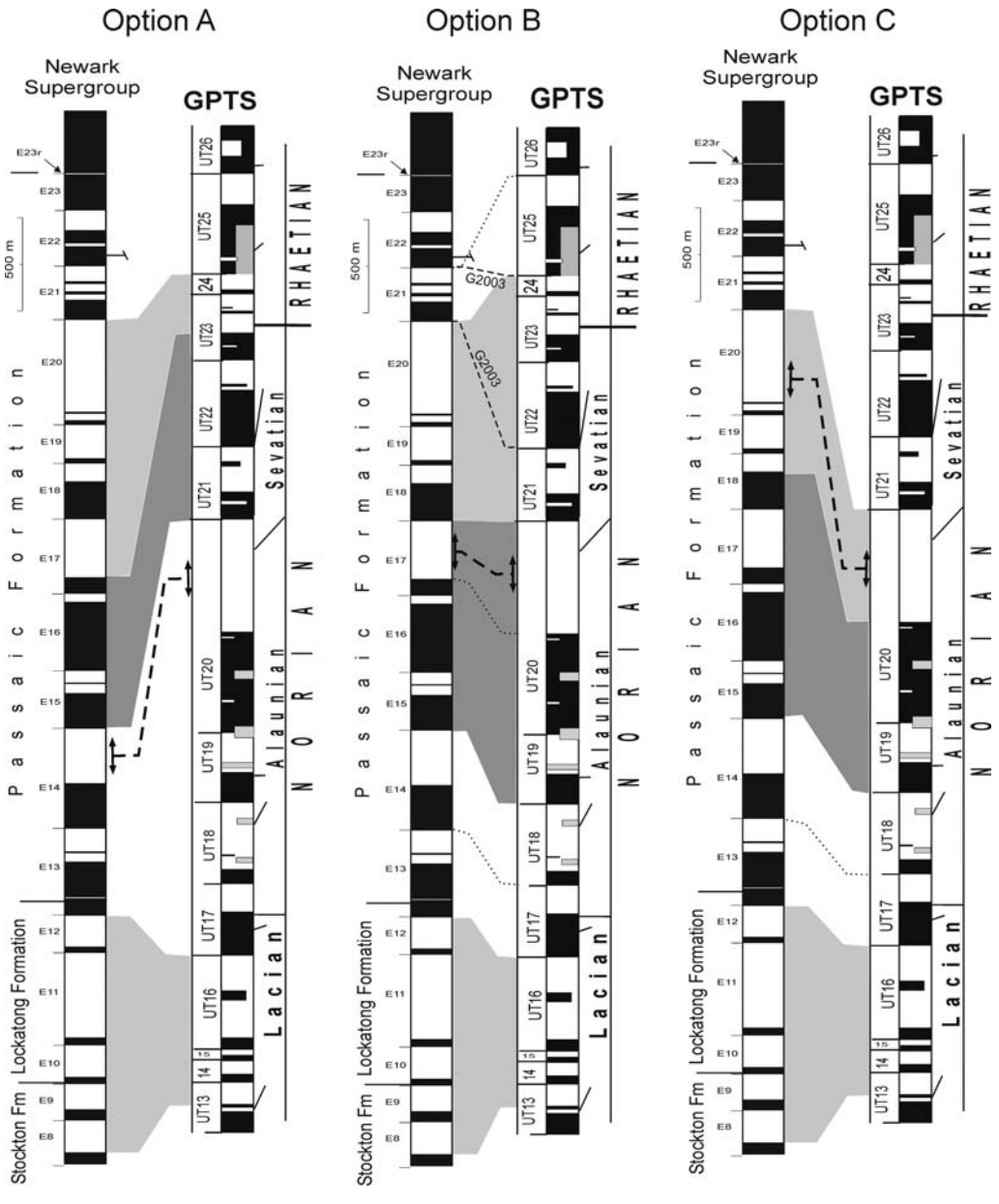

Fig. 12. The main options for correlating the Newark Supergroup magnetostratigraphy to the GPTS from Figures 9 and 10. Double-headed dashed line emphasises the key interval of E20r and its suggested correlation to key intervals in the Newark Supergroup for these three options. See text for discussion. G2003 – alternative correlations for option B proposed by Gallet *et al.* (2003). See Figure 1 for key.

Norian–Rhaetian boundary in the Passaic Fm., correlation option A suggesting the lowest and option C the highest (Fig. 12).

Option A has been proposed by Muttoni *et al.* (2004*b*, 2010), working from the Carnian–Norian boundary upwards (based on the above statistical matching approach), suggesting the base Rhaetian correlates approximately with Newark Supergroup magnetozone E17 (Fig. 12), or somewhat above, at a level similar to the original palynological and astrochronological estimate of Olsen & Kent (1999). Channell *et al.* (2003) had reached much

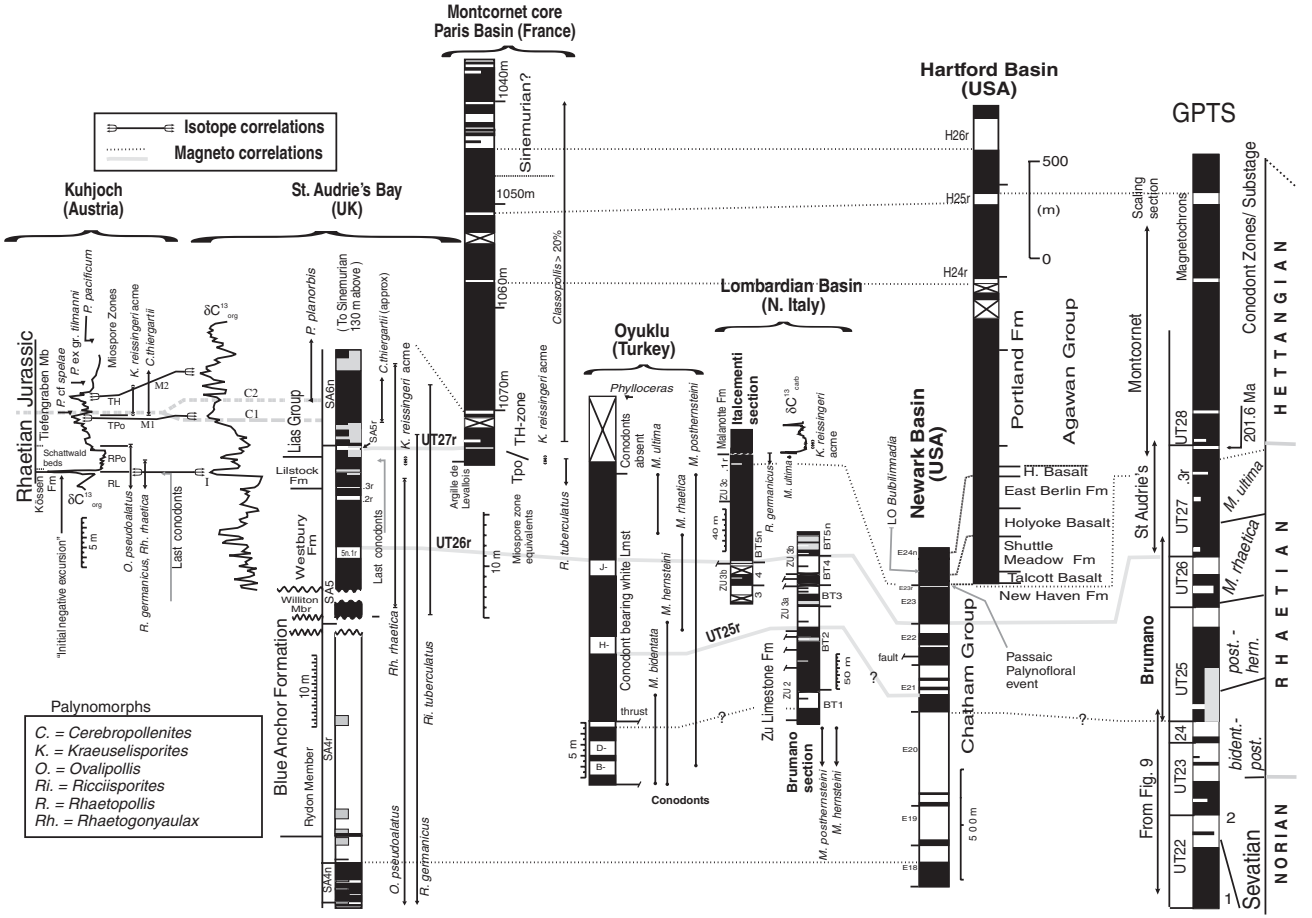

Fig. 13. Summary magnetostratigraphy of the Triassic–Jurassic boundary. Section data from left to right: Kuhjoch (Kuerschner *et al.* 2007; von Hillebrandt *et al.* 2007); St Audrie's Bay (Hesselbo *et al.* 2002; Hounslow *et al.* 2004); Montcornet core (Yang *et al.* 1996); Oyuklu (Gallet *et al.* 2007); Lombardian basin (Muttoni *et al.* 2010), Newark and Hartford basins (Kent *et al.* 1995; Kent & Olsen 2008). Thickness scales different for each section. See Figure 1 for additional keys. See Figures 9 and 10 for conodont genus abbreviations, and Sevatian sub-divisions. Ammonoid genus abbreviations, *P.* = *Psiloceras*. I, M1, M2 negative isotopic excursions at Kujoch. C1, C2 possible correlation options between the Kujoch and St Audrie's Bay sections (see text).

the same conclusion using the fragmented stratigraphy at Silická Brezová. Option A implies that the Newark interval E13–E14 interval is incomplete in comparison to the marine sections, and that the interval UT23r–UT24r in the GPTS is equivalent to E17r to E20r in the Newark Supergroup (Fig. 12).

Option B (Fig. 12) and variations on this option have been proposed by Krystyn *et al.* (2002), Gallet *et al.* (2003) and option 1 of Gallet *et al.* (2007). The strength of this option is the good polarity pattern match between the lower part of the Passaic Fm. and the UT17 to UT20r interval in the GPTS. A weakness is the absence of a clear match to the reverse polarity dominated interval in the E18r–E20r interval in the Newark Supergroup (Fig. 12). Gallet *et al.* (2003) proposed correlations between the base of E21n and UT22n, whereas a variation shown in Figure 12 is a higher correlation between E21n and UT25n that is more consistent with the underlying reverse polarity dominated interval UT23r to UT24r (Fig. 12). This option tends to imply large sedimentation rates changes in the marine successions around the Sevatian–Rhaetian boundary interval. A dramatic reduction in sedimentation rate in the studied marine sections in the lowest Rhaetian, and large within-section sedimentation rate changes in the Sevatian, is a characteristic which is shown in the ST4/STK-A sections at Steinbergkogel (Fig. 10). In the nonmarine European sections the interval correlated to E18r to E20r (Fig. 11) certainly witnessed dramatic environmental changes related to much wetter environments and initiation of marine transgressions. This may be reflected in the Tethyan pelagic sections around this interval by large reductions in sedimentation rates.

Magnetozone UT20r has been an attractive target for correlation to the E18r–E20r interval (i.e. option C in Fig. 12) because it has relatively the thickest reverse magnetozone in the Pizzo Mondello, Kavur Tepe and Kavaalani sections. This option has been proposed by Hounslow *et al.* (2004) and option 2 of Gallet *et al.* (2007). The correlation in option C implies that both the UT17–UT20n interval in the marine sections and the E21 to E22 interval in the Newark Supergroup are incomplete (Gallet *et al.* 2007). Support for this option comes from: (a) the absence of typical European latest Triassic miospores from the Newark Supergroup (Van Veen 1995; Kuerschner *et al.* 2007), although this may be a reflection of the differing floral province of the Newark Basin; (b) the mid Norian GPTS through the interval UT17–UT20n is the most fragmented, and therefore might be expected to be incomplete; and (c) the only substantial fault in the cored Passaic Fm. appears to be in magnetozone E22n (Olsen *et al.* 1996).

Weaknesses of correlation option C are: (a) it lacks the additional thin normal magnetozones characteristic of the E18r–E20r interval in the Newark Supergroup; (b) within the Blue Anchor Fm. in the UK the dinoflagellate cyst *Rhaetogonyaulux rhaetica* is known from lower, reverse polarity, levels (Orbell 1973) than those reported by Hounslow *et al.* (2004). In Tethyan sections in the Alps, *R. rhaetica* appears to characterise the middle and upper Rhaetian (Krystyn *et al.* 2007*a*), suggesting that the base of the Rhaetian probably lies within or below the level of SA4r and its correlative interval E19r–E20r (Figs 11 & 12).

There is no current resolution to these correlation problems, so the cyclostratigraphy timescale from the Newark Supergroup cannot be easily applied to the GPTS (Fig. 14) through the Norian and Rhaetian. The fact that other nonmarine sections through this interval seem to confirm the polarity character from the Newark Supergroup below E21n (Fig. 11) suggests that the problems largely reside with the marine section data: either missing or duplicated intervals or large within-section changes in sedimentation rates.

A common assumption made for the Newark Supergroup magnetostratigraphy is that because of the very large sedimentation rate, it is the most complete record of the magnetic polarity in the Norian–Rhaetian (Gallet *et al.* 2007). This assumption is only valid if the coring obtained a complete succession. In the Newark Supergroup coring program, intercore-correlation was supported by ground mapping along with horizon correlation based on lithology and colour, supported by magnetostratigraphic correlation from core and limited outcrops (Olsen *et al.* 1996). Nevertheless, full succession recovery can be difficult to confirm in cyclically bedded red-beds like the Passaic Fm., because of small faults, unless very good well-log coverage and seismic surveys exist.

The Triassic–Jurassic boundary

The Triassic–Jurassic boundary (TJB) is proposed to be defined in the Kuhjoch section in Austria (von Hillebrandt *et al.* 2007) at the FO of the ammonoid *Psiloceras* cf. *spelae*. Since this or nearby sections have no magnetostratigraphy and no sections containing this ammonoid have a magnetostratigraphy, the identification of this boundary in other sections with magnetostratigraphy, such as St Audrie's Bay and Oyuklu, is based on other correlation criteria. The two best possibilities are the use of carbon-isotopic curves, and palynological changes near the boundary, which demonstrate correlation to the St Audrie's Bay magnetostratigraphy.

The organic carbon isotopic data at Kuhjoch and St Audrie's Bay are quite similar, both display a

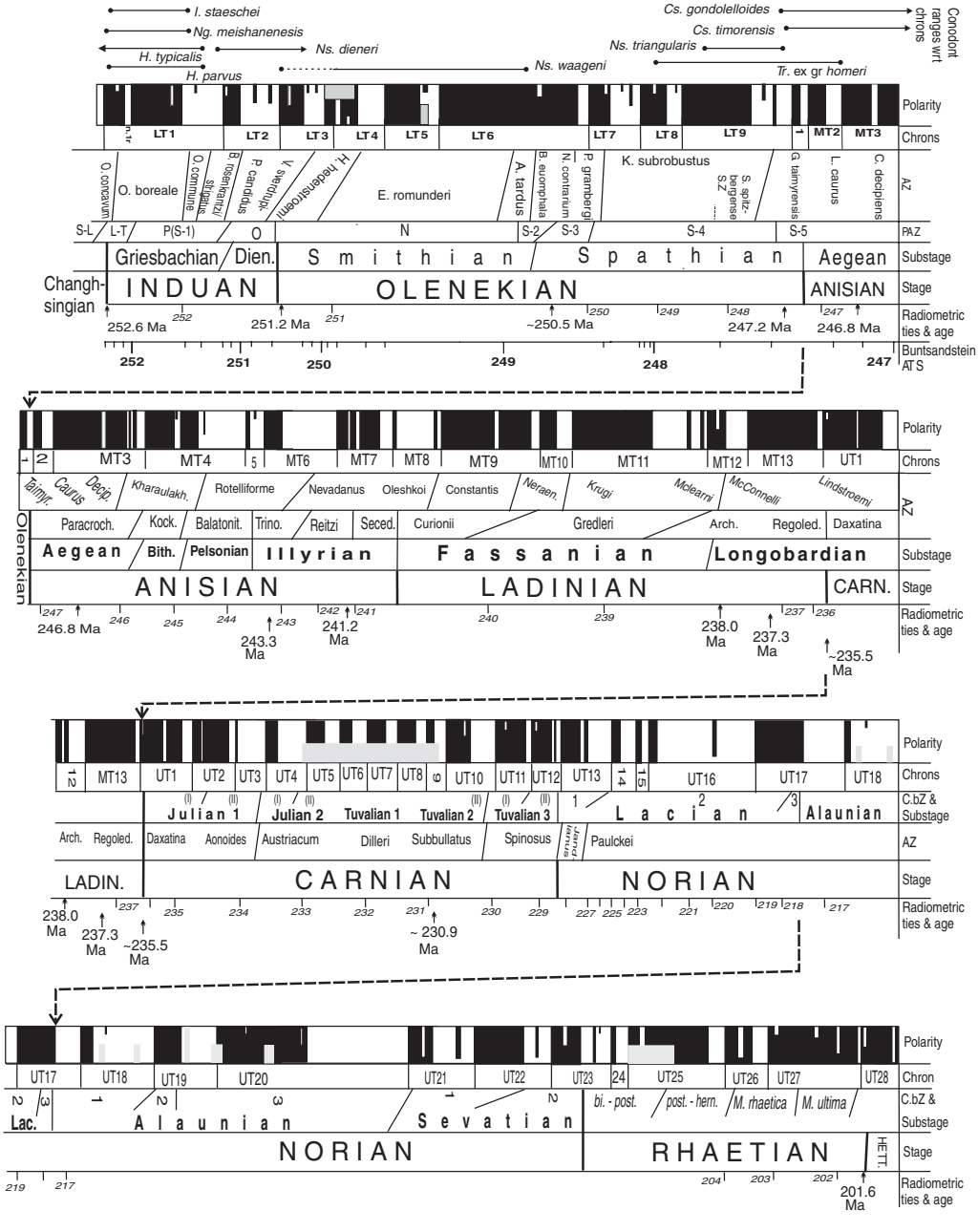

Fig. 14. Summary bio-magnetostratigraphic timescale for the Triassic, based on joint scaling of Figures 1, 2, 3, 5, 7, 8, 9, 10 and 12. No attempt is made to standardize the linked biostratigraphic zonations, which simply show the character of the supporting biostratigraphy (see text and previous figures for details). Radiometric ages from Brack *et al.* (2001), Mundil *et al.* (2004), Furin *et al.* (2006), Lehrmann *et al.* (2006), Galfetti *et al.* (2007*a*), Schaltegger *et al.* (2008), with additional discussion in text. Age in 1 Ma increments based on linear interpolations of radiometric ages for Induan to Carnian. Buntsandstein astronomical timescale (ATS) from Szurlies (2007), based on Figure 4 correlations. See Figure 1 for key. C.bZ, conodont biozones; AZ, Ammonoid zones; PAZ, Miospore assemblage zones (Lower Triassic from Hounslow *et al.* 2008*a*, *b*). See Figures 8, 9, 10 and 12 for details of Upper Triassic bio-zonations.

dual-peaked initial negative isotopic excursion, prior to the first *Psiloceras* (marked 'I' in Fig. 13). At Kuhjoch, this initial dual peak is concentrated in the 10 cm at the base of the Tiefengraben Mb (von Hillebrandt *et al.* 2007), whereas at St Audrie's Bay, it extends through the upper part of the Lilstock Fm. (Hesselbo *et al.* 2002; Fig. 13). In both sections, this initial negative peak includes the LO of conodonts. Above this level both sections show a peak in positive $\delta^{13}C_{org}$ values (at the position of magnetozone SA5r at St Audrie's Bay and within the Schattwald beds at Kuhjoch; Fig. 13), followed above by a decline to more negative values, with *Psiloceras* cf. *spelae* at Kuhjoch about 0.5 m above a peak in negative $\delta^{13}C_{org}$ (marked M1 in Fig. 13), and coinciding with a second smaller positive peak in $\delta^{13}C_{org}$ (Fig. 13). Using only the isotope record for correlation suggests that the TJB proposed at Kuhjoch is approximately coincident with the first *P. planorbis* at the St Audrie's Bay section (correlation C2 in Fig. 13). At Kuhjoch, above the TJB, there is a second negative excursion in $\delta^{13}C_{org}$ (marked M2 in Fig. 13), which appears to be shown at St Audrie's Bay within the lower range of *P. planorbis* (Fig. 13), although this later peak is not shown in other TJB interval isotopic records (McRoberts *et al.* 2007).

Kuerschner *et al.* (2007) suggested a correlation at a slightly lower level using the FO of *Cerebropollenites thiergartii* (correlation C1 in Fig. 13). The last occurrences of other significant miospore species (e.g. *Ovalipollis pseudoalatus*, *Rhaetopollis germanicus and Ricciisporites tuberculatus*) fall at different correlated levels, with only *R. germanicus* showing a LO within the main positive peak in the isotopic curve (Fig. 13). At Kuhjoch, the boundary between the TPo (*Trachysporites–Porcellispora*) and TH (*Trachysporites–Heliosporites*) zones is similar to that near the top of the Lilstock Fm., with both displaying an abundance peak in *Kraeuselisporites* (*Heliosporites*) *reissingeri* (Hounslow *et al.* 2004; Kuerschner *et al.* 2007), although the timing of these events appears to be different with respect to the carbon isotope data (Fig. 13). The Malanotte Fm. in the Lombardian Basin displays a similar association to that seen at St Audrie's Bay (Fig. 13), with an initial peak in negative $\delta^{13}C_{carb}$ and an acme of *K. reissingeri* a little above (Galli *et al.* 2007).

Support for the lower correlation level (i.e. C1 in Fig. 13) is consistent with a wider set of much debated ammonite data. Whilst global correlation of species of *Psiloceras* is difficult, *P. planorbis* is commonly inferred to be age-equivalent or younger than the *Psiloceras pacificum* ammonite faunas (Guex *et al.* 2002; von Hillebrandt *et al.* 2007). Similarly, the ammonites of the genus *Neophyllites*, occurr prior to *P. planorbis* in NW Europe, but in the New York Canyon area (Nevada, USA) it overlaps the range of *Psiloceras tilmanni* group ammonites (Guex *et al.* 2002). The lower correlation level (i.e. C1; Fig. 13) implies that the M1 isotopic negative excursion at St Audrie's Bay occupies about 3 m of strata across the TJB at Kuhjoch.

The magnetostratigraphy of the Montcornet core from the Paris Basin can be easily related to that from St Audrie's Bay in that a detailed palynostratigraphy exists for both sections near the boundary (Yang *et al.* 1996; Hounslow *et al.* 2004). The upper boundary of the Argille de Levollois at 1075 m in the Montcornet core is closely coincident with a palynological change, very similar to that at the Lilstock Fm.–Lias Group boundary at St Audrie's Bay. Both sections show abundance peaks of *K. reissingeri* followed closely above by low diversity miospore assemblages dominated by *Classopollis*. The LO of *Ricciisporites tuberculatus* also occurs slightly above the acme of *K. reissingeri*. For this reason, the reverse magnetozone at 1073.8 m in the Montcornet core is probably the equivalent of SA5r, some metres below the likely position of the TJB at St Audrie's Bay (Fig. 13). Between 1075 m and 1067 m in the Montcornet core are acmes of *K. reissingeri* (1074.9–1074.23 m), *Deltoidospora* (1074.9–1067.8 m), and *Concavisporites* (1074.9– 1070.1 m). As in the St Audrie's Bay section, this acme interval appears to be the equivalent of the upper part of the TPo or lower part of the TH assemblage zones of Kuerschner *et al.* (2007). Other thin (<0.3 m) reverse magnetozones occur higher in the Hettangian part of the Montcornet core, but have not apparently been detected at St Audrie's Bay, probably because of insufficient sampling density and the much thicker Hettangian succession (some 140 m) in the latter area.

The best constraint on the correlation of the Oyuklu section magnetostratigraphy with that from St Audrie's Bay, is provided by the LO of conodonts, which at St Audrie's Bay have their highest occurrence close to the initial negative δC^{13}_{org} peak. In some other sections, conodonts may range into younger strata closer to the positive peak in $\delta^{13}C$ (Lucas & Tanner 2007; McRoberts *et al.* 2007). At Oyuklu, the presence of the ammonite *Phylloceras* some 6 m above the last conodonts is the only solid evidence of truly Jurassic strata. The highest of the reverse magnetozones at Oyuklu (i.e. J−; Fig. 13) is probably the equivalent of SA5n.1r at St Audrie's Bay, and BT4r at the Brumano section. The Rhaetian nature of the Williton Mb. and Westbury Fm. in St Audrie's Bay is shown by the dinoflagellate cyst *Rhaetogonyaulax rhaetica*, whose first occurrence appears to be younger than Sevatian-1 (Krystyn *et al.* 2007*a*), although its first occurrence is often strongly influenced by

environmental conditions in the Germanic facies rocks of the UK, France and Germany.

There has been much discussion about correlating from marine successions within the TJB interval into the thick nonmarine successions of eastern North American (Kent & Olsen 1995; Muttoni *et al.* 2010; Hounslow *et al.* 2004; Whiteside *et al.* 2007; Lucas & Tanner 2007; Gallet *et al.* 2007). The most recent synthesis places the TJB interval somewhere within the succession of interbedded basalts and sedimentary units above the Passaic palynofloral event (Lucas & Tanner 2007). A magnetostratigraphic constraint is provided by the good match between the lower part of the St Audrie's Bay succession and the Newark Supergroup-Hartford Basin magnetozones E14 to E20 (Fig. 11), which suggests Newark Supergroup magnetozone E23 is Rhaetian (Fig. 13). A further constraint is provided by the magnetostratigraphy of the Portland Fm. in the Hartford Basin, overlying the basalt succession, which based on magnetostratigraphic correlation, probably places the base of the Sinemurian around magnetozone H26r (Kent & Olsen 2008). Around the Passaic palynofloral event, Whiteside *et al.* (2003) have an associated negative peak in $\delta^{13}C_{org}$ which is similar to that from marine successions. An alternative, supported by the magnetostratigraphy, is that this event may be a negative excursion in $\delta^{13}C_{org}$ equivalent to that in the Westbury Fm. close to SA5n.1r (Fig. 13). This suggests that Newark Supergroup magnetozone E23r may be the equivalent of BT5n.1r in the Italcementi section and UT27n.3r in the composite GPTS, a correlation which is consistent with the conclusions of Lucas & Tanner (2007).

Conclusions

The duration of the Triassic is some 51.1 Ma using the Changhsingian–Induan boundary at 252.6 Ma (Mundil *et al.* 2004) and the Rhaetian–Hettangian boundary at about 201.6 Ma (Schaltegger *et al.* 2008). Using linear extrapolation in the pseudo-height composite (Fig. 14) the base of the MT magnetochrons are very close to 247.2 Ma, essentially those radiometric dates from the Guando sections (Lehrmann *et al.* 2006). The age for the base of the UT magnetochrons is approximately 235.5 Ma based on the arguments presented previously for the Middle Triassic (Fig. 5).

Linear interpolations (using the pseudo-height composite) of the radiometric ages have been used to add 1 Ma increments for the Induan through to the early Norian GPTS (Fig. 14). Those for the upper part of the Rhaetian are based on the Newark Supergroup APTS, which are constrained by a similar upper tie-point at *c*. 201.6 Ma (Schaltegger *et al.* 2008). This cannot be usefully performed for the Norian, since its *c*. 25 Ma duration is not well constrained with radiometric ages, and there is no certainty in how to best correlate the Newark APTS to the marine-based GPTS.

The GPTS for the Triassic has some 133 magnetozones that appear to be soundly validated by existing data, but with some 37 additional tentative sub-magnetozones (Fig. 14). We have divided these into 50 magnetochrons corresponding to major N–R couplets. The validated magnetozones give a reversal rate of 2.6 rev/Ma, and average magnetochron duration of 0.38 Ma (Table 1). This reversal rate is similar to that in the Cenozoic. The Cande & Kent (1995) timescale has 171 reversals from the base of magnetochron C29n at 64.745 Ma to the base of C1n at 0.78 Ma, yielding a mean reversal frequency of 2.64 rev/Ma with a mean magnetochron duration of 0.379 Ma. The Lower and Middle Triassic have similar reversal rates of *c*. 4 rev/Ma, but the Upper Triassic has a reversal rate which is approximately half of this (Table 1), indicating that the maximum magnetostratigraphic resolution available for dating and correlation is during the Lower and Middle Triassic.

The proposed and ratified Triassic stage boundaries are for the most part reasonably well

Table 1. *Statistical information about the Triassic magnetic field divided into intervals corresponding to the chron numbering and radiometric age scaling used in Figure 14. Statistics are shown for validated polarity boundaries, and additional tentative, often short duration magnetozones. [..] indicates the number of magnetozones*

Chron Interval	Age range (Ma)	Validated magnetozones		Including tentative sub-magnetozones	
		Reversal rate (rev/Ma)	Mean chron duration (Ma)	Reversal rate (rev/Ma)	Mean chron duration (Ma)
UT	33.9	1.9 [64]	0.53	3.0 [102]	0.33
MT	11.7	3.8 [45]	0.26	4.4 [51]	0.23
LT	5.5	4.4 [24]	0.23	9.8 [54]	0.10
Triassic	51.1	2.6 [133]	0.38	4.1 [207]	0.25

characterised by a known and validated magnetic polarity pattern. The Induan, Anisian and Ladinian are perhaps the best characterized with multiple studies, along with the lower Norian and upper Carnian. In the Lower Triassic the lower part of the Olenekian appears to be not strongly validated by data from multiple sections, which in part may relate to inadequate biostratigraphic constraints. The Middle Triassic GPTS is for the most part well characterized by conodonts and secondarily by ammonoids, with low to high palaeolatitude correlations of the biozones supported by magnetostratigraphy (Hounslow *et al.* 2008*b*). Conodont biozonations provide the primary means of age calibrating the Upper Triassic GPTS. Parts of the Upper Triassic GPTS are not strongly validated in multiple sections with the existing data. The GPTS in the middle parts of the Carnian is the least well documented (UT5 to UT9), with intervals in the middle Norian (UT17 to UT20n) and middle Rhaetian (UT24 to UT26) possessing somewhat lesser degrees of uncertainty.

For the Lower Triassic, the ages based on the radiometric control points, and the Buntsandstein astronomical timescale (ATS), are in some parts more than 1 Ma divergent. Some of this, particularly in the Olenekian, relates to the uncertainty in how to best correlate the magnetostratigraphy between the marine and nonmarine successions. Part of the reason for the 'bunching' of the 0.2 Ma intervals in the Buntsandstein ATS presumably relates to the likely out-of-phase sedimentation rates, between these interior continental basins (i.e. Buntsandstein) and continental margin (i.e. Sverdrup–Barents Sea) records of magnetic polarity.

The apparent confirmation of the Newark Supergroup magnetostratigraphy by data from other nonmarine sections (Fig. 11) indicates the generally robust nature of the Newark Supergroup APTS. Therefore the problems in relating this to the GPTS are either omission (or duplication) in the marine Norian–Rhaetian section data, or that Upper Triassic, nonmarine clastic and marine carbonate successions have strongly out of phase sedimentation rates: problems that will tax future research. Both of the enormously detailed magnetostratigraphic studies on the Buntsandstein and Newark Supergroup indicate that without additional correlation constraints there will often be additional uncertainty in using such polarity records for age control. This suggests that better integrated, multi-tool studies will be required to provide more detailed and better understanding of environmental and sedimentary systems in the nonmarine Triassic.

Jonathan Glen kindly allowed use of his unpublished/in press manuscript. Carmen Heunisch allowed use of unpublished data on the palynology of the Buntsandstein. Tyler Beatty and Morten Bergan allowed use of inpress and unpublished data. Leopold Krystyn, Mike Orchard, Steve Hesselbo, and Dennis Kent provided helpful discussion. Detailed comments from Geoff Warrington were provided on an earlier draft. Jim Ogg and Robert Scholger improved the text with thoughtful reviews. Russian translations by Vassil Karloukovski.

References

ANGIOLINI, L., DRAGONETTI, L., MUTTONI, G. & NICORA, A. 1992. Triassic stratigraphy in the island of Hydra (Greece). *Rivista Italiana di Paleontologia e Stratigrafia*, **98**, 137–180.

ARCHE, A., LOPEZ-GOMEZ, J., MARZO, M. & VARGAS, H. 2004. The siliciclastic Permian-Triassic deposits in the central and northeastern Iberian Peninsula (Iberian, Ebro and Catalan Basins): a proposal for correlation. *Geologica Acta*, **2**, 305–320.

AS, J. A. & ZIJDERVELD, J. D. A. 1958. Magnetic cleaning of rocks in palaeomagnetic research. *Geophysical Journal of the Royal Astronomical Society*, **1**, 308–319.

BAUD, A., NAKREM, H.-A., BEAUCHAMP, B., BEATTY, T. W., EMBRY, A. F. & HENDERSON, C. M. 2008. Lower Triassic bryozoan beds from Ellesmere Island, High Arctic, Canada. *Polar Research*, **27**, 428–440.

BAYER, C. & LUNDSCHIEN, B. A. 1998. Establishment of a magnetostratigraphic framework for sequence stratigraphic modelling of fluvial reservoirs in the Lunde Formation. *In*: GRADSTEIN, F. M., SANDVIK, K. O. & MILTON, N. J. (eds) *Sequence stratigraphy – concepts and applications*. Norwegian Petroleum Society Special Publication, **8**, 251–262.

BEATTY, T. W., ZONNEVELD, J.-P. & HENDERSON, C. M. 2008. Anomalously diverse Early Triassic ichnofossil assemblages in northwest Pangea: a case for a shallow-marine habitable zone. *Geology*, **36**, 771–774.

BERGAN, M. 2005. Correlation in fluvial deposits – ideas for use of various techniques, FORCE seminar. *Statfjord and Triassic Formations Workshop*, Norwegian Petroleum Directorate, Stavanger, 5–6 Dec.

BENTON, M. J. 1997. The Triassic reptiles from Devon. *Proceedings of the Ussher Society*, **9**, 141–152.

BISSEL, H. J. 1973. Permian–Triassic boundary in the eastern Great Basin area. *In*: LOGAN, A. & HILLS, L. V. (eds) *The Permian and Triassic systems and their mutual boundary*. Canadian Society of Petroleum Geologists Memoir, **2**, Calgary, 318–344.

BOND, J. 1997. Late Triassic stratigraphy of the Beryl Field. *In*: OAKMAN, C. D., MARTIN, J. H. & CORBETT, P. M. W. (eds) *Cores from the Northwest European hydrocarbon province: an illustration of geological applications from exploration development*. British Geological Survey, 79–95.

BOYD, D. W. & MAUGHAN, E. K. 1973. Permian-Triassic boundary in the middle Rocky Mountains. *In*: LOGAN, A. & HILLS, L. V. (eds) *The Permian and Triassic systems and their mutual boundary*. Canadian Society of Petroleum Geologists Memoir, **2**, Calgary, 294–317.

BRACK, P. & MUTTONI, G. 2000. High-resolution magnetostratigraphic and lithostratigraphic correlations in Middle Triassic pelagic carbonates from the Dolomites (northern Italy). *Palaeogeography, Palaeoclimatology, Palaeoecology*, **161**, 361–380.

BRACK, P., MUNDIL, R., OBERLI, F., MEIER, M. & RIEBER, H. 1996. Biostratigraphic and radiometric age data question the Milankovitch characteristics of the Latemar cycles (Southern Alps, Italy). *Geology*, **24**, 371–375.

BRACK, P., SCHLAGER, W., STEFANI, M., MAURER, F. & KENTER, J. 2000. The Seceda drill hole in the Middle Triassic Buchenstein beds (Livinallongo Formation, Dolomites, Northern Italy) a progress report. *Rivista Italiana di Paleontologia e Stratigrafia*, **106**, 283–292.

BRACK, P., MUTTONI, G. & RIEBER, H. 2001. Comment on: 'Magnetostratigraphy and biostratigraphy of the Middle Triassic Margon section (Southern Alps, Italy)' by GIALANELLA, P. R., HELLER, F., MIETTO, P., INCORONATO, A., DE ZANCHE, V., GIANOLLA, P. & ROGHI, G. [*Earth Planet. Sci. Lett.* 187(2001) 17–25]. *Earth and Planetary Science Letters*, **193**, 253–255.

BRACK, P., RIENER, H., NICORA, A. & MUNDIL, R. 2005. The global boundary stratotype and point (GSSP) of the Ladinian Stage (Middle Triassic) at Bagolino (Southern Alps, Northern Italy) and its implication for the Triassic timescale. *Episodes*, **28**, 233–244.

BRACK, P., RIEBER, H., MUNDIL, R., BLENDINGER, W. & MAURER, F. 2007. Geometry and chronology of growth and drowning of Middle Triassic carbonate platforms (Cernera and Bivera/Clapsavon) in the Southern Alps (northern Italy). *Swiss Journal of Geosciences*, **100**, 327–348.

BROGLIO LORIGA, C., CIRILLI, S. *ET AL*. 1999. The Prati di Stuores/Stuores Wiesen section (Dolomites, Italy): a candidate Global Stratotype Section and Point for the base of the Carnian stage: *Rivista Italiana di Paleontologia e Stratigrafia*, **105**, 37–78.

BRUNHES, B. 1906. Recherches sur le direction d'aimantation des roches volcaniques. *Journal of Physics*, **5**, 705–724.

BUREK, P. J. 1967. Korrelation revers magnetisierter Gesteinsfolgen im Oberen Buntsandstein S.W. Deutchlands. *Geologisches Jahrbuch*, **84**, 591–616.

BUREK, P. J. 1970. Magnetic reversals: their application to stratigraphic problems. *American Association of Petroleum Geologists Bulletin*, **54**, 1120–1139.

CANDE, S. C. & KENT, D. V. 1995. Revised calibration of the geomagnetic polarity timescale for the Late Cretaceous and Cenozoic. *Journal of Geophysical Research*, **B100**, 6093–6095.

CHANNELL, J. E. T., LOWRIE, W. & MEDIZZA, F. 1979. Middle and Early Cretaceous magnetic stratigraphy from the Cismon Section, Northern Italy. *Earth and Planetary Science Letters*, **43**, 153–166.

CHANNELL, J. E. T., KOZUR, H. W., SIEVERS, T., MOCL, R., AUBRECHT, R. & SYKORA, M. 2003. Carnian–Norian biomagnetostratigraphy at Silická Brezová (Slovakia): correlation to other Tethyan sections and to the Newark Basin. *Palaeogeography, Palaeoclimatology, Palaecology*, **191**, 65–109.

CHEN, H.-H., SUN, S. & LI, J.-L. 1994. Permo Triassic magnetostratigraphy in Wulong area, Sichuan, China. *Science in China (series B)*, **37**, 203–212.

CIRILLI, S., RADRIZZANI, C. P., PONTON, M. & RADRIZZANI, S. 1998. Stratigraphical and palaeoenvironmental analysis of the Permian–Triassic transition in the Badia Valley (Southern Alps, Italy). *Palaeogeography, Palaeoclimatology, Palaecology*, **138**, 85–113.

CLEGG, J. A., ALMOND, M. & STUBBS, P. B. H. 1954. The remanent magnetization of some sedimentary rocks in Britain. *Philosophical Magazine*, **45**, 583–598.

COLLINSON, D. W., CREER, K. M., IRVING, E. & RUNCORN, S. K. 1957. The measurement of the permanent magnetization of rocks. *Philosophical Transactions of the Royal Society of London, Series A*, **250**, 73–82.

CORNET, B. 1993. Applications and limitations of palynology in age, climatic and paleoenvironmental analyses of Triassic sequences in North America. *In*: LUCAS, S. G. & MORALES, M. (eds) *The non-marine Triassic*. New Mexico Museum of Natural History & Science Bulletin, **3**, 73–93.

CREER, K. M. 1958. The remanent magnetization of unstable Keuper Marls. *Philosophical Transactions of the Royal Society of London, Series A*, **250**, 130–143.

CREER, K. M. 1959. AC demagnetisation of unstable Triassic Keuper Marls from SW England. *Geophysical Journal of the Royal Astronomical Society*, **2**, 261–275.

CREER, K. M., IRVING, E. & RUNCORN, S. K. 1954. The direction of the geomagnetic field in remote epochs in Britain. *Philosophical Transactions of the Royal Society of London, Series A*, **250**, 144–156.

DINARÈS-TURELL, J., DIEZ, J. D., REY, D. & ARNAL, I. 2005. 'Buntsandstein' magnetostratigraphy and biostratigraphic reappraisal from eastern Iberia: Early and Middle Triassic stage boundary definitions through correlation to Tethyan sections. *Palaeogeography, Palaeoclimatology, Palaeoecology*, **229**, 158–177.

DU BOIS, P. M. 1957. Comparison of palaeomagnetic results for selected rocks of Great Britain and North America. *Advances in Physics*, **6**, 177–186.

EDWARDS, L. E. 1989. Supplemented graphic correlation: a powerful tool for paleontologists and nonpaleontologists. *Palaios*, **4**, 127–143

EIDE, F. 1989. Biostratigraphic correlation within the Triassic Lunde Formation in the Snorre area. *In*: COLLINSON, J. D. (ed.) *Correlation in Hydrocarbon Exploration*. Norwegian Petroleum Society, London, Graham and Trotman, 291–297.

FIJALKOWSKA, A. 1995. Palynostratigraphy and palynofacies of the Permian–Triassic transitional sequence in the Zary Pericline (SW Poland). *Geological Quarterly*, **39**, 307–332.

FOWELL, S. J. & OLSEN, P. E. 1993. Time calibration of Triassic/Jurassic microfloral turnover, eastern North America. *Tectonophysics*, **222**, 361–369.

FURIN, S., PRETO, N., RIGO, M., ROGHI, G., GIANOLLA, P., CROWLEY, J. L. & BOWRING, S. A. 2006. High-precision U–Pb zircon age from the Triassic of Italy: implications for the Triassic time scale and the Carnian origin of calcareous nannoplankton and dinosaurs. *Geology*, **34**, 1009–1012.

GALFETTI, T., BUCHER, H. *ET AL*. 2007*a*. Timing of the Early Triassic carbon cycle perturbations inferred from new U–Pb ages and ammonoid biochronozones. *Earth and Planetary Science Letters*, **258**, 593–604.

GALFETTI, T., HOCHULI, P. A., BRAYARD, A., BUCHER, H., WESSERT, H. & VIGRAN, J. O. 2007*b*. Smithian-Spathian boundary event: evidence from global climatic change in the wake of the end-Permian biotic crisis. *Geology*, **35**, 291–294.

GALLET, Y., BESSE, J., KRYSTYN, L., MARCOUX, J. & THEVENIAUT, H. 1992. Magnetostratigraphy of the Late Triassic Bolücektasi Tepe section (southwestern Turkey): implications for changes in magnetic reversal frequency. *Physics of the Earth and Planetary Interiors*, **73**, 85–108.

GALLET, T., BESSE, J., KRYSTYN, L., THEVENIAUT, H. & MARCOUX, J. 1993. Magnetostratigraphy of the Kavur Tepe section (south western Turkey): a magnetic polarity time scale for the Norian. *Earth and Planetary Science Letters*, **117**, 443–456.

GALLET, T., BESSE, J., KRYSTYN, L. & MARCOUX, J. 1996. Norian magnetostratigraphy from the Scheiblkogel section, Austria: constraints on the origin of the Antalya Nappes, Turkey. *Earth and Planetary Science Letters*, **140**, 113–122.

GALLET, Y., KRYSTYN, L. & BESSE, J. 1998. Upper Anisian to Lower Carnian magnetostratigraphy from the Northern Calcareous Alps (Austria). *Journal of Geophysical Research*, **103**, 605–621.

GALLET, Y., BESSE, J., KRYSTYN, L., MARCOUX, J., GUEX, J. & THEVENIAUT, H. 2000*a*. Magnetostratigraphy of the Kavaalani section (southwestern Turkey): consequences for the origin of the Antalya Calcareous Nappes (Turkey) and for the Norian (Late Triassic) magnetic polarity timescale. *Geophysical Research Letters*, **27**, 2033–2036.

GALLET, Y., KRYSTYN, L., BESSE, J., SAIDI, A. & RICOU, L.-E. 2000*b*. New constraints on the Upper Permian and Lower Triassic geomagnetic polarity timescale from the Abadeh section (central Iran). *Journal of Geophysical Research*, **105**, 2805–2815.

GALLET, Y., KRYSTYN, L., BESSE, J. & MARCOUX, J. 2003. Improving the Upper Triassic numerical timescale from cross-correlation between Tethyan marine sections and the continental Newark Basin sequence. *Earth and Planetary Science Letters*, **212**, 255–261.

GALLET, Y., KRYSTYN, L., MARCOUX, J. & BESSE, J. 2007. New constraints on the end-Triassic (Upper Norian–Rhaetian) magnetostratigraphy. *Earth and Planetary Science Letters*, **255**, 458–470.

GELUK, M. C. & RÖHLING, H.-G. 1999. High-resolution sequence stratigraphy of the Lower Triassic Buntsandstein: a new tool for basin analysis. *In*: BACHMANN, G. H. & LERCHE, I. (eds) *Epicontinental Triassic.* Zentralblatt fur Geologie und Palaontologie, E. Schweizerbart'sche Verlagsbuchhandlung, Stuttgart, T1, 1998 (7–8), 727–745.

GIALANELLA, P. R., HELLER, F., MIETTO, P., INCORONATO, A., DE ZANCHE, V., GIANOLLA, P. & ROGHI, G. 2001. Magnetostratigraphy and biostratigraphy of the Middle Triassic Margon section (Southern Alps, Italy). *Earth and Planetary Science Letters*, **187**, 17–25.

GLEN, J. M., NOMADE, S., LYONS, J. L., METCALFE, I., MUNDIL, R. & RENNE, P. R. 2009. Magnetostratigraphic correlations of Permian–Triassic marine-to-terrestrial sections from China. *Journal of Asian Earth Sciences*, **36**, 521–540.

GLEN, W. 1982. *The road to Jaramilo. Critical years of the revolution in Earth Sciences*. Stanford, Stanford University Press.

GOREE, W. S. & FULLER, M. 1976. Magnetometers using RF-driven SQUIDS and their applications in rock magnetism and paleomagnetism. *Journal of Geophysical Research*, **84**, 5480–5486.

GOUGH, D. I. 1964. A spinner magnetometer. *Journal of Geophysical Research*, **69**, 2455–2463.

GRĂDINARU, E., ORCHARD, M. J. *ET AL*. 2007. The Global Boundary Stratotype Section and Point (GSSP) for the base of the Anisian: Dęsli Caira Hill, North Dobrogea, Romania. *Albertiana*, **36**, 54–71.

GRADSTEIN, F. M., AGTERBERG, F. P., OGG, J. G., HARDENBOL, J., VAN VEEN, P., THIERRY, J. & HUANG, Z. 1994. A Mesozoic time scale. *Journal of Geophysical Research*, **99**, 24051–24074.

GRAHAM, J. W. 1949. The stability and significance of magnetism in sedimentary rocks. *Journal of Geophysical Research*, **54**, 131–167.

GRAHAM, J. W. 1955. Evidence of polar shift since Triassic time. *Journal of Geophysical Research*, **61**, 735–739.

GUEX, J., BARTOLINI, A. & TAYLOR, D. 2002. Discovery of *Neophyllites* (Ammonitina, Cephalopoda, Early Hettangian) in the New York Canyon sections (Gabbs Valley Range, Nevada) and discussion of the $\delta^{13}C$ negative anomalies located around the Triassic–Jurassic boundary. *Bulletin de Géologie de l'Université de Lausanne*, **354**, 247–254.

GULLO, M. 1996. Conodont biostratigraphy of uppermost Triassic deep-water calcilutites from Pizzo Mondello (Sicani Mountains): evidence for Rhaetian pelagites in Sicily. *Palaeogeography, Palaeoclimatology, Palaeoecology*, **126**, 309–323.

HAILWOOD, E. A. 1989. *Magnetostratigraphy*. Geological Society London, Special Report, **19**, Geological Society, Blackwell, London.

HELLER, F. 1977. Palaeomagnetism of Upper Jurassic limestones from southern Germany. *Journal of Geophysics*, **42**, 475–488.

HELLER, F., CHEN, H., DOBSON, J. & HAAG, M. 1995. Permian–Triassic magnetostratigraphy – new results from South China. *Earth and Planetary Science Letters*, **89**, 281–295.

HELLER, F., LOWRIE, W., HUANMEI, L. & JUNDA, W. 1988. Magnetostratigraphy of the Permo–Triassic boundary section at Shangsi (Guangyuan, Sichuan Province, China). *Earth and Planetary Science Letters*, **88**, 348–356.

HELSLEY, C. E. 1969. Magnetic reversal stratigraphy of the Lower Triassic Moenkopi Fm. of West Colorado. *Geological Society of America Bulletin*, **80**, 2431–2450.

HELSLEY, C. E. & STEINER, M. B. 1974. Paleomagnetism of the Lower Triassic Moenkopi Formation. *Geological Society of America Bulletin*, **85**, 457–464.

HENDERSON, C. & BAUD, A. 1997. Correlation of the Permian–Triassic boundary in Arctic Canada and comparison with Meishan, China. *In*: NAIWEN, W. &

REMANE, J. (eds) *Stratigraphy*. Proceedings of the 30th International Geological Congress, Beijing, VSP-Brill Publishing, **11**, 143–152.

HESSELBO, S. P., ROBINSON, S. A., SURLYK, F. & PIASECKI, S. 2002. Terrestrial and marine extinction at the Triassic–Jurassic boundary synchronized with major carbon–cycle perturbation: a link to initiation of massive volcanism. *Geology*, **30**, 251–254.

HEUNISCH, C. 1999. Die Bedeutung der Palynologie für Biostratigraphie und Fazies in der Germanischen Trias. *In*: HAUSCHKE, N. & WILDE, V. (eds) *Trias – eine ganz andere Welt, Europa am Beginn des Erdmittelalters*. Müchen, Verlag dur Friedrich Feil, 207–220.

HIETE, M., BERNER, U., HEUNISCH, C. & RÖHLING, H.-G. 2005. Organic carbon isotopic and palynological excursions near the PTB in NW-Germany. *Workshop on Permian–Triassic Paleobotany and Palynology*. Bolzano/Bozen (Italy), June 16–18, 2005.

HIETE, M., BERNER, U., HEUNISCH, C. & RÖHLING, H.-G. 2006. A high-resolution inorganic geochemical profile across the Zechstein–Buntsandstein boundary in the North German Basin. *Zeitschrift der Deutschen Gesellschaft für Geowissenschaften*, **157**, 77–105.

HINNOV, L. A. & GOLDHAMMER, R. K. 1991. Spectral analysis of the Middle Triassic Latemar Limestone. *Journal of Sedimentary Petrology*, **61**, 1173–1193.

HOLSER, W. T., SCHÖNLAUB, H.-P. *ET AL*. 1989. A unique geochemical record at the Permian/Triassic boundary. *Nature*, **337**, 39–44.

HORACEK, M., BRANDNER, R. & ABART, R. 2007. Carbon isotope record of the P/T boundary and the Lower Triassic in the Southern Alps: evidence for rapid changes in storage of organic carbon. *Palaeogeography, Palaeoclimatology, Palaeoecology*, **252**, 347–354.

HOUNSLOW, M. W. & MCINTOSH, G. 2003. Magnetostratigraphy of the Sherwood Sandstone Group (Lower and Middle Triassic), south Devon, UK: detailed correlation of the marine and non-marine Anisian. *Palaeogeography, Palaeoclimatology, Palaeoecology*, **193**, 325–348.

HOUNSLOW, M. W., MAHER, B. A., THISTLEWOOD, L. & DEAN, K. 1995. Magnetostratigraphic correlations in two cores from the late Triassic Lunde Formation, Beryl Field, northern North Sea, UK. *In*: TURNER, P. & TURNER, A. (eds) *Palaeomagnetic applications in hydrocarbon exploration and production*. Geological Society, London, Special Publications, **98**, 163–172.

HOUNSLOW, M. W., POSEN, P. E. & WARRINGTON, G. 2004. Magnetostratigraphy and biostratigraphy of the Upper Triassic and lowermost Jurassic succession, St. Audrie's Bay. *Palaeogeography, Palaeoclimatology, Palaeoecology*, **213**, 331–358.

HOUNSLOW, M. W., HU, M., MØRK, A., VIGRAN, J. O., WEITSCHAT, W. & ORCHARD, M. J. 2007*a*. Magnetobiostratigraphy of the lower part of the Kapp Toscana Group (Carnian), Vendomdalen, central Spitsbergen, arctic Norway. *Journal of the Geological Society, London*, **164**, 581–597.

HOUNSLOW, M. W., SZURLIES, M., MUTTONI, G. & NAWROCKI, J. 2007*b*. The magnetostratigraphy of the Olenekian–Anisian boundary and a proposal to define the base of the Anisian using a magnetozone datum. *Albertiana*, **36**, 62–67.

HOUNSLOW, M. W., PETERS, C., MØRK, A., WEITSCHAT, W. & VIGRAN, J. O. 2008*a*. Biomagnetostratigraphy of the Vikinghøgda Formation, Svalbard (arctic Norway) and the geomagnetic polarity timescale for the Lower Triassic. *Geological Society of America Bulletin*, **120**, 1305–1325.

HOUNSLOW, M. W., HU, M., MØRK, A., WEITSCHAT, W., VIGRAN, J. O., KARLOUKOVSKI, V. & ORCHARD, M. J. 2008*b*. Intercalibration of Boreal and Tethyan timescales: the magneto-biostratigraphy of the Middle Triassic and the latest Early Triassic, central Spitsbergen (arctic Norway). *Polar Research*. **27**, 469–490.

HUANG, K. & OPDYKE, N. D. 2000. Magnetostratigraphic investigation of the Badong Formation in South China. *Geophysical Journal International*, **142**, 74–82.

IRVING, E. 1964. *Paleomagnetism and its application to Geological and Geophysical Problems*. New York, John Wiley.

ISING, G. 1942. On the magnetic properties of varved clay. *Arkiv for Matematik, Astronomic och Fysik*, **29A**, 1–37.

JACOBS, J. A. 1963. *The Earth's core and Geomagnetism*. Oxford, Pergammon Press.

JIN, Y. G., SHANG, Q. H. & CAO, C. Q. 2000. Late Permian magnetostratigraphy and its global correlation. *Chinese Science Bulletin*, **45**, 698–704.

KENT, D. V. & OLSEN, P. E. 1997. Paleomagnetism of Upper Triassic continental sedimentary rocks from Dan River–Danville rift basin (eastern North America). *Geological Society of America Bulletin*, **109**, 366–377.

KENT, D. V. & OLSEN, P. E. 1999. Astronomically tuned geomagnetic polarity time scale for the Late Triassic. *Journal of Geophysical Research*, **104**, 12831–12841.

KENT, D. V. & OLSEN, P. E. 2000. Magnetic polarity stratigraphy and paleolatitude of the Triassic–Jurassic Blomidon Formation in the Fundy Basin (Canada): implications for Early Mesozoic tropical climate gradients. *Earth and Planetary Science Letters*, **179**, 311–324.

KENT, D. V. & OLSEN, P. E. 2008. Early Jurassic magnetostratigraphy and paleolatitudes from the Hartford continental rift basin (eastern North America): testing for polarity bias and abrupt polar wander in association with the central Atlantic Magmatic province. *Journal of Geophysical Research*, **113**, B06105, doi: 10.1029/2007JB005407.

KENT, D. V., OLSEN, P. E. & WITTE, W. K. 1995. Late Triassic–earliest Jurassic geomagnetic polarity sequence and paleolatitudes from drill cores in the Newark rift basin, eastern North America. *Journal of Geophysical Research*, **100**, 14965–14998.

KENT, D. V., MUTTONI, G. & BRACK, P. 2004. Magnetostratigraphic confirmation of a much faster tempo for sea-level change for the Middle Triassic Latemar platform carbonates. *Earth and Planetary Science Letters*, **228**, 369–377.

KENT, D. V., MUTTONI, G. & BRACK, P. 2006. Reply to 'Discussion of "Magnetostratigraphic confirmation of a much faster tempo for sea-level change for the Middle Triassic Latemar platform carbonates" by D. V. KENT, G. MUTTONI & P. BRACK [Earth Planet. Sci. Lett.

228 (2004), 369–377]' by L. HINNOV. *Earth and Planetary Science Letters*, **243**, 847–850.

KHRAMOV, A. N. 1958. *Palaeomagnetism and stratigraphic correlation*. Gostoptechizdat Press, Leningrad [published & translated into English as Khramov and Irving, 1960, Canberra, Australian National University].

KHRAMOV, A. N. 1963. Paleomagnetic study of Upper Permian and Lower Triassic sections in the north and east of the Russian Platform. *In*: KHRAMOV, A. N. (ed.) *Paleomagnetic Stratigraphic Investigations*. Gostoptechizdat Press, Leningrad, 145–174 [in Russian].

KHRAMOV, A. N. 1987. *Paleomagnetology*. Berlin, Springer–Verlag.

KIRSCHVINK, J. L. 1980. The least squares line and plane and the analysis of palaeomagnetic data. *Geophysical Journal of the Royal Astronomical Society*, **62**, 699–718.

KOZUR, H. W. 1999. The correlation of the Germanic Buntsandstein and Muschelkalk with the Tethyan scale. *Zentralblatt fur Geologie und Palaontologie, E. Schweizerbart'sche Verlagsbuchhandlung, Stuttgart*, T1, Jb 1998, H7–8, 701–725.

KOZUR, H. W. & BACHMANN, G. H. 2005. Correlation of the Germanic Triassic with the international scale. *Albertiana*, **32**, 21–35.

KRASSILOV, V. A., AFONIN, S. A. & LOZOVSKY, V. R. 1999. Floristic evidence of transitional Permian–Triassic deposits of the Volga–Dvina region. *Permophiles*, **34**, 12–14.

KRYSTYN, L., GALLET, Y., BESSE, J. & MARCOUX, J. 2002. Integrated Upper Carnian to Lower Norian biochronology and implications for the Upper Triassic magnetic polarity time scale. *Earth and Planetary Science Letters*, **203**, 343–351.

KRYSTYN, L., RICHOZ, S., GALLET, Y., BOUQUEREL, H., KÜRSCHNER, W. M. & SPÖTL, C. 2007*a*. Updated bio- and magnetostratigraphy from Steinbergkogel (Austria), candidate GSSP for the base of the Rhaetian stage. *Albertiana*, **36**, 164–172.

KRYSTYN, L., BHARGAVA, O. N. & RICHOZ, S. 2007*b*. A candidate GSSP for the base of the Olenekian Stage: Mud at Pin Valley; district Lahul & Spiti, Hamachal Pradesh (Western Himalaya), India. *Albertiana*, **35**, 5–29.

KUERSCHNER, W. M., BONIS, N. R. & KRYSTYN, L. 2007. Carbon-isotope stratigraphy and palynostratigraphy of the Triassic–Jurassic transition in the Tiefengraben section – Northern Calcareous Alps (Austria). *Palaeogeography, Palaeoclimatology, Palaeoecology*, **244**, 257–280.

LAI, X., YANG, F., HALLAM, A. & WIGNALL, P. B. 1996. The Shangsi Section, candidate of the Global Stratotype Section and Point of the Permian–Triassic Boundary. *In*: YIN, H. F. (ed.) *The Paleozoic–Mesozoic Boundary*. Wuhan, China University of Geosciences Press, 113–124.

LANGEREIS, C. G., DEKKERS, M. J., DE LANGE, G. J., PATERNE, M. & VAN SANTVOORT, P. J. M. 1997. Magnetostratigraphy and astronomical calibration of the last 1.1 Myr from the eastern Mediterranean piston core and dating of short events in the Brunhes. *Geophysical Journal International*, **129**, 75–94.

LEHRMANN, D. J., RAMEZANI, J. *ET AL*. 2006. Timing of recovery from the end-Permian extinction: geochronologic and biostratigraphic constraints from south China. *Geology*, **34**, 1053–1056.

LE TOURNEAU, P. M. 1999. *Depositional history and tectonic evolution of the Late Triassic age rifts of the U.S. central Atlantic margin: results of an integrated palaeomagnetic analysis of the Taylorville and Richmond basins*. Unpublished PhD thesis, Columbia University, New York.

LI, H. & WANG, J. 1989. Magnetostratigraphy of the Permo-Triassic boundary section of Meishan of Cangxing, Zhejang. *Science in China*, **8**, 652–658.

LOOY, C. V., TWITCHETT, R. J., DILCHER, D. L., VAN KONIJNENBURG-VAN CITTERT, J. H. A. & VISSCHER, H. 2001. Life in the end-Permian dead Zone. *Proceedings of the National Academy Science, USA*, **98**, 7879–7883.

LOWRIE, W. & ALVAREZ, W. 1977. Late Cretaceous geomagnetic polarity sequence: detailed rock and palaeomagnetic studies of the Scaglia Rossa limestone at Gubbio, Italy. *Geophysical Journal of the Royal Astronomical Society*, **51**, 561–581.

LOWRIE, W. & KENT, D. V. 2004. Geomagnetic polarity timescales and reversal frequency regimes. *In*: CHANNELL, J. E. T., KENT, D. V., LOWRIE, W. & MEERT, J. (eds) *Timescales of the palaeomagnetic field*. America Geophysical Union, Washington DC, 117–129.

LOZOVSKY, V. R. 1998. The Permian–Triassic boundary in the continental series of Eurasia. *Palaeogeography, Palaeoclimatology, Palaeoecology*, **143**, 273–283.

LOZOVSKY, V. R. & MOLOSTOVSKY, E. A. 1993. Constructing the Early Triassic magnetic polarity time scale. *In*: LUCAS, S. G. & MORALES, M. (eds) *The Nonmarine Triassic*. New Mexico Museum of Natural History and Science Bulletin, **3**, 297–300.

LUCAS, S. G. 1999. Tetrapod based correlation of the nonmarine Triassic. *In*: BACHMANN, G. H. & LERCHE, I. (eds) *Epicontinental Triassic.* Zentralblatt fur Geologie und Palaontologie, E. Schweizerbart'sche Verlagsbuchhandlung, Stuttgart, T1, Jb 1998, H7–8, 497–521.

LUCAS, S. G. & TANNER, L. H. 2007. The nonmarine Triassic–Jurassic boundary in the Newark Supergroup of eastern North America. *Earth–Science Reviews*, **84**, 1–20.

LUCAS, S. G., HECKERT, A. B., SPIELMANN, J. A., TANNER, L. & HUNT, A. P. 2007*a*. Second day: Early and Middle Triassic stratigraphy, palaeontology and correlation in northeastern Arizona. *In*: LUCAS, A. G. & SPIELMANN, J. A. (eds) *The Global Triassic*. New Mexico Museum of Natural History and Science Bulletin, **40**, 181–187.

LUCAS, S. G., KRAINER, K. & MILNER, A. R. C. 2007*b*. The type section and age of the Timpoweap Member and stratigraphic nomenclature of the Triassic Moenkopi Group in south western Utah. *In*: LUCAS, A. G. & SPIELMANN, J. A. (eds) *Triassic of the American West*. New Mexico Museum of Natural History and Science Bulletin, **40**, 109–118.

MAGARITZ, M., BAR, R., BAUD, A. & HOLSER, W. T. 1988. The carbon–isotope shift at the Permian/Triassic

boundary in the southern Alps is gradual. *Nature*, **331**, 337–339.

MÁRTON, E., BUDAI, T., HAAS, J., KOVÁCS, S., SZABO, I. & VÖRÖS, A. 1997. Magnetostratigraphy and biostratigraphy of the Anisian–Ladinian boundary section Felsöörs (Balaton Highland, Hungary). *Albertiana*, **20**, 50–57.

MARTIN, D. L. 1975. A paleomagnetic polarity transition in the Devonian Columbus Limestone of Ohio: a possible stratigraphic tool. *Tectonophysics*, **28**, 125–134.

MATUYAMA, M. 1929. On the direction of magnetization in basalt in Japan, Tyosen and Manchuria. *Proceedings of the Imperial Academy of Japan*, **5**, 203–205.

MCELHINNY, M. W. & BUREK, P. J. 1971. Mesozoic palaeomagnetic stratigraphy. *Nature*, **232**, 98–102.

MCELHINNEY, M. W. & MCFADDEN, P. L. 2000. *Paleomagnetism – continents and oceans*. San Diego, Academic Press.

MCFADDEN, P. L., MA, X. H., MCELHINNY, M. H. & ZHANG, Z. K. 1988. Permo-Triassic magnetostratigraphy in China: Northern Tarim. *Earth and Planetary Science Letters*, **87**, 152–160.

MCNISH, A. G. & JOHNSON, E. A. 1938. Magnetization of unmetamorphosed varves and marine sediments. *Journal of Geophysical Research*, **43**, 401–407.

MCROBERTS, C. A., WARD, P. D. & HESSELBO, S. 2007. A proposal for the base Hettangian Stage (= base Jurassic System) GSSP at New York Canyon (Nevada, USA) using carbon isotopes. *International Subcommission of Jurassic Stratigraphy Newsletter*, **34**, 43–49.

METCALFE, I., FOSTER, C. B., AFONIN, S. A., NICOLL, R. S., MUNDIL, R., XIAOFENG, W. & LUCAS, S. G. 2009. Stratigraphy, biostratigraphy and C-isotopes of the Permian–Triassic non-marine sequence at Dalongkou and Lucaogou, Xinjiang Province, China. *Journal of Asian Earth Sciences*, **36**, 503–520.

MIETTO, P., ANDREETTA, R. *ET AL*. 2007. A candidate of the global boundary stratotype section and point for the base of the Carnian stage (Upper Triassic): GSSP at the base of the canadensis Subzone (FAD of *Daxatina*) in the Prati di Stuores/Stuores Wiesen section (Southern Alps, NE Italy). *Albertiana*. **36**, 78–97.

MOLINA-GARZA, R. S., GEISSMANN, J. W., LUCAS, S. G. & VAN DER VOO, R. 1996. Palaeomagnetism and magnetostratigraphy of Triassic strata in the Sangre de Cristo Mountains and Tucumcari Basin, New Mexico, U.S.A. *Geophysical Journal International*, **124**, 935–953.

MOLOSTOVSKY, E. A. 1983. *Paleomagnetic stratigraphy of the eastern European part of the USSR*. Saratov, University of Saratov [in Russian].

MOLOSTOVSKY, E. A. 1996. Some aspects of magnetostratigraphic correlation. *Stratigraphy and Geological Correlation*, **4**, 231–237.

MOLOSTOVSKY, E. A., PEVZNER, M. A. & PECHERSKY, D. M. 1976. Phanerozoic magnetostratigraphic scale and regime of magnetic field reversals. *In*: Geomagnetic Investigations (Radiosvyaz', Moscow), 45–52 [in Russian].

MOLOSTOVSKY, E. A., MOLOSTOVSKAYA, I. I. & MINIKH, M. G. 1998. Stratigraphic correlations of the Upper Permian and Triassic beds from the Volga-Ural and Cis-Caspian. *In*: CRASQUIN-SOLEAU, S. & BARRIER, É. (eds) *Peri-Tethys memoir 3: Stratigraphy and Evolution of Peri-Tethyan platforms*. Mémoires du Muséum national d'histoire naturelle, Paris, **177**, 35–44.

MØRK, A., ELVEBAKK, G. *ET AL*. 1999. The type section of the Vikinghøgda Formation: a new Lower Triassic unit in central and eastern Svalbard. *Polar Research*, **18**, 51–82.

MUNDIL, R., BRACK, P., MEIER, M., RIEBER, H. & OBERLI, F. 1996. High-resolution U–Pb dating of Middle Triassic volcaniclastics: time-scale calibration and verification of tuning parameters for carbonate sedimentation. *Earth and Planetary Science Letters*, **141**, 137–151.

MUNDIL, R., ZÜHLKE, R. *ET AL*. 2003. Cyclicity in Triassic platform carbonates: synchronizing radio-isotopic and orbital clocks. *Terra Nova*, **15**, 81–87.

MUNDIL, R., LUDWIG, K. R., METCALFE, I. & RENNE, P. R. 2004. Age and timing of the Permian mass extinctions: U/Pb dating of closed-system zircons. *Science*, **305**, 1760–1763.

MUTTONI, G. & KENT, D. V. 1994*a*. Paleomagnetism of latest Anisian (Middle Triassic) sections of the Prezzo Limestone and the Buchenstein Formation, Southern Alps, Italy. *Earth and Planetary Science Letters*, **122**, 1–18.

MUTTONI, G., CHANNELL, J. E. T., NICORA, A. & RETTORI, R. 1994*b*. Magnetostratigraphy and biostratigraphy of an Anisian-Ladinian (Middle Triassic) boundary section from Hydra (Greece). *Palaeogeography, Palaeoclimatology, Palaeoecology*, **111**, 249–262.

MUTTONI, G., KENT, D. V. & GAETANI, M. 1995. Magnetostratigraphy of the Lower–Middle Triassic boundary section from Chios (Greece). *Physics of the Earth and Planetary Interiors*, **92**, 245–260.

MUTTONI, G., KENT, D. V. *ET AL*. 1996*a*. Magnetobiostratigraphy of the Spathian to Anisian (Lower to Middle Triassic) Kçira section, Albania. *Geophysical Journal International*, **127**, 503–514.

MUTTONI, G., KENT, D. V., NICORA, A., RIEBER, H. & BRACK, P. 1996*b*. Magneto-biostratigraphy of the 'Buchenstein Beds' at Frötschbach (Western Dolomites, Italy). *Albertiana*, **17**, 51–56.

MUTTONI, G., KENT, D. V., BRACK, P., NICORA, A. & BALINI, M. 1997. Middle Triassic magnetobiostratigraphy from the Dolomites and Greece. *Earth and Planetary Science Letters*, **146**, 107–120.

MUTTONI, G., KENT, D. V. *ET AL*. 1998. Towards a better definition of the Middle Triassic magnetostratigraphy and biostratigraphy in the Tethyan realm. *Earth and Planetary Science Letters*, **164**, 285–302.

MUTTONI, G., GAETANI, M. *ET AL*. 2000. Middle Triassic palaeomagnetic data from northern Bulgaria: constraints on Tethyan magnetostratigraphy and palaeogeography. *Palaeogeography, Palaeoclimatology, Palaeoecology*, **160**, 223–237.

MUTTONI, G., KENT, D. V. & ORCHARD, M. 2001*a*. Paleomagnetic reconnaissance of early Mesozoic carbonates from Williston Lake, northeastern British Columbia, Canada: evidence for late Mesozoic remagnetization. *Canadian Journal of Earth Sciences*, **38**, 1157–1168.

MUTTONI, G., KENT, D. V., DI STEFANO, P., GULLO, M., NICORA, A., TAIT, J. & LOWRIE, W. 2001*b*. Magnetostratigraphy and biostratigraphy of the Carnian/Norian boundary interval from the Pizzo Mondello section (Sicani Mountains, Sicily). *Palaeogeography, Palaeoclimatology, Palaeoecology*, **166**, 383–399.

MUTTONI, G., NICORA, A. M., BRACK, P. & KENT, D. V. 2004*a*. Integrated Anisian–Ladinian boundary chronology. *Palaeogeography, Palaeoclimatology, Palaeoecology*, **208**, 85–102.

MUTTONI, G., KENT, D. V., OLSEN, P. E., DI STEFANO, P., LOWRIE, W., BERNASCONI, S. M. & HERNANDEZ, F. M. 2004*b*. Tethyan magnetostratigraphy from Pizzo Mondello (Sicily) and correlation to the Late Triassic Newark astrochronological polarity time scale. *Geological Society of America Bulletin*, **116**, 1043–1058.

MUTTONI, G., MECO, S. & GAETANI, M. 2005. Carnian–Norian boundary magneto-biostratigraphy from Guri Zi (Albania). *Rivista Italiana di Paleontologia e Stratigrafia*, **111**, 233–245.

MUTTONI, G., KENT, D. V., JADOUL, F., OLSEN, P. E., RIGO, M., GALLIC, M. T. & NICORA, A. 2010. Rhaetian magnetobiostratigraphy from the Southern Alps (Italy): constraints on Triassic chronology. *Palaeogeography, Palaeoclimatology, Palaeoecology*, **285**, 1–16.

NAGATA, T. 1945. Natural remanent magnetization of sedimentary rocks, Part II. *Bulletin of Earthquake Research Institute*, **23**, 94–95.

NAKREM, H. A., ORCHARD, M. J., WEITSCHAT, W., HOUNSLOW, M. W., BEATTY, T. W. & MØRK, A. 2008. Triassic conodonts from Svalbard and their Boreal correlation. *Polar Research*, **27**, 523–539.

NAWROCKI, J. 1997. Permian to early Triassic magnetostratigraphy from the central European basin in Poland: implications on regional and worldwide correlations. *Earth Planetary Science Letters*, **152**, 37–58.

NAWROCKI, J. & SZULC, J. 2000. The Middle Triassic magnetostratigraphy from the Peri-Tethys basin in Poland. *Earth and Planetary Science Letters*, **182**, 77–92.

NICOLL, R. T., METCALFE, I. & CHENG-YUAN, W. 2002. New species of the conodont genus *Hindeodus* and the conodont biostratigaphy of the Permian–Triassic boundary interval. *Journal of Asian Earth Science*, **20**, 609–631.

NICORA, A., BALINI, M. *ET AL*. 2007. The Carnian/Norian boundary interval at Pizzo Mondello (Sicani Mountains, Sicily) and its bearing for the defnition of the GSSP of the Norian Stage. *Albertiana*, **36**, 102–115.

NYSTUEN, J. P., KNARUD, R. & JORDE, K. 1989. Correlation of Triassic to Lower Jurassic sequences, Snorre Field and adjacent areas, northern North Sea. *In*: COLLINSON, J. D. (ed.) *Correlation in hydrocarbon exploration*. Norwegian Petroleum Society, London, Graham & Trotman, 273–289.

OGG, J. G. & STEINER, M. B. 1991. Early Triassic polarity time-scale: integration of magnetostratigraphy, ammonite zonation and sequence stratigraphy from stratotype sections (Canadian Arctic Archipelago). *Earth and Planetary Science Letters*, **107**, 69–89.

OLSEN, P. E., KENT, D. V., CORNET, B., WITTE, W. K. & SCHLISCHE, R. W. 1996. High-resolution stratigraphy of the Newark rift basin (early Mesozoic, eastern North America). *Geological Society of America Bulletin*, **108**, 40–77.

OLSEN, P. E. & KENT, D. V. 1999. Long-period Milankovitch cycles from the Late Triassic and Early Jurassic of eastern North America and their implications for the calibration of the Early Mesozoic time-scale and the long-term behaviour of the planets. *Philosophical Transactions of the Royal Society of London, Series A*, **357**, 1761–1786.

OPDYKE, N. D. & CHANNELL, J. E. 1996. *Magnetic Stratigraphy*. International Geophysical Series, **64**, London, Academic Press.

ORBELL, G. 1973. Palynology of the British Rhaeto–Liassic. *Bulletin Geological Survey of Great Britain*, **11**, 1–44.

ORCHARD, M. J. 2007. A proposed Carnian–Norian Boundary GSSP at Black Bear Ridge, northeast British Columbia, and a new conodont framework for the boundary interval. *Albertiana*, **36**, 129–141.

ORCHARD, M. J. 2008. Lower Triassic conodonts from the Canadian arctic, their intercalibration with ammonoid-based stages and a comparison with other North American Olenekian faunas. *Polar Research*, **27**, 393–412.

ORCHARD, M. J., ZONNEVELD, J. P., JOHNS, M. J., MCROBERTS, C. A., SANDY, M. R., TOZER, E. T. & CARRELLI, G. G. 2001. Fossil succession and sequence stratigraphy of the Upper Triassic of Black Bear Ridge, northeast British Columbia, a GSSP prospect for the Carnian-Norian boundary. *Albertiana*, **25**, 10–22.

ORCHARD, M. J., LEHRMANN, D. J., JIAYONG, W., HONGMEI, W. & TAYLOR, H. J. 2007. Conodonts from the Olenekian–Anisian boundary beds, Guandao, Guizhou province, China. *In*: LUCAS, A. G. & SPIELMANN, J. A. (eds) *The Global Triassic*. New Mexico Musuem of Natural History and Science Bulletin, **41**, 347–354.

PÄLIKE, H., MOORE, T., BACKMAN, J., RAFFI, I., LANCI, L., PARÉS, J. M. & JANECEK, T. 2005. Integrated stratigraphic correlation and improved composite depth scales for ODP Sites 1218 and 1219. *In*: WILSON, P. A., LYLE, M. & FIRTH, J. V. (eds) *Paleogene equatorial transect*. Proceedings Ocean Drilling Program Scientific Results, **199**, 1–41.

PÁLFY, J., PARRISH, R. R. & VÖRÖS, A. 2003. Mid-Triassic integrated U–Pb geochronology and ammonoid biochronology from the Balaton Highland (Hungary). *Journal of the Geological Society, London*, **160**, 271–284.

PAYNE, J. L., LEHRMANN, D. J., WEI, J., ORCHARD, M. J., SCHRAG, D. P. & KNOLL, A. H. 2004. Large perturbations of the carbon cycle during recovery from the end-Permian extinction. *Science*, **305**, 506–509.

PECHERSKY, D. M. & KHRAMOV, A. N. 1973. Mesozoic palaeomagnetic scale of the USSR. *Nature*, **244**, 499–501.

PERGAMENT, M. A., PECHERSKY, D. M. & KHRAMOV, A. N. 1971. *On the Paleomagnetic Timescale of the Mesozoic*. Izvestiya of the Academy of Sciences of the USSR, Geologic Series, **10**, 3–11.

PERRI, M. C. & FARABEGOLI, E. 2003. Conodonts across the Permian-Triassic boundary in the southern Alps. *Courier Forschungsinstitut Senckenberg*, **245**, 281–313.

PERRI, M. C. & SPALLETTA, C. 1998. *Southern Alps Field Trip Guidebook*, ECOS VII: Giornale di Geologia, **60** (special issue).

PICARD, M. D. 1964. Paleomagnetic correlation of units of the Chugwater (Triassic) Formation west-central Wyoming. *American Association of Petroleum Geologists Bulletin*, **48**, 269–291.

POSENATO, R. 2009. Global correlations of the mid Early Triassic events: the Induan/Olenekian boundary in the Dolomites (Italy). *Earth Science Reviews*, **91**, 93–105.

PRETO, N., HINNOV, L. A., HARDIE, L. A. & DE ZANCHE, V. 2001. Middle Triassic orbital signature recorded in the shallow-marine Latemar carbonate buildup (Dolomites, Italy). *Geology*, **29**, 1123–1126.

REEVE, S. C. & HELSLEY, C. E. 1972. Magnetic reversal sequence in the upper part of the Chinle Formation, Montoya, New Mexico. *Geological Society of America Bulletin*, **83**, 3795–3812.

REY, D., TURNER, P. & RAMOS, A. 1996. Palaeomagnetism of the Middle Triassic in the Iberian ranges (central Spain). *In*: MORRIS, A. & TARLING, D. H. (eds) *Palaeomagnetism and tectonics of the Mediterranean region*. Geological Society, London, Special Publications, **105**, 59–82.

RICHOZ, S., KRYSTYN, L., HORACEK, M. & SPÖTL, C. 2007. Carbon isotope record of the Induan Olenekian candidate GSSP, Mud and comparison with other sections. *Albertiana*, **35**, 35–40.

ROGHI, G. 2004. Palynological investigations in the Carnian of the Cabe del Predil area (Julian Alps, NE Italy). *Review of Palaeobotany and Palynology*, **132**, 1–35.

RUNCORN, S. K. 1955. Palaeomagnetism of sediments from the Colorado Plataeu. *Nature*, **176**, 505–506.

SCHALTEGGER, U., GUEX, J., BARTOLINI, A., SCHOENE, B. & OVTCHAROVA, M. 2008. Precise U–Pb age constraints for end-Triassic mass extinction, its correlation to volcanism and Hettangian post-extinction recovery. *Earth and Planetary Science Letters*, **267**, 266–275

SCHOLGER, R., MAURITSCH, H. J. & BRANDNER, R. 2000. Permian–Triassic boundary magnetostratigraphy from the southern Alps (Italy). *Earth and Planetary Science Letters*, **176**, 495–508.

SEPHTON, M. A., LOOY, C. V., BRINKHUIS, H., WIGNALL, P. B., DE LEEUW, J. W. & VISSCHER, H. 2005. Catastrophic soil erosion during the end-Permian biotic crisis. *Geology*, **33**, 941–944.

SHAW, A. B. 1964. *Time in Stratigraphy*. New York, McGraw-Hill.

SHIVE, P. N., STEINER, M. B. & HUYCKE, D. T. 1984. Magnetostratigraphy, palaeomagnetism and remanence acquisition in the Triassic Chugwater Formation of Wyoming. *Journal of Geophysical Research*, **89**, 1801–1815.

STEINER, M. B. 2006. The magnetic polarity timescale across the Permian–Triassic boundary. *In*: LUCAS, S. G., CASSINIS, G. & SCHNEIDER, J. W. (eds) *Nonmarine Permian biostratigraphy and biochronology*. Geological Society, London, Special Publications, **265**, 15–38.

STEINER, M. B., OGG, J., ZHANG, Z. & SUN, S. 1989. The Late Permian/Early Triassic magnetic polarity time scale and plate motions of south China. *Journal Geophysical Research*, **94**, 7343–7363.

STEINER, M. B., MORALES, M. & SHOEMAKER, E. M. 1993. Magnetostratigraphic, biostratigraphic and lithological correlations in Triassic strata of the western United States. *In*: AISSAOUUI, D. M., MCNEIL, D. F. & HURLEY, N. F. (eds) *Applications of paleomagnetism to sedimentary geology*. Society of Economic Palaeontologists and Mineralogists Special Publications, **49**, 41–57.

STEINER, M. B., ESHET, Y., RAMPINO, M. R. & SCHWINDT, D. M. 2003. Fungal abundance spike and the Permian–Triassic boundary in the Karoo Supergroup (South Africa). *Palaeogeography, Palaeoclimatology, Palaeoecology*, **194**, 405–414.

SUN, Z., HOUNSLOW, M. W., PEI, J., ZHAO, L., TONG, J. & OGG, J. G. 2007. Magnetostratigraphy of the West Pingdingshan section, Chaohu, Anhui Province: relevance for base Olenekian GSSP selection. *Albertiana*, **36**, 22–32.

SUN, Z., HOUNSLOW, M. W., PEI, J., ZHAO, L., TONG, J. & OGG, J. G. 2009. Magnetostratigraphy of the Lower Triassic beds from Chaohu (China), and its implications for the Induan–Olenekian stage boundary. *Earth and planetary Science Letters*, **279**, 350–361.

SZURLIES, M. 2007. Latest Permian to Middle Triassic cyclo-magnetostratigraphy from the Central European Basin, Germany: implications for the geomagnetic polarity timescale. *Earth and Planetary Science Letters*, **261**, 602–619.

SZURLIES, M., BACHMANN, G. H., MENNING, M., NOWACZYK, N. R. & KÄDING, K.-C. 2003. Magnetostratigraphy and high resolution lithostratigraphy of the Permian–Triassic boundary interval in Central Germany. *Earth and Planetary Science Letters*, **212**, 263–278.

TAYLOR, G. K., TUCKER, C. *ET AL*. 2009. Magnetostratigraphy of Permian/Triassic boundary sequences in the Cis-Urals, Russia: no evidence for a major temporal hiatus. *Earth and Planetary Science Letters*, **281**, 36–47.

TONG, J., ZUO, J. & CHEN, Z. Q. 2007. Early Triassic carbon isotope excursions from South China: proxies for devastation and restoration of marine ecosystems following the end-Permian mass extinction. *Geological Journal*, **42**, 371–389.

TORRESON, O. W., MURPHY, T. & GRAHAM, J. W. 1949. Magnetic polarization of sedimentary rocks and the Earth's magnetic history. *Journal of Geophysical Research*, **54**, 111–129.

VAN VEEN, P. M. 1995. Time calibration of Triassic/Jurassic microfloral turnover, eastern North America–comment. *Tectonophysics*, **245**, 93–95.

VIGRAN, J. O., MANGERUD, G., MØRK, A., BUGGE, T. & WEITSCHAT, W. 1998. Biostratigraphy and sequence stratigraphy of the Lower and Middle Triassic deposits from the Svalis Dome, Central Barents Sea, Norway. *Palynology*, **22**, 89–141.

VINE, F. J. & MATTHEWS, D. H. 1963. Magnetic anomalies over ocean ridges. *Nature*, **199**, 947–949.

VISSCHER, H., BRUGMAN, W. A. & VAN HOUTE, M. 1993. Chronostratigraphical and sequence stratigraphic

interpretation of the palynomorph record from the Muschelkalk of the Obernsees well, south Germany. *In*: HAGDORN, H. & SEILACHER, A. (eds) *Muschelkalk*. Schöntaler Symposium 1991. Sonderbände der Gesellschaft für Naturkunde, Württemberg, **2**, 145–152.

VON HILLEBRANDT, A., KRYSTYN, L. *ET AL*. 2007. A candidate GSSP for the base of the Jurassic in the Northern Calcareous Alps (Kuhjoch section, Karwendel Mountains, Tyrol, Austria). *International Subcommission of Jurassic Stratigraphy Newsletter*, **34**, 2–20.

VÖRÖS, A., BUDAI, T., HAAS, J., KOVÁCS, S., KOZUR, H. & PÁLFY, J. 2003. GSSP (Global Boundary Stratotype Section and Point) proposal for the base of the Ladinian (Triassic) – a proposal for the GSSP at the base of the Reitzi Zone (sensu stricto) at Bed 105 in the Felsöörs section, Balaton Highland, Hungary. *Albertiana*, **28**, 35–47.

WARD, P. D., BOTHA, J. *ET AL*. 2005. Abrupt and gradual extinction among Late Permian land vertebrates in the Karoo Basin, South Africa. *Science*, **307**, 709–714.

WHITESIDE, J. H., OLSEN, P. E., KENT, D. V., FOWELL, S. J. & EL-TOUHAMI, M. 2007. Synchrony between the Central Atlantic magmatic province and the Triassic–Jurassic mass-extinction event? *Palaeogeography, Palaeoclimatology, Palaeoecology*, **244**, 345–367.

WHITESIDE, J. H., OLSEN, P. E. & SAMBROTTO, R. N. 2003. Negative $\delta^{13}C$ carbon isotopic anomaly in continental strata at the Triassic–Jurassic boundary in eastern North America (Newark Basin, Pennsylvania, USA). *Geological Society of America Abstracts*, **34**, 160.

WIGNALL, P. B., HALLAM, A., XULONG, L. & FENGQUING, Y. 1995. Palaeoenvironmental changes across the Permian/Triassic boundary at Shangsi (N. Sichuan, China). *Historical Biology*, **10**, 175–189.

WILSON, R. L. 1961. Palaeomagnetism in Northern Ireland Pt. 1. The thermal demagnetisation of natural magnetic moments of rocks. *Geophysical Journal of the Royal Astronomical Society*, **5**, 45–69.

YANG, Z., MOREAU, M.-G., BUCHER, H., DOMMERGUES, J.-L. & TROUILLER, A. 1996. Hettangian and Sinemurian magnetostratigraphy from the Paris Basin. *Journal Geophysical Research*, **101**, 8025–8042.

YAROSHENKO, O. P. 2005. Reorganisation of palynofloras across the Permian–Triassic boundary (examples from the east European platform). *Stratigraphy and Geological Correlation*, **13**, 408–415.

YAROSHENKO, O. P. & LOZOVSKY, V. R. 2004. Palynological assemblages of the continental Lower Triassic in western Europe and their interregional correlation. Paper 1. Palynological assemblages of the Induan stage. *Stratigraphy and Geological Correlation*, **12**, 65–73.

YIN, H., ZHANG, K., TONG, J., YANG, Z. & WU, S. 2001. The Global stratotype section and point (GSSP) of the Permian–Triassic Boundary. *Episodes*, **24**, 102–114.

YIN, H., TONG, J. & ZHANG, K. 2005. A review on the Global stratotype section and point of the Permian–Triassic boundary. *Acta Geologica Sinica*, **79**, 715–728

ZHAO, L., ORCHARD, M. J., TONG, J., SUN, Z., ZUO, J., ZHANG, S. & YUN, A. 2007. Lower Triassic conodont sequence in Chaohu, Anhui Province, China and its global correlation. *Palaeogeography, Palaeoclimatology, Palaeoecology*, **252**, 24–38.